ISSN 0097-3157

Proceedings of the Academy of Natural Sciences of Philadelphia 167: 85-146 2020

A reappraisal of phylogenetic relationships among auchenipterid catfishes of the subfamily Centromochlinae and diagnosis of its genera (Teleostei: Siluriformes)

Luisa Maria Sarmento-Soares

Programa de Pós-Graduação em Biologia Animal, Universidade Federal do Espírito Santo. Prédio Bárbara Weinberg, Campus de Goiabeiras, 29043-900, Vitória, ES, Brasil. http://orcid.org/0000-0002-8621-1794
Laboratório de Ictiologia, Universidade Estadual de Feira de Santana. Av. Transnordestina s/no., Novo Horizonte, 44036-900, Feira de Santana, BA, Brasil
Instituto Nossos Riachos, INR, Estrada de Itacoatiara, 356 c4, 24348-095, Niterói, RJ. www.nossosriachos.net
E-mail: sarmento.soares@gmail.com

Ronaldo Fernando Martins-Pinheiro

Instituto Nossos Riachos, INR, Estrada de Itacoatiara, 356 c4, 24348-095, Niterói, RJ. www.nossosriachos.net
E-mail: pinheiro.martins@gmail.com

ABSTRACT.—A hypothesis of phylogenetic relationships is presented for species of the South American catfish subfamily Centromochlinae (Auchenipteridae) based on parsimony analysis of 133 morphological characters in 47 potential ingroup taxa and one outgroup taxon. Of the 48 species previously considered valid in the subfamily, only one, *Centromochlus steindachneri*, was not evaluated in the present study. The phylogenetic analysis generated two most parsimonious trees, each with 202 steps, that support the monophyly of Centromochlinae composed of five valid genera: *Glanidium*, *Gephyromochlus*, *Gelanoglanis*, *Centromochlus* and *Tatia*. Although those five genera form a clade sister to the monotypic *Pseudotatia*, we exclude *Pseudotatia* from Centromochlinae. The parsimony analysis placed *Glanidium* (six species) as the sister group to all other species of Centromochlinae. *Gephyromochlus* contained a single species, *Gephyromochlus leopardus*, that is sister to the clade *Gelanoglanis* (five species) + *Centromochlus* (eight species). Based on the new taxonomic arrangement herein, *Balroglanis* Grant 2015 and *Sauronglanis* Grant 2015 are placed in the synonymy of *Centromochlus*. *Tatia* is the most diverse genus within Centromochlinae, with twenty-six species in three monophyletic clades. The species composition of *Tatia* differs from that of Calegari et al. (2019). *Duringlanis* Grant 2015 and *Ferrarissoaresia* Grant 2015 are considered synonyms of *Tatia*. All generic taxa within Centromochlinae are diagnosed based on synapomorphic morphological characters. An identification key for Centromochlinae is provided.

RESUMO.—Uma hipótese de relações filogenéticas é apresentada para as espécies da subfamília sul americana de bagres Centromochlinae (Auchenipteridae) baseada em análise de parcimônia de 133 caracteres morfológicos em 47 potenciais taxa internos e um táxon externo. Das 48 espécies previamente consideradas válidas na subfamília apenas uma, *Centromochlus steindachneri*, não foi avaliada no presente estudo. A análise filogenética gerou duas árvores mais parcimoniosas, cada uma com 202 passos, que suportam o monofiletismo de Centromochlinae em uma composição de cinco gêneros válidos: *Glanidium*, *Gephyromochlus*, *Gelanoglanis*, *Centromochlus* and *Tatia*. Apesar destes cinco gêneros formarem um clado irmão ao monotípico *Pseudotatia*, nós excluímos *Pseudotatia* de Centromochlinae. A análise parcimoniosa colocou *Glanidium* (seis espécies), como o grupo-irmão de todas as espécies de Centromochlinae. *Gephyromochlus* contém uma única espécie, *Gephyromochlus leopardus*, que é irmã do clado *Gelanoglanis* (cinco espécies) + *Centromochlus* (oito espécies). Baseado no novo arranjo taxonômico aqui proposto, *Balroglanis* Grant 2015 e *Sauronglanis* sensu Grant 2015 são colocados na sinonímia de *Centromochlus*. *Tatia* é o mais diversificado gênero em Centromochlinae, com vinte e seis espécies em três clados monofiléticos. A composição de espécies em *Tatia* se modifica em relação ao arranjo de Calegari et al. (2019). *Duringlanis* Grant 2015 e *Ferrarissoaresia* Grant 2015 são considerados sinônimos de *Tatia*. Todos os taxa genéricos de Centromochlinae são diagnosticados com base em caracteres morfológicos sinapomórficos. Uma chave de identificação para Centromochlinae é fornecida.

Submitted: 3 Jun 2019, Accepted 11 Aug 2020.

INTRODUCTION

The Neotropical catfish family Auchenipteridae (Fig. 1) is composed of two monophyletic clades: Centromochlinae and Auchenipterinae (Ferraris, 1988; Soares-Porto, 1998; Akama, 2004; Birindelli, 2014; Calegari et al., 2019). Although some authors (Miranda Ribeiro, 1968; Ferraris, 1988) previously elevated Centromochlinae to family level, most recent classifications treat it as a subfamily. For more details, see Birindelli (2014) who reviewed the systematic history of Auchenipteridae as well as its sister family Doradidae.

The monophyly of Centromochlinae is well supported by unique reproductive features in mature males associated with insemination: a urogenital papilla emerging from a skin flap at the anal-fin origin; anal-fin proximal radials partially or completely fused into a single ossification; and anal-fin proximal radials oblique to body axis, not interdigitated with hemal spines (Ferraris, 1988; Soares-Porto, 1998; Birindelli, 2014; Calegari et al., 2019). The recent combined analysis of morphological and molecular evidence by Calegari et al. (2019) divided Centromochlinae into four tribes: Centromochlini, Gelanoglanini, Gladiniini and Pseudotatiini.

The Centromochlinae includes up to 48 species arranged in nine genera (Calegari et al., 2019), but the limits and validity of several taxa remain questionable. For example, *Gelanoglanis* was thought to nest deeply within *Centromochlus* (Soares-Porto, 1998), but remains valid by most authors due to its several unique autapomorphies (Soares-Porto et al., 1999; Ferraris, 2007; Rengifo et al., 2008; Calegari et al., 2014; Calegari & Reis, 2016, Calegari et al. 2019). Sarmento-Soares & Martins-Pinheiro (2008; 2013) transferred *Glanidium bockmanni* and *Tatia musaica* to *Centromochlus*, but other authors (Vari & Ferraris, 2013; Calegari et al., 2019) refer those species to *Tatia*. The validity and assignment of other nominal species to *Centromochlus* also needs further investigation. For examples, *Centromochlus steindachneri* was tentatively considered a junior synonym of *C. heckelii* by Mees (1974) and Calegari et al. (2019), but is possibly valid (LMSS, pers. obs.); *Centromochlus megalops* was considered valid by Royero (1999), a *species inquirendae* in *Centromochlus* by Ferraris (2007), and a junior synonym of *C. heckelii* by Mees (1974) and Calegari et al. (2019); and *Centromochlus simplex* was *incertae sedis* in Centromochlinae according to Sarmento-Soares & Martins Pinheiro (2008), valid in *Centromochlus* by Sarmento-Soares & Birindelli (2015) and valid in *Tatia* by Calegari et al. (2019).

Grant (2015) proposed four new subgenera in *Centromochlus*: *Balroglanis*, *Duringlanis*, *Ferrarissoaresia* and *Sauronglanis*. In subgenus *Balroglanis*, Grant (2015) placed eight nominal species: *Centromochlus schultzi* Rössel, 1962 (type of subgenus); *Glanidium bockmanni* Sarmento-Soares & Buckup, 2005; *Tatia concolor* Mees, 1974; *Centromochlus macracanthus* Soares-Porto, 2000; *Tatia punctata* Mees, 1974; *Tatia reticulata* Mees, 1974; *Tatia simplex* Mees, 1974 and *Centromochlus britskii* Sarmento-Soares & Birindelli, 2015. Calegari et al. (2019) elevated *Balroglanis* to genus and restricted it to three species: *B. schultzi*, *B. macracanthus* and the newly added *B. carolae* (Vari & Ferraris, 2013). Grant (2015) recognized three species in subgenus *Duringlanis*: *Centromochlus perugiae* Steindachner, 1882 (type of subgenus), *Centromochlus altae* Fowler, 1945 and *Tatia romani* Mees, 1988. Calegari et al. (2019) subsequently elevated *Duringlanis* to generic level with the same composition. Grant (2015) erected monotypic subgenus *Ferrarissoaresia* for *Centromochlus meridionalis* Sarmento-Soares et al., 2013. Calegari et al. (2019) elevated *Ferrarissoaresia* to generic level and expanded it to include *Ferrarissoaresia ferrarisi* (Birindelli, Sarmento-Soares & Lima, 2015). To the subgenus *Sauronglanis*, Grant (2015) assigned four nominal and one undescribed species: *Tatia musaica* Royero, 1992 (type of subgenus); *Tatia carolae* Vari & Ferraris, 2013; *Tatia marthae* Vari & Ferraris, 2013, *Tatia melanoleuca* Vari & Calegari, 2014; and *Centromochlus* (*Sauronglanis*) sp. Ninja, from Lago Balbina, Amazonas, Brazil. Calegari et al. (2019) did not comment on *Sauronglanis* and effectively synonymized this subgenus with *Tatia*. Birindelli (2014) placed the monotypic *Pseudotatia* sister to *Pseudauchenipterus* in Auchenipterinae. The recent transfer of *Pseudotatia* to Centromochlinae by Calegari et al. (2019) deserves additional investigation.

The primary objective of this study is to provide a comprehensive phylogenetic analysis based on morphological data for nearly all valid species of Centromochlinae. Based on those results, valid genera are newly diagnosed and a key to their identification is provided. This study aims to create a new framework for considering the evolution of morphological features within Centromochlinae.

MATERIAL AND METHODS

Morphological analysis.—Measurements for comparisons follow Sarmento-Soares & Martins-Pinheiro (2008), except for the depth of eye socket. This depth was measured in cleared and stained specimens using backlighting and a microscope eyepiece reticle; head width was measured in the same manner for comparative purposes. Osteological nomenclature follows Dahdul et al. (2010), with some exceptions based on Birindelli (2014). Osteological features were examined in cleared and stained

(cs) specimens prepared according to the procedures of Taylor & Van Dyke (1985), dry skeletons (Sk) prepared with dermestid larvae following Meeuse (1965) and radiographs (Rx). Data on rare taxa (e.g., *Gelanoglanis travieso* and *Tatia marthae*) were derived solely from radiographs, images of alcohol preserved specimens and original descriptions. Prior to clearing and staining, specimens were dissected whenever possible to study myology and determine sexual maturity of gonads. Morphology of pectoral-fin spine and serrations follows Vanscoy et al. (2015). Muscle names follow Datovo & Vari (2013; 2014) with references to alternative names used in previous studies (e.g., Sarmento-Soares & Porto, 2006). Abbreviations in myological character descriptions are: M., muscle; AM., adductor mandibulae and IA., intersegmental aponeurosis. Muscle illustrations were produced over photographs of dissected specimens. Drawings of muscle parts were sketched by hand based on photographs and direct observations of the specimens under a stereomicroscope. Drawings of cleared and stained specimens were rendered using a camera lucida. Structural details were photographed using a digital camera attached to a stereomicroscope. Due to the lack of specimens available for dissection, gonadal and myological features were coded as missing data for *Gephyromochlus leopardus, Gelanoglanis stroudi, Gelanoglanis nanonocticolus, Gelanoglanis travieso, Gelanoglanis pan, Gelanoglanis varii, Tatia caudosignata, Tatia concolor, T. marthae,* and *T. punctata*. For material examined, institutional abbreviations follows Sabaj (2020).

Taxon sampling.—The monophyly of family Auchenipteridae is well established (Britski, 1972; Ferraris, 1988; Curran, 1989; Walsh, 1990; Royero, 1999; Akama, 2004; Birindelli, 2014; Calegari et al., 2019). Auchenipteridae is composed of two subfamilies, Auchenipterinae and Centromochlinae, considered to be monophyletic sister clades following Ferraris (1988), Soares-Porto (1998), Akama (2004), Birindelli (2014) and Calegari et al. (2019). *Tocantinsia piresi* represents a basal lineage in Auchenipterinae based on morphological (Birindelli, 2014) and molecular evidence (Arce et al., 2013; Calegari et al., 2019). As TNT does not allow for multiple outgroups (P. Goloboff, pers. comm.), *T. piresi* was designated as the outgroup taxon. When appropriate, character state descriptions include comparisons to other catfish groups, reference(s) to previous phylogenetic studies, and discussion of polymorphic features. Most comparisons are within the clade Doradidae + Auchenipteridae, following the results of Birindelli (2014). The nominal species *Centromochlus steindachneri* Gill, 1870 was not evaluated in the present study and its validity remains obscure. *Centromochlus megalops*, long recognized as a *species inquirendae* in *Centromochlus* (sensu Ferraris, 2007), is treated as a junior synonym of *Centromochlus heckelii* following Mees (1974) and examination of type specimens by Calegari et al. (2019).

Species coded as missing data for morphological features under parsimony analysis are: *Gephyromochlus leopardus* (characters #13, #14, #62), *Pseudotatia parva* (#18, #19, #20), *Tatia concolor* (#13, #14, #18, #19, #20), *Tatia marthae* (#13, #14, #17, #18, #19, #20, #46, #48, #49, #51, #55, #56, #66, #67, #93, #95, #96, #97, #98, #99, #102, #103, #104, #105, #106, #107, #109, #111, #112, #113, #114, #115, #118) and *Tatia punctata* (#13, #14, #18, #19, #20). No specimens were available for myological dissections of *Gelanoglanis stroudi*, *G. nanonocticolus*, *G. travieso, G. pan, Tatia altae*, *T. ferrarisi*, *T. concolor, T. marthae, T. punctata*; thus, myological characters for those species were coded as missing data. See Appendix A for material examined.

Phylogenetic analysis.—Hypotheses are based on the cladistic method as originally proposed by Hennig (1950; 1966). The character matrix (Appendix B) was edited using WinClada (Nixon, 1999–2002). Unknown or missing data were entered as '?', and data for inapplicable characters were entered as '-'; both states were treated as missing data in the parsimony analysis. All characters were equally weighted. Multistate characters were ordered only when it was reasonable to infer *a priori* the nature of the transformational series or ontogenetic sequence. The parsimony analysis was performed using TNT (Goloboff & Catalano, 2016). Character numbers begin with 0, following the default in TNT and WinClada. The parsimony analysis included 47 potential ingroup taxa rooted with one outgroup, *Tocantinsia piresi* (Table 1). A heuristic (traditional) search using Tree-Bisection-Reconnection (TBR) was performed with 1,000,000 replicates. Consistency (CI) and Retention (RI) indices of fundamental cladograms and characters (on fundamental trees) were calculated using TNT via scripts 'wstats' and 'stats'. Ambiguous characters were reconstructed under ACCTRAN criteria (Swofford and Maddison, 1987; Maddison & Maddison, 2001). Character statements were described according to Sereno (2007). Nodal support was evaluated with 1000 non-parametric bootstrap pseudoreplicates. All of the support values were plotted on the strict consensus tree. For nodal support, we calculated Absolute Bremer support in TNT retaining 100 suboptimal trees. Achieved values referred to as weakly supported (Absolute Bremer support 1–2), moderately supported (3–4), well supported (5–8), and very well supported (> 8). Bremer support values for each genus represented by more than one species are presented in Table 2.

Table 1. Classification of nominal taxa assigned to subfamily Centromochlinae Bleeker 1862 (Auchenipteridae Bleeker 1862) in current study compared to classifications of previous studies (* denotes type species).

	Nominal species	Ferraris, 2007
Valid Genus		
***Centromochlus* Kner, 1857**		
1	*Auchenipterus heckelii* De Filippi 1853	valid as *Centromochlus heckelii*
2	*Centromochlus existimatus* Mees 1974	valid as *Centromochlus existimatus*
3	*Centromochlus macracanthus* Soares-Porto 2000	valid as *Centromochlus macracanthus*
	**Centromochlus megalops* Kner 1858 [type species of *Centromochlus*]	Species *inquirenda* in *Centromochlus*
4	*Centromochlus orca* Sarmento-Soares, Lazarotto, Py-Daniel & Leitão 2017	—
5	**Centromochlus schultzi* Rössel 1962 [type species of subgenus *Balroglanis*]	valid as *Centromochlus schultzi*
6	*Centromochlus steindachneri* Gill 1870	valid as *Centromochlus steindachneri*
7	*Tatia carolae* Vari & Ferraris 2013	—
8	*Tatia melanoleuca* Vari & Calegari 2014	—
9	**Tatia musaica* Royero 1992 [type species of subgenus *Sauronglanis*]	valid as *Tatia musaica*
***Gelanoglanis* Böhlke 1980**		
10	*Gelanoglanis nanonocticolus* Soares-Porto, Walsh, Nico & Netto 1999	valid as *Gelanoglanis nanonocticolus*
11	*Gelanoglanis pan* Calegari, Reis & Vari 2014	—
12	**Gelanoglanis stroudi* Böhlke 1980 [type species of *Gelanoglanis*]	valid as *Gelanoglanis stroudi*
13	*Gelanoglanis travieso* Rengifo & Lujan 2008	—
14	*Gelanoglanis varii* Calegari & Reis 2016	—
***Gephyromochlus* Hoedeman 1961**		
15	**Centromochlus* (*Gephyromochlus*) *leopardus* Hoedeman 1961 [type species of *Gephyromochlus*]	valid as *Glanidium leopardum*
***Glanidium* Lütken, 1874**		
16	**Glanidium albescens* Reinhardt in Lütken, 1874 [type species of *Glanidium*]	valid as *Glanidium albescens*
17	*Glanidium botocudo* Sarmento-Soares & Martins-Pinheiro 2013	
18	*Glanidium catharinensis* Miranda Ribeiro 1962	valid as *Glanidium catharinensis*
19	*Glanidium cesarpintoi* Ihering, 1928	valid as *Glanidium cesarpintoi*
20	*Glanidium melanopterum* Miranda Ribeiro 1918	valid as *Glanidium melanopterum*
21	*Glanidium ribeiroi* Haseman 1911	valid as *Glanidium ribeiroi*

Table 1. cont.

Grant, 2015	Calegari et al., 2019	Sarmento-Soares & Martins-Pinheiro 2020 [current study]
—	valid as *Centromochlus heckelii*	valid as *Centromochlus heckelii*
—	valid as *Centromochlus existimatus*	valid as *Centromochlus existimatus*
valid as *Centromochlus* (*Balroglanis*) *macracanthus*	valid as *Balroglanis macracanthus*	valid as *Centromochlus macracanthus*
—	synonym of *Centromochlus heckelii*	synonym of *Centromochlus heckelii* [not examined]
—	valid as *Tatia orca*	valid as *Centromochlus orca*
valid as *Centromochlus* (*Balroglanis*) *schultzi*	valid as *Balroglanis schultzi*	valid as *Centromochlus schultzi*
—	synonym of *Centromochlus heckelii*	possibly valid as *Centromochlus steindachneri* [not examined]
valid as *Centromochlus* (*Sauronglanis*) *carolae*	valid as *Balroglanis carolae*	valid as *Centromochlus carolae*
valid as *Centromochlus* (*Sauronglanis*) *melanoleucus*	valid as *Tatia melanoleuca*	valid as *Centromochlus melanoleucus*
valid as *Centromochlus* (*Sauronglanis*) *musaicus*	valid as *Tatia musaica*	valid as *Centromochlus musaicus*
—	valid as *Gelanoglanis nanonocticolus*	valid as *Gelanoglanis nanonocticolus*
—	valid as *Gelanoglanis pan*	valid as *Gelanoglanis pan*
—	valid as *Gelanoglanis stroudi*	valid as *Gelanoglanis stroudi*
—	valid as *Gelanoglanis travieso*	valid as *Gelanoglanis travieso*
—	valid as *Gelanoglanis varii*	valid as *Gelanoglanis varii* [not examined]
—	valid as *Gephyromochlus leopardus*	valid as *Gephyromochlus leopardus*
—	valid as *Glanidium albescens*	valid as *Glanidium albescens*
—	valid as *Glanidium botocudo*	valid as *Glanidium botocudo*
—	valid as *Glanidium catharinensis*	valid as *Glanidium catharinensis*
—	valid as *Glanidium cesarpintoi*	valid as *Glanidium cesarpintoi*
—	valid as *Glanidium melanopterum*	valid as *Glanidium melanopterum*
—	valid as *Glanidium ribeiroi*	valid as *Glanidium ribeiroi*

Table 1. cont.

***Tatia* Miranda Ribeiro 1911 [Clade A]**		
22	*Tatia aulopygia* (Kner 1857)	valid as *Tatia aulopygia*
23	*Tatia boemia* Koch & Reis 1996	valid as *Tatia boemia*
24	*Tatia brunnea* Mees 1974	valid as *Tatia brunnea*
25	*Tatia caudosignata* DoNascimiento, Albornoz-Garzón & García-Melo 2019	—
26	*Tatia caxiuanensis* Sarmento-Soares & Martins-Pinheiro 2008	—
	Centromochlus creutzbergi Boseman 1953	valid as *Tatia creutzbergi*
27	*Tatia dunni* (Fowler 1945)	valid as *Tatia dunni*
28	*Tatia galaxias* Mees 1974	valid as *Tatia galaxias*
29	*Tatia gyrina* (Eigenmann & Allen, 1942)	valid as *Tatia gyrina*
30	**Tatia intermedia* (Steindachner 1877) [type species of Tatia]	valid as *Tatia intermedia*
31	*Tatia jaracatia* Pavanelli & Bifi 2009	—
32	*Tatia meesi* Sarmento-Soares & Martins-Pinheiro 2008	—
33	*Tatia neivai* (Ihering 1930)	valid as Tatia neivai
34	*Tatia nigra* Sarmento-Soares & Martins-Pinheiro 2008	—
35	*Tatia strigata* Soares-Porto 1995	valid as *Tatia strigata*
***Tatia* Miranda Ribeiro 1911 [Clade B]**		
36	*Centromochlus altae* Fowler,1945	valid as *Centromochlus altae*
37	*Centromochlus ferrarisi* Birindelli, Sarmento-Soares & Lima 2015	—
38	**Centromochlus meridionalis* Sarmento-Soares, Cabeceira, Carvalho, Zuanon & Akama 2013 [type species of subgenus *Ferrarissoaresia*]	—
39	**Centromochlus perugiae* Steindachner 1882 [type species of subgenus *Duringlanis*]	valid as *Centromochlus perugiae*
40	*Tatia reticulata* Mees 1974	valid as *Centromochlus reticulatus*
41	*Tatia romani* Mees 1988	valid as *Centromochlus romani*
***Tatia* Miranda Ribeiro 1911 [Clade C]**		
42	*Centromochlus britskii* Sarmento-Soares & Birindelli 2015	—
43	*Glanidium bockmanni* Sarmento-Soares & Buckup 2005	—
44	*Tatia concolor* Mees 1974	valid as *Centromochlus concolor*
45	*Tatia marthae* Vari & Ferraris 2013	—
46	*Tatia punctata* Mees 1974	valid as *Centromochlus punctatus*
47	*Tatia simplex* Mees 1974	valid as *Tatia simplex*

Table 1. cont.

—	valid as *Tatia aulopygia*	valid as *Tatia aulopygia*
—	valid as *Tatia boemia*	valid as *Tatia boemia*
—	valid as *Tatia brunnea*	valid as *Tatia brunnea*
—	valid as *Tatia caudosignata*	valid as *Tatia caudosignata* [not examined]
—	valid as *Tatia caxiuanensis*	valid as *Tatia caxiuanensis*
	valid as *Tatia creutzbergi*	synonym of *Tatia gyrina*
—	valid as *Tatia dunni*	valid as *Tatia dunni*
—	valid as *Tatia galaxias*	valid as *Tatia galaxias*
—	valid as *Tatia gyrina*	valid as *Tatia gyrina*
—	valid as *Tatia intermedia*	valid as *Tatia intermedia*
—	valid as *Tatia jaracatia*	valid as *Tatia jaracatia*
—	valid as *Tatia meesi*	valid as *Tatia meesi*
—	valid as *Tatia neivai*	valid as *Tatia neivai*
—	valid as *Tatia nigra*	valid as *Tatia nigra*
—	valid as *Tatia strigata*	valid as *Tatia strigata*
valid as *Centromochlus* (*Duringlanis*) *altae*	valid as *Duringlanis altae*	valid as *Tatia altae*
—	valid as *Ferrarissoaresia ferrarisi*	valid as *Tatia ferrarisi*
valid as *Centromochlus* (*Ferrarissoaresia*) *meridionalis*	valid as *Ferrarissoaresia meridionalis*	valid as *Tatia meridionalis*
valid as *Centromochlus* (*Duringlanis*) *perugiae*	valid as *Duringlanis perugiae*	valid as *Tatia perugiae*
valid as *Centromochlus* (*Balroglanis*) *reticulatus*	valid as *Tatia reticulata*	valid as *Tatia reticulata*
valid as *Centromochlus* (? *Duringlanis*) *romani*	valid as *Duringlanis romani*	valid as *Tatia romani*
valid as *Centromochlus* (*Balroglanis*) *britskii*	valid as *Tatia britskii*	valid as *Tatia britskii*
valid as *Centromochlus* (*Balroglanis*) *bockmanni*	valid as *Tatia bockmanni*	valid as *Tatia bockmanni*
valid as *Centromochlus* (*Balroglanis*) *concolor*	valid as *Tatia concolor*	valid as *Tatia concolor*
valid as *Centromochlus* (*Sauronglanis*) *marthae*	valid as *Tatia marthae*	valid as *Tatia marthae*
valid as *Centromochlus* (*Balroglanis*) *punctatus*	valid as *Tatia punctata*	valid as *Tatia punctata*
valid as *Centromochlus* (*Balroglanis*) *simplex*	valid as *Tatia simplex*	valid as *Tatia simplex*

Table 2. Support values for each genus recognized in this study and represented by more than one species (monotypic *Gephyromochlus* not listed).

Genus	Bremer support	Bootstrap
Centromochlus	3	70
Gelanoglanis	22	100
Glanidium	8	100
Tatia	3	91

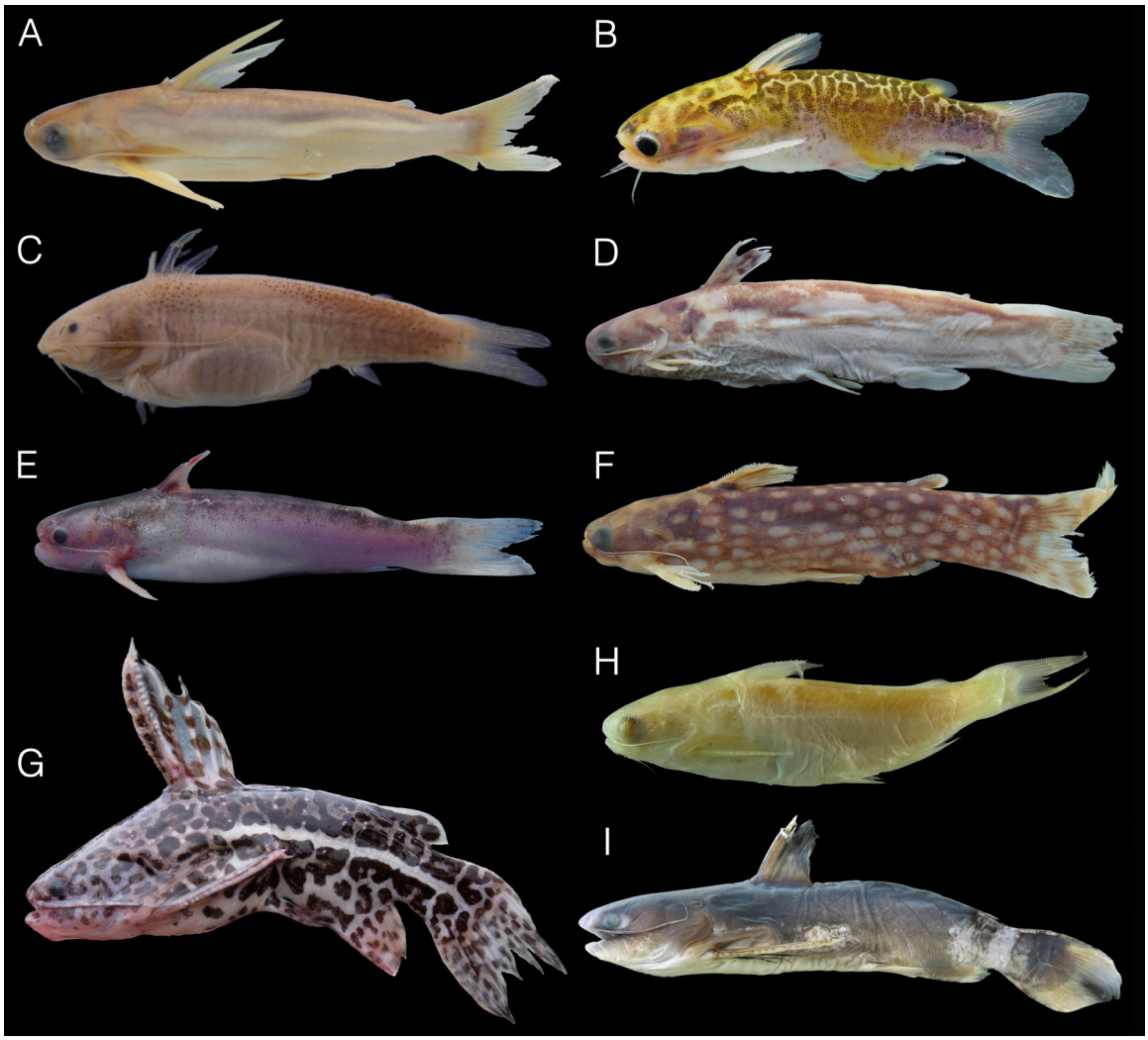

Fig. 1. Representative species in Auchenipteridae. A. *Centromochlus heckelii*, MCNG 23921, 78.5 mm SL. B. *Tatia perugiae*, INPA uncatatogued, 36.0 mm SL. C. *Gelanoglanis stroudi*, MBUCV-V 27965, 24.0 mm SL. D. *Gephyromochlus leopardus*, ZMA 105.854, 103.0 mm SL. E. *Glanidium albescens*, DZUFMG uncatalogued, 110.0 mm SL. F. *Tatia intermedia*, ZMA 105.791, 74.2 mm SL. G. *Liosomadoras oncinus*, MZUSP 105828, 98.0 mm SL. H. *Pseudotatia parva*, FMNH 70580, 47.2 mm SL, holotype. I. *Tocantinsia piresi*, UFOPA, uncatalogued, 120.0 mm SL.

RESULTS

Phylogenetic reconstruction.—The Tree-Bisection-Reconnection (TBR) heuristic search algorithm resulted in two most parsimonious trees, each with 202 steps, CI 0.69 and RI 0.93 (see Fig. 26). The new classification for Centromochlinae is summarized in Table 1.

CHARACTER DESCRIPTIONS AND INTERPRETATIONS

External morphology.—Characters 0–11 pertain to various externally visible features.

0. *Mouth, shape* (CI 1.0, RI 1.0). State 0: mouth gape straight (Figs. 2A,B,D,E,F); state 1: mouth gape sinuous (Fig. 2C). The derived condition is unique to *Gelanoglanis* wherein the sinuous gape is limited by a free fleshy flange around its angle (Figs. 1C, 2C; Curran, 1989: #22). In all other species the mouth gape is straight, with a short fold at its angle. The somewhat sinuous mouth of *Gelanoglanis* was first noticed by Böhlke (1980: 151) in his description of *Gelanoglanis stroudi*. The same feature is present in all congeners, as described by Soares Porto et al. (1999), Rengifo et al. (2008) and Calegari et al. (2014). No other centromochlins exhibit such an unusual mouth shape.

1. *Olfactory rosette in posterior nare, size* (CI 1.0, RI 1.0). State 0: small, posterior nare opening similar in size as anterior one (Figs. 2A,B,D,E,F); state 1: large with well-developed lamellae, posterior nare opening enlarged (Fig. 2C). In all species of *Gelanoglanis* the posterior nasal cavity is enlarged to shelter a well-developed olfactory rosette. The nasal cavity is lined with the olfactory epithelium, organized into a series of lamellae appearing as a rosette. The arrangement, shape and degree of development of the lamellae in the olfactory rosette vary considerably among fishes (Hara, 1994). As Centromochlinae catfishes are active at night, *Gelanoglanis* may use olfactory signals during feeding (F.C.T. Lima, pers. comm.). Böhlke (1980: 150) noted the enlargement of posterior nare opening as a diagnostic feature of *Gelanoglanis*.

2. *Eye socket, depth* (CI 1.0, RI 1.0). State 0: eye depth 30–45% head width (Fig. 2D); state 1: eye depth more than 60% head width (Fig. 2A). Derived condition synapomorphic for *Centromochlus*. Extremely large ventrolateral eye occupying almost entire head depth is noticed in *Centromochlus* and *Tympanopleura* (Calegari et al., 2019: #3491). The depth of the eye socket is associated with eye mobility; features linked with the size of the visual field (Collin & Shand, 2003). In the Auchenipteridae, the eye is lateral, generally situated below the cranial border and protected by a cranial roof (Britski, 1972). The ventrolateral placement of the eye in species of *Centromochlus* may be an adaptation for swimming close to the surface in pelagic habits, a behavior reported for species *C. heckelii* and *C. existimatus* (Sazima et al., 2005).

3. *Eye, size* (unordered; CI 0.67, RI 0.90). State 0: intermediate to large, more than 20% HL (Figs. 2D, E, F); state 1: small, about 15% HL (Fig. 2B); state 2: very small, less than 10% HL (Fig. 2C). State 1 present in *Tatia meridionalis* and *T. ferrarisi*. State 2 synapomorphic for *Gelanoglanis*. This multistate character is left unordered because there is no obvious transformational series.

4. *Adipose fin* (CI 1.0, RI 1.0). State 0: present (Figs. 3A,B,D,E,G,H); state 1: absent (Fig. 3F). Adipose fin is absent in *Tatia britskii*. Anatomical and phylogenetic evidence suggest that the adipose fin has multiple origins in teleost fishes (Stewart et al., 2014). To attribute functions to the adipose fin is a complex task given its diversity in size, position and composition. Evolutionarily, an adipose fin is typically present in most catfish families, including Auchenipteridae and Doradidae, although absent in their closest relative Aspredinidae (Friel, 1994: #126; Cardoso, 2008: #125). The absence of an adipose fin has been interpreted as derived within the auchenipterins *Epapterus, Trachelyichthys, Trachelyopterichthys,* and *Trachelyopterus coriaceus* (Ferraris, 1988: #O2; Curran, 1989: #12; Royero, 1999: #143; Akama, 2004: #186; Birindelli, 2014: #4). The absence of an adipose fin is stated as a derived character for the same auchenipterins plus all members of the Aspredinidae in the analysis by Calegari et al. (2019), but the authors did not examine *Tatia britskii*. This character was coded as inapplicable for species of *Gelanoglanis* in which an adipose fin fold is present and interpreted as distinct (see character 5). The extremely reduced adipose fin in *Tatia simplex,* much smaller than in all other species (Mees, 1974: 93), is an independent distinctive condition (see character 6).

5. *Adipose fin fold* (CI 1.0, RI 1.0). State 0: present in larva or post-larva only (for early ontogeny images of centromochlins see Nakatani et al., 2001; Pereira et al., 2017; Santos et al., 2017); state 1: retained in adults (Fig. 3C). An adipose fin fold is retained in adult *Gelanoglanis nanonocticolus*, *G. pan* and *G. varii*, and likely represents a paedomorphic feature. In other ostariophysan fishes, the development of the adipose fin is characterized by an outgrowth after the complete reduction of the larval fin fold (Stewart et al., 2014). During development of *Tatia neivai*, the adipose fin fold appears after the notochord

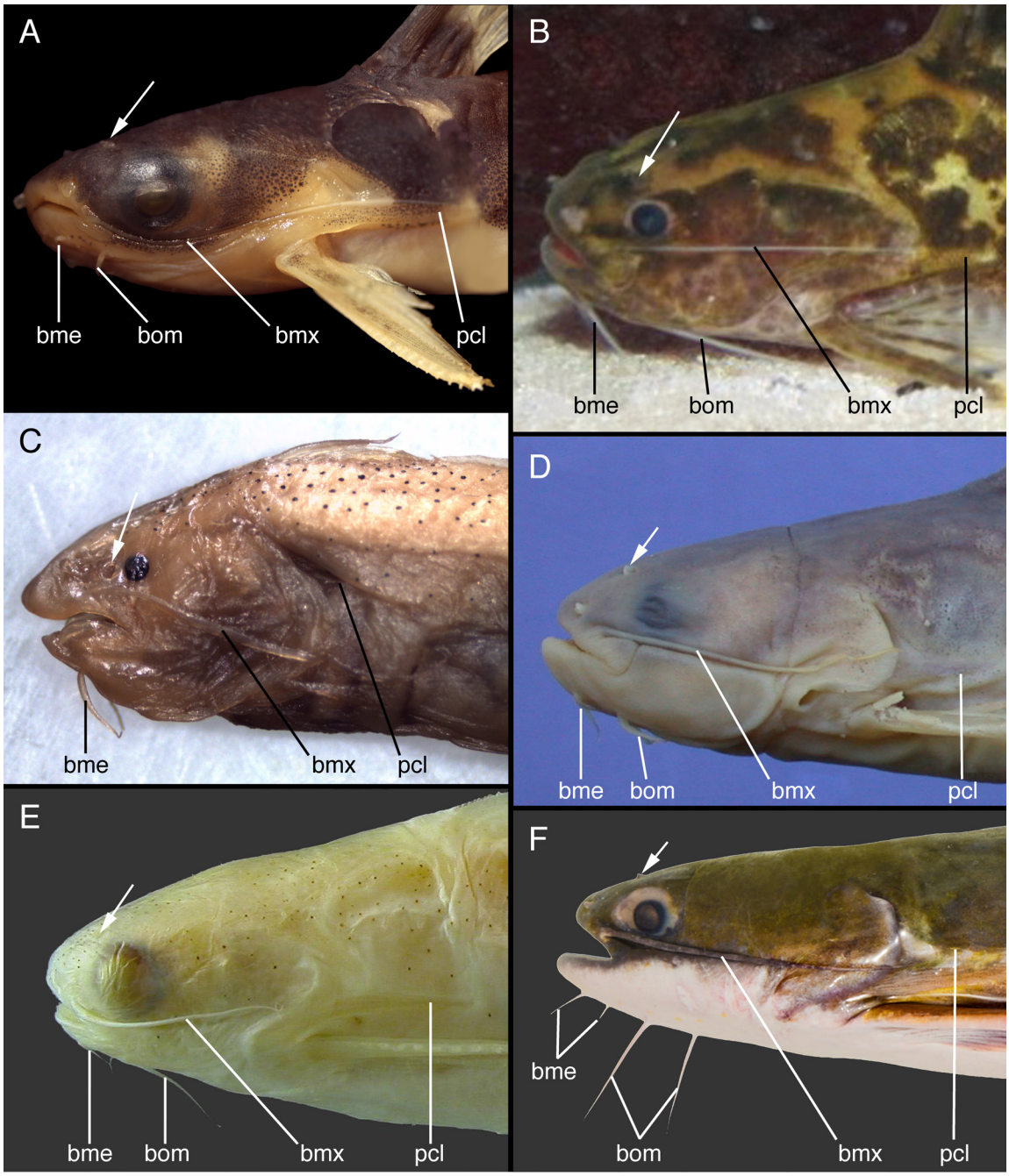

Fig. 2. Head in left lateral view. A. *Centromochlus orca*, INPA 35086, 53.8 mm SL. B. *Tatia meridionalis*, INPA 37893, 46.0 mm SL. C. *Gelanoglanis* cf. *pan*, INPA 12419, 20.1 mm SL. D. *Glanidium botocudo*, DZUFMG 047, 95.2 mm SL, paratype. E. *Pseudotatia parva*, FMNH 70580, 47.2 mm SL, holotype. F. *Tocantinsia piresi*, CAS 6573, holotype of *Tocantinsia depressa*. Abbreviations: bmx, maxillary barbel; bom, lateral mental barbel; bme, mental barbel; pcl, postcleitral process. Arrow indicates posterior nasal opening.

flexion stage and persists until larval stage (specimens <10 mm SL; Nakatani et al., 2001). In *Gelanoglanis nanonocticolus* and *G. pan*, the adipose tissue forms a thin skin fold; both keep a post anal fin fold in adults. An adipose preceded by a thin, long skin ridge is stated by Calegari et al. (2019: #3494) as a derived feature in *Gelanoglanis nanonocticolus*, *Gelanoglanis varii* and the doradids *Rhinodoras* and *Megalodoras*. Coded as inapplicable for *Tatia britskii*, the only centromochlin that lacks an adipose fin.

6. *Adipose fin, size* (unordered; CI 1.0, RI 1.0). State 0: normally developed, 5.8–11.2% SL (Fig. 3G); State 1: small, 2.5–4.0% SL (Fig. 3A); state 2: reduced, 1.3–2.0% SL (Fig. 3F). State 1 is synapomorphic for *Centromochlus* and present in all eight species: *C. carolae, C. musaicus, C. existimatus, C. heckelii, C. macracanthus, C. melanoleucus, C. schultzi, and C. orca*. State 2 (reduced) is in *T. simplex*. The condition in *Gelanoglanis* in which fin fold substitutes adipose fin (Fig. 3C) was coded as inapplicable (-). Absence vs. presence of adipose fin included in character 4.

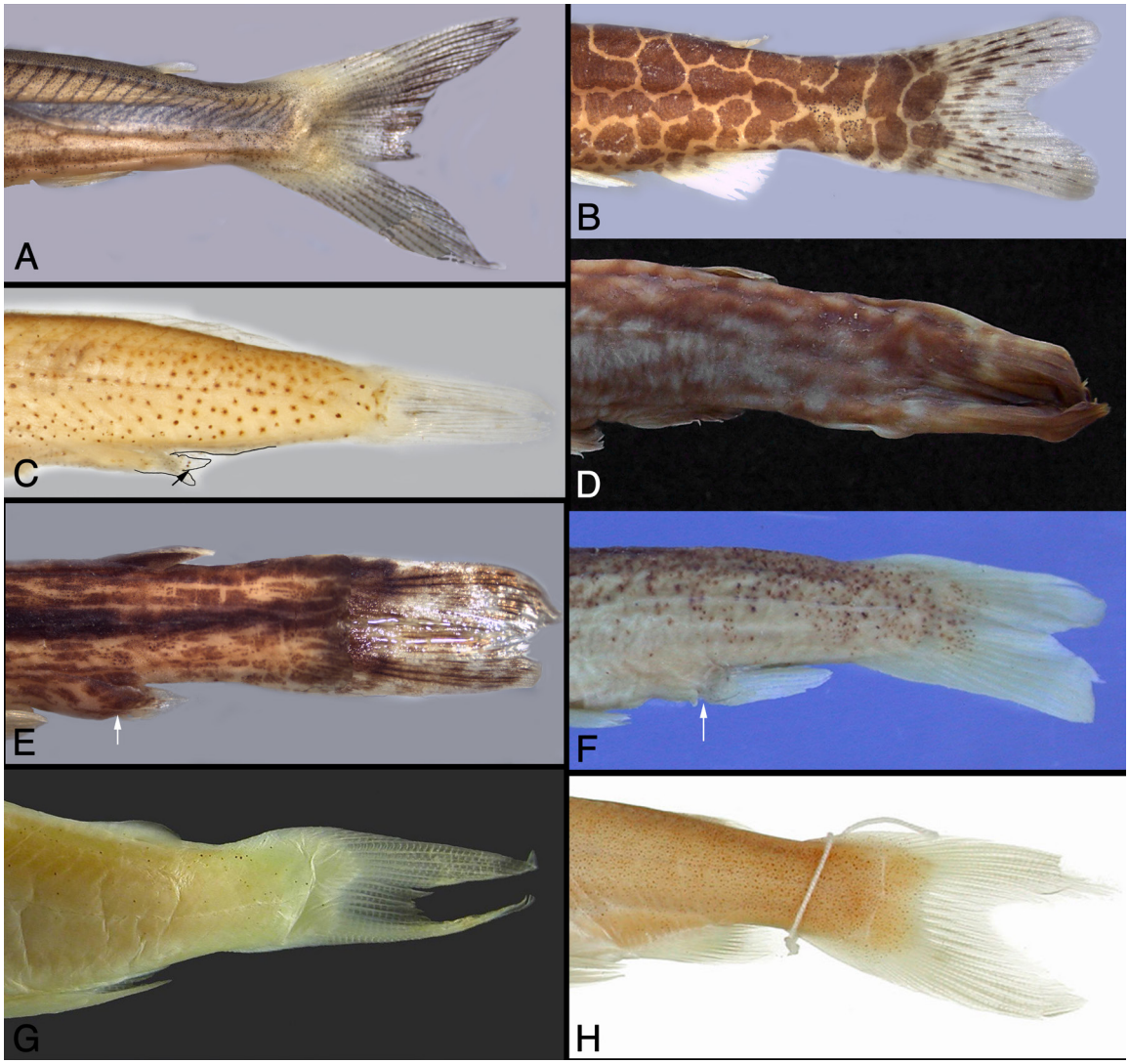

Fig. 3. Caudal peduncle in lateral view. A. *Centromochlus existimatu*s INPA 40662, 59.0 mm SL. B. *Tatia reticulata*, INPA 35394, 28.8 mm SL. C. *Gelanoglanis nanonocticolus*, MZUSP 28308, 16.8 mm SL. D. *Tatia aulopygia*, INPA 11078, 76.2 mm SL. E. *Tatia gyrina*, INPA 20970, 36.2 mm SL. F. *Tatia britskii*, MZUSP 43251, 38.6 mm SL, holotype. G. *Pseudotatia parva*, FMNH 70580 47.2 mm SL, holotype. H. *Tocantinsia piresi*, CAS 6573, Holotype of *Tocantinsia depressa* Mees 1974. Arrow indicates position of urogential papilla.

7. *Caudal peduncle, shape* (CI 1.0, RI 1.0). State 0: caudal peduncle cylindrical (Figs. 3A–C, F–H); state 1: caudal peduncle compressed immediately posterior to adipose fin, forming a tall middorsal keel (Figs. 3D–E). Synapomorphic for ten species of *Tatia*: *T. aulopygia*, *T. boemia, T. brunnea*, *T. caudosignata*, *T. dunni, T. galaxias, T. intermedia, T. jaracatia, T. neivai, T. nigra* and *T. strigata*. Hypothesized as synapomorphic for *Tatia* by Soares-Porto (1998: #25) and Sarmento-Soares & Martins-Pinheiro (2008), but condition herein restricted to certain species of *Tatia*.

8. *Papilla-like tubercles on ventral surface of head in mature males* (CI 1.0, RI 1.0). State 0: absent; state 1: present. Derived condition unique to *Gelanoglanis nanonocticolus*, *G. pan* and *G. varii* (Figs. 4 A,B). Papillae are not common structures among siluriforms, although reported in other genera of auchenipterids such as *Auchenipterus* spp. and *Trachelyopterus insignis* (Ferraris & Vari, 1999). Species of the auchenipterin genus *Pseudauchenipterus* have papilla-like tubercles in the tympanic region (Royero, 1999: #148; Akama, 2004: #183; Birindelli, 2014: #29), but not on the ventral surface of head. The nature of papillae, ducts and gonads vary among centromochlin species, giving way to unique morphological conditions associated with breeding and insemination. Nuptial males of the aforementioned *Gelanoglanis* exhibit secondary sexually dimorphic features such as gular papillae, a filamentous unbranched pectoral-fin ray and a falcate pelvic-fin margin. Other centromochlins do not have such secondary dimorphic features, and primary dimorphic changes are limited to inseminating male modified anal fin.

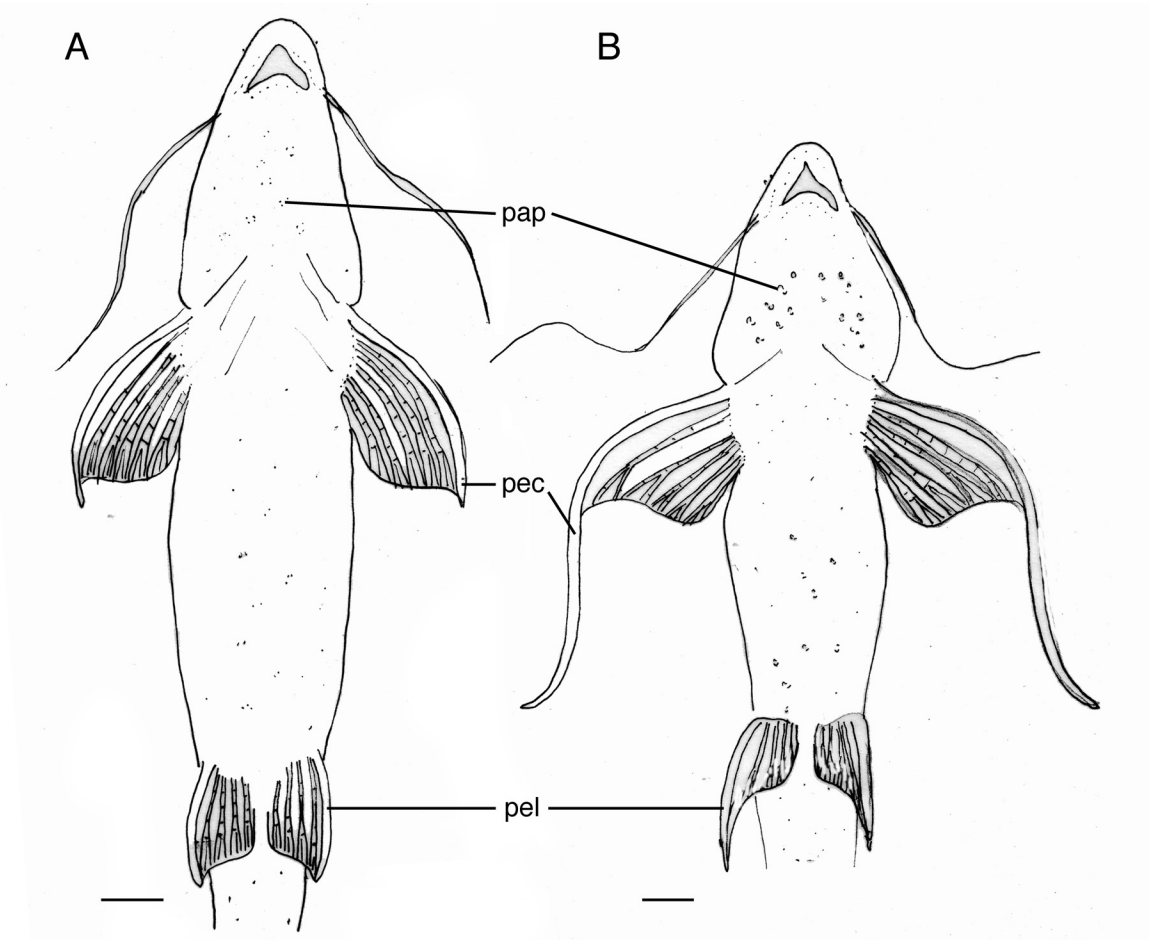

Fig. 4. Ventral view of body illustrating sexual dimorphism in *Gelanoglanis nanonocticolus*, MZUSP 81212: A. female, 23.3 mm SL. B. male, 20.5 mm SL. Abbreviations: pap, gular papillae (much concentrated in male); pec, pectoral fin, filamentous in male; pel, pelvic fin, falcate in male. Mental barbels omitted. Scale bar = 2 mm.

9. *Mental barbels, size* (CI 1.0, RI 1.0). State 0: mental barbels moderately reduced, length 50% of outer mental barbel; state 1: both mental barbels extremely reduced, length 13% of outer mental barbel (Birindelli, 2014: #19; Calegari et al., 2019: #3508). Derived condition exhibited by *Centromochlus existimatus* and *C. heckelii*. In fishes, barbels are skin appendages for taste and/or mechanoreception, with variable construction between species and occupying multiple areas of the jaws, lips and/or head (LeClair & Topczewski, 2010). Birindelli (2014: #19) referred to the relative lengths of the inner and outer mental barbels. In *C. existimatus* and *C. heckelii,* both mental barbels are extremely reduced, differing from the usual condition observed in most centromochlins in which the medial mental barbel is about half the size of the lateral mental barbel (Soares-Porto, 1998). This character was coded as inapplicable (-) for *Gelanoglanis* which lacks the lateral pair of mental barbels.

10. *Mental barbels, number of pairs* (CI 1.0, RI 1.0). State 0: two pairs (Figs. 2A,B,D–F); state 1: one pair (Fig. 2C; Ferraris, 1988: #J19; Curran, 1989: #23; Birindelli, 2014: #16; and Calegari et al., 2019: #3504). All species of *Gelanoglanis* have a single pair of mental barbels interpreted as the medial pair. Böhlke (1980) considered this condition to be diagnostic of *Gelanoglanis*.

11. *Papillae along maxillary barbel* (CI 1.0, RI 1.0). State 0: absent, maxillary barbel not modified; state 1: present anterolaterally, appearing as regularly arranged bumps. Derived condition observed in *Gelanoglanis nanonocticolus*, *G. pan* and *G. varii*. Calegari et al. (2014) noticed soft papillae arranged in a single discrete row along the length of the maxillary barbel in both juveniles and adults of *G. pan*. Soft papilla on maxillary barbel is stated as a derived feature by Clagari et al. (2019: #3502). The barbels of mature males develop sexually dimorphic breeding tubercles in some species of Auchenipterinae, especially *Auchenipterus, Entomocorus, Pseudepapterus, Epapterus* and *Tetranematichthys* (Ferraris & Vari, 1999; Akama, 2004: #177; Birindelli, 2014: #25). The maxillary barbel tubercles arranged in regular bumps is an apomorphic feature uniquely observed in *Gelanoglanis nanonocticolus* and *G. pan*, and treated as a synapoporphy for these two sister species. The association of papillae with sexual dimorphism deserves further investigation.

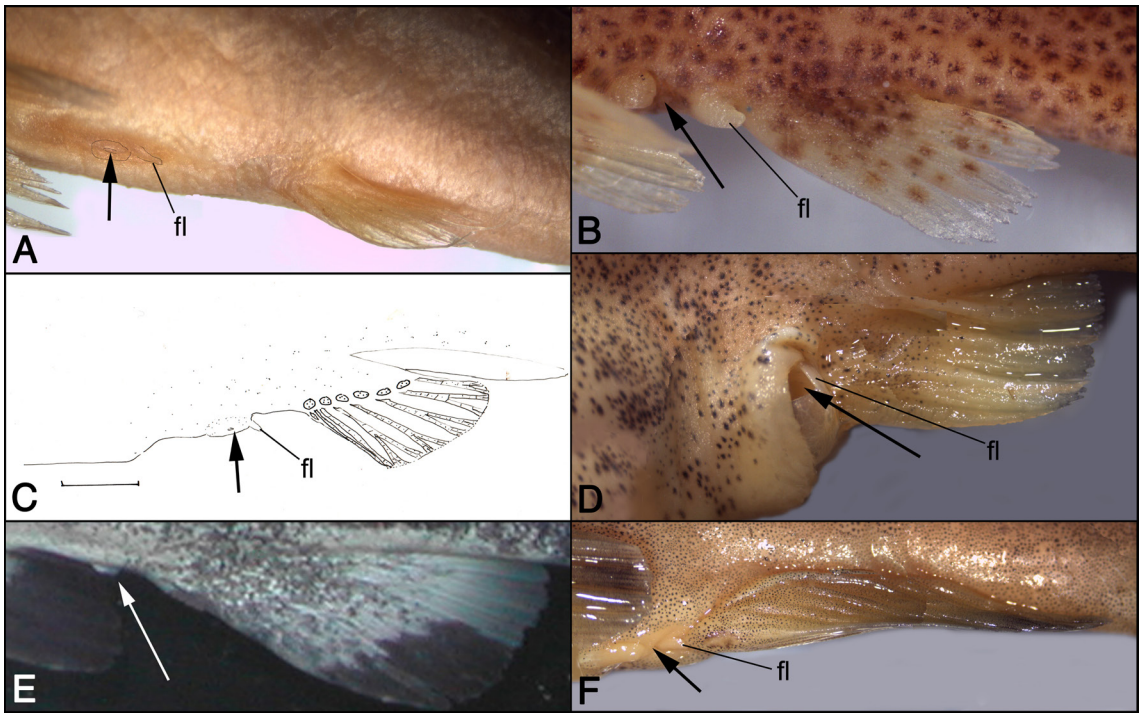

Fig. 5. Lateral view of female genital papilla. A. *Centromochlus heckelii*, INPA 12643, 90.1 mm SL. B. *Tatia romani*, MCNG 14896, 29.0 mm SL. C. *Gelanoglanis nanonocticolus*, MZUSP 81524, 25.3 mm SL. D. *Glanidium albescens*, MCNIP 1084, 111.3 mm SL. E. *Tocantinsia piresi,* aquarium specimen. F. *Tatia nigra*, INPA 43876, 100.5 mm SL. Abbreviations: fl, skin flap. Arrow indicates genital opening.

Reproductive system.—Characters 12–20 pertain to a variety of sexually dimorphic features associated with reproduction by insemination, a strategy unique to Auchenipteridae among catfishes. Insemination has been documented via aquarium observations and is inferred to be synapomorphic for Auchenipteridae based on morphological studies (Akama, 2004; Birindelli, 2014). In males, the testes consist of two chaplets of fringed testicular lobes, whereas in females the ovaries are sac shaped (Loir et al., 1989). Thus, sexual determination is relatively easy in most auchenipterid catfishes. Furthermore, inseminating features in centromochlin catfishes are likely transitory (Franke, 1990), limited to the reproductive season, and therefore rarely observed. Sperm storage in bundles are reported for some centromochlin species, and possibly all these catfishes are inseminating, although seminal vesicles are not evident as in other inseminating auchenipterid catfishes (Loir et al., 1989; Mazzoldi et al., 2006).

12. *Female urogenital papilla flap* (CI 1.0, RI 1.0). State 0: flap absent (Fig. 5E); state 1: flap present (Figs. 5 A–D,F). Although not easily observed, some auchenipterid females develop a genital papilla as they mature, and a flap is associated with papilla in most centromochlin catfishes. In *Pseudotatia parva* and *Tocantinsia piresi* (Fig. 5E) such a flap is absent.

13. *Female urogenital papilla, size of flap* (CI 0.20, RI 0.43). State 0: thin flap; state 1: thick flap around genital duct (Fig. 5D). In most centromochlins a thin skin flap is observed (Figs. 5A–C). In *Centromochlus* and *Gelanoglanis*, the female genital papilla is oval (see Fig. 5A for *C. heckelii* and Fig. 5C for *G. nanonocticolus*) or slit-like (e.g., *C. musaicus*), with a thin flap associated with genital duct. We assume ripe females develop an oval genital papilla that becomes slit-like after insemination. State 2 observed in *Glanidium albescens* (Fig. 5D) and *G.*

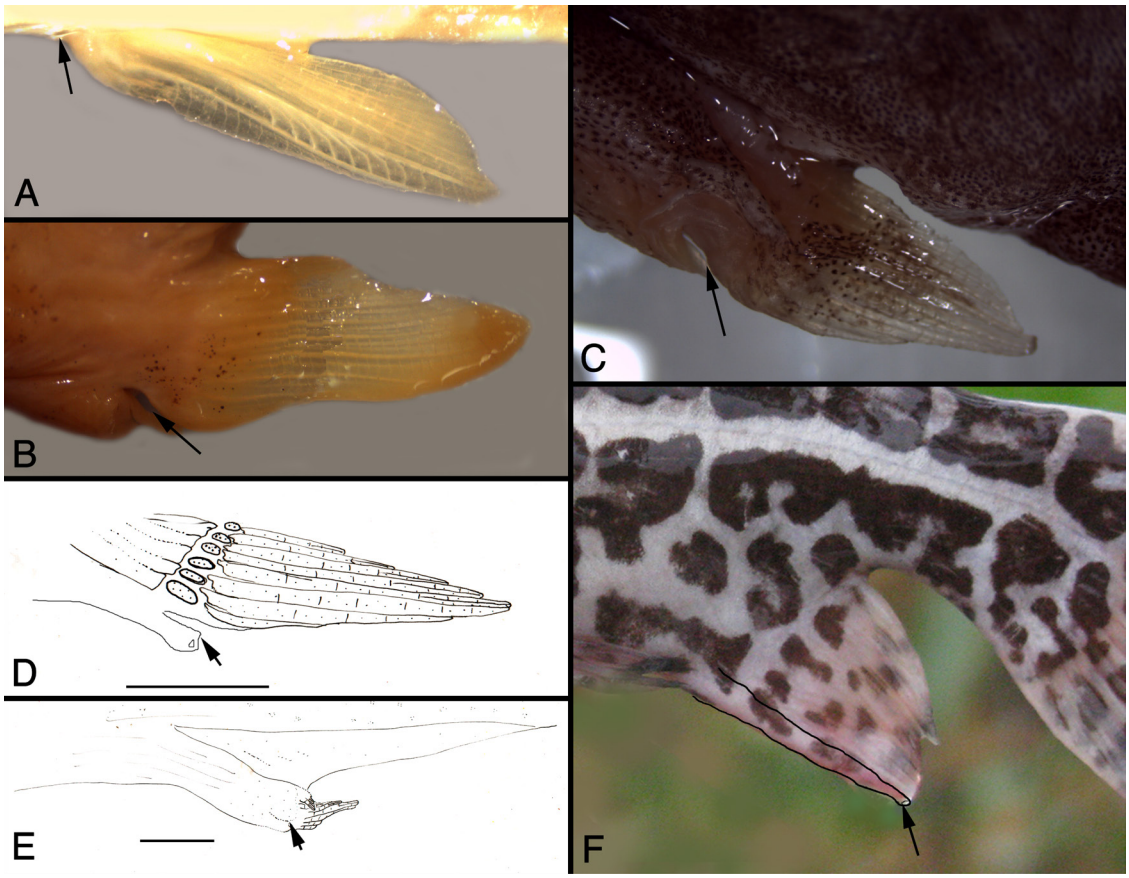

Fig. 6. Left lateral view of male urogenital papilla. A. *Centromochlus heckelii*, MZUSP 57643, 80.1 mm SL. B. *Glanidium botocudo*, MNRJ 32538, 93.2 mm SL, holotype. C. *Tatia intermedia*, INPA 47933, 124.0 mm SL. D. *Gelanoglanis stroudi*, ANSP 142938, 36.6 mm SL. E. *Gelanoglanis nanonocticolus*, MZUSP 81212, 20.5 mm SL. F. *Liosomadoras oncinus*, MZUSP 105828. Arrow indicates genital opening.

botocudo. Ripe specimens have a bulging abdomen, soft to the touch. A thick flap around genital duct is uniquely observed in females of some *Glanidium*. In *Pseudotatia parva* and *Tocantinsia piresi* the flap is absent (-).

14. *Shape of female urogenital opening* (CI 0.50, RI 0.95). State 0: rounded; state 1: slit-like (Fig. 5F). Derived condition found in *Tatia,* and independently acquired in *Centromochlus existimatus* and *C. heckelii*. Our observations on reproductive specimens showed a slit-like urogenital opening in *Tatia*, which differs from the rounded opening characteristic of remaining auchenipterids (compare Figs. 5A–D with Birindelli, 2014: fig. 19). In some *Tatia* species a slit-like opening is accompanied by an intumescent papilla (see character #16). A slit-like shallow papillae is independently acquired in *C. existimatus* and *C. heckelii*.

15. *Position of male urogenital opening* (CI 1.0, RI 1.0). State 0: opening at anterior distal end of anal fin (Fig. 6F); state 1: opening at anterior base of anal fin (Figs. 6A–E). State 0 in *Pseudotatia parva*. In Auchenipterinae, the genital papilla forms a tube attached to the anterior border of the anal fin and the urogenital opening is displaced towards the distal end of the last unbranched fin ray (Fig. 6F; Birindelli & Zuanon, 2012). The condition diagnostic for Centromochlinae, in which the urogenital opening emerges from anterior base of anal fin, is considered synapomorphic (Ferraris, 1988: #A4; Curran, 1989: #18; Soares Porto, 1998: #29; Reis & Borges, 2006; Birindelli, 2014: #46; Calegari et al., 2019: #3736).

16. *Male urogenital papilla, thickness* (CI 1.0, RI 1.0). State 0: simple (Fig. 6A); state 1: swollen (Fig. 3E). Among centromochlins a swollen urogenital papilla is only observed in *Tatia caxiuanensis, T. gyrina*, and *T. meesi* (Fig. 3E; Soares-Porto, 1998: #32). In these three species, the swollen urogenital papilla is possibly restricted to nuptial males.

17. *Mature male deferent duct skin flap* (CI 0.50, RI 0.67). State 0: present (Figs. 6 B–E); state 1: absent (Fig. 6A). The skin flap of deferent duct in mature males is absent in *Centromochlus heckelii* and *C. existimatus*, and independently lost in *Tatia dunni* and *T. brunnea*. In most centromochlin catfishes, the deferent duct is protected by a skin flap.

18. *Testicular lobes, shape* (CI 1.0, RI 1.0). State 0: filiform (Figs. 7B–E); state 1: rounded (Fig. 7A). Derived condition found in *Centromochlus existimatus*, *C. heckelii* and *C. macracanthus*. In Siluriformes,

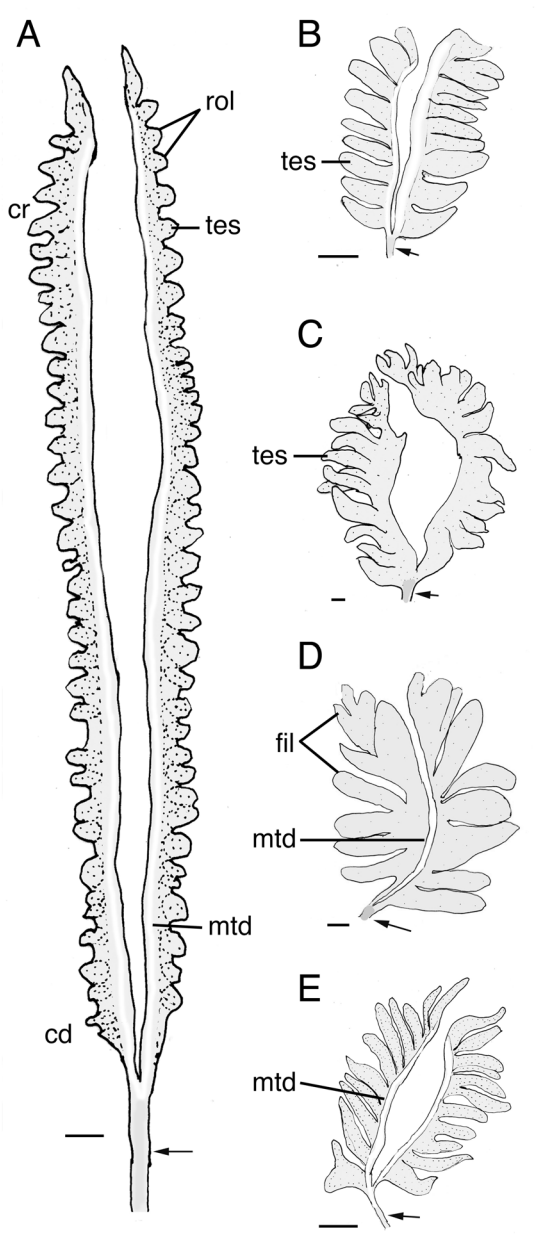

Fig. 7. Ventral view of male reproductive apparatus. A. *Centromochlus heckelii*, MZUSP 83268, 80.2 mm SL. B. *Tatia reticulata*, MNRJ 30492, 30.8 mm SL. C. *Glanidium ribeiroi*, MZUSP 45044, 82.2 mm SL. D. *Glanidium albescens*, MCNIP 1084, 23.9 mm SL. E. *Tatia caxiuanensis*, MPEG 6201, 30.2 mm SL, paratype, cs. Abbreviations: cr, cranial region; cd, caudal region; fil, filiform testicular lobes; mtd, main testicular duct; rol, rounded testicular lobes; tes, testis. Arrow indicates spermatic duct. Scale bar =1 mm.

testes are generally formed by tufts of irregular filiform spermatogenic lobes along a deferent duct (Britski, 1972: 34). Coded as missing data for *Pseudotatia parva, Tatia concolor*, *T. marthae* and *T. punctata* as there were no specimens available for dissection.

19. *Testicular lobes, coalescence* (CI 1.0, RI 1.0). State 0: testis with separate, individualized lobes (Figs. 7A–C,E); state 1: testis with coalesced lobes (Fig. 7D). Individualized lobes are observed in testis of *Glanidium ribeiroi* (Fig.7C) and the remaining Centromochlinae. *Glanidium albescens*, *G. botocudo*, and *G. cesarpintoi* have coalesced, fused testicular lobes (Fig. 7D). The variability observed in the number and the relative development of fringes in multilobular testis might be indicative of interspecific differences in the sexual activity (Meisner et al., 2000).

20. *Testicular lobes, relative size* (CI 0.33, RI 0.91). State 0: irregular, with distinct sizes (Figs. 7C,D); state 1: regular testicular lobes, each of about same size (Figs. 7B,E). The testicular lobes are foliated and regularly shaped in *Centromochlus existimatus* and *C. heckelii* (Fig. 7A) and all species of *Tatia* except *T. bockmanni*, *T. britskii*, and *T. simplex*. Irregular, thick lobes of varied morphology observed in the testes of the Auchenipterinae (Meisner et al., 2000; Mazzoldi et al., 2007; Melo et al., 2011). Although difficult to examine, the thin lobes regularly arranged along the main duct of the testis needs further investigation to understand its function.

Neurocranium.—Characters 21–30 pertain to certain neurocranial bones and associated fontanels.

21. *Mesethmoid length/width I* (CI 1.0, RI 1.0). State 0: width equal to or greater than length (Figs. 8A–C, 9C,D); state 1: width approximately half of length (Fig. 8D). The general condition in auchenipterids is a large mesethmoid, observed in demersal fishes such as *Tocantinsia piresi*. State 1 is synapomorphic for pelagic *Gelanoglanis*. The mesethmoid width is reduced in pelagic juveniles of *Centromochlus*, such as *C. musaicus* and *C. orca*, and interpreted as independent acquisition for those two species.

22. *Mesethmoid length/width II* (CI 0.50, RI 0.67). State 0: length moderate to long, greater than about 75% of width (Fig. 8A); state 1: length extremely short, about 50% of width (Figs. 8C). State 1 in *Tatia perugiae*, *T. altae*, *T. romani*, and independent acquired in *Tatia gyrina*. *Tatia gyrina* (Soares-Porto, 1998; Sarmento-Soares & Martins-Pinheiro, 2008) has a short mesethmoid and its condition is interpreted as non-homologous relative to that observed in *Tatia perugiae*, *T. altae*, and *T. romani*.

23. *Anterior cranial fontanel opening* (CI 0.50, RI 0.50). State 0: open, replacing anterior suture between frontals (Figs. 8A–C); state 1: completely occluded, frontals sharing complete suture (Fig. 8D; Calegari et al., 2019: #3539). State 0 is present in all Centromochlinae, with exception of *Gelanoglanis*. State 1 interpreted as a synapomorphy of *Gelanoglanis,* with a reversal in *Gelanoglanis pan*. In small adults (< 25 mm SL) of *G. pan*, the cranial fontanel opening is round and bordered by frontals (Birindelli, 2014: #56; Calegari et al., 2014). In *Gelanoglanis stroudi*, *G. nanonocticolus, G. travieso,* and *G. varii* the anterior cranial fontanel is completely occluded in adults and the frontals are conjoined along their entire medial margin (Ferraris, 1988: #N6; Soares- Porto, 1998: #6; Soares-Porto et al., 1999).

24. *Anterior cranial fontanel position* (CI 0.33, RI 0.33). State 0: anterior cranial fontanel located between mesethmoid and frontals (Figs. 8A,B); state 1: anterior cranial fontanel located between the frontals (Fig. 8C; Soares-Porto, 1998: #6; Calegari et al. 2019: #3541). The anterior cranial fontanel limited to frontals is interpreted to have evolved independently in three centromochlin lineages: *Gelanoglanis pan, Tatia aulopygia* and the clade comprising *Tatia altae* and *T. perugiae*. Within the Auchenipterinae, a cranial fontanel between frontals is observed in *Liosomadoras oncinus* (Birindelli & Zuanon, 2012). The character is inaplicable in *Gelanoglanis stroudi, G. nanonocticolus* and *G. travieso,* species in which cranial fontanel is occluded.

25. *Posterior cranial fontanel* (CI 1.0, RI 1.0). State 0: Anterior cranial fontanel a continuous opening (Fig. 9A); state 1: posterior cranial fontanel present (Fig. 9B; Calegari et al., 2019: #3540). The anterior and posterior cranial fontanels are separated by an epiphyseal bar in *Glanidium albescens*, *G. botocudo* and *G. cesarpintoi* (Fig. 9B; Royero, 1999: #3; Akama, 2004: #12, #13, #14; Sarmento-Soares & Martins-Pinheiro, 2013: fig. 2; Birindelli, 2014: #57). Birindelli (2014: #57) coded this character as polymorphic for *Tatia* and *Centromochlus*, and our observations corroborate polymorphism in *T. meesi, C. existimatus* and *Gephyromochlus leopardus*, which are coded as polymorphic.

Fig. 8. (Page 101) Neurocranium in dorsal view. A. *Centromochlus heckelii*, MNRJ 12135, 50.0 mm SL. B. *Centromochlus musaicus*, MBUCV-V 17727, paratype, 26.8 mm SL. C. *Tatia perugiae*, FMNH 92005. D. *Gelanoglanis stroudi*, ANSP 142940, paratype, 24.8 mm SL. Abbreviations: afo, anterior fontanel; epo, epiotic; epop, epiotic process; fro, frontal; io1, first infraorbital; io5, posterior ossified infraorbital; let, lateral ethmoid; max, maxilla; mes, mesethmoid; nas, nasal; np1, anterior nuchal plate; np2, middle nuchal plate; np3, posterior nuchal plate; pal, palatine; pmx, premaxilla; pto, pterotic; scl, posttemporal-supracleitrum; soc, parietal-supraoccipital; sop, suprapreopercle; sph, sphenotic. Scale bar = 1 mm.

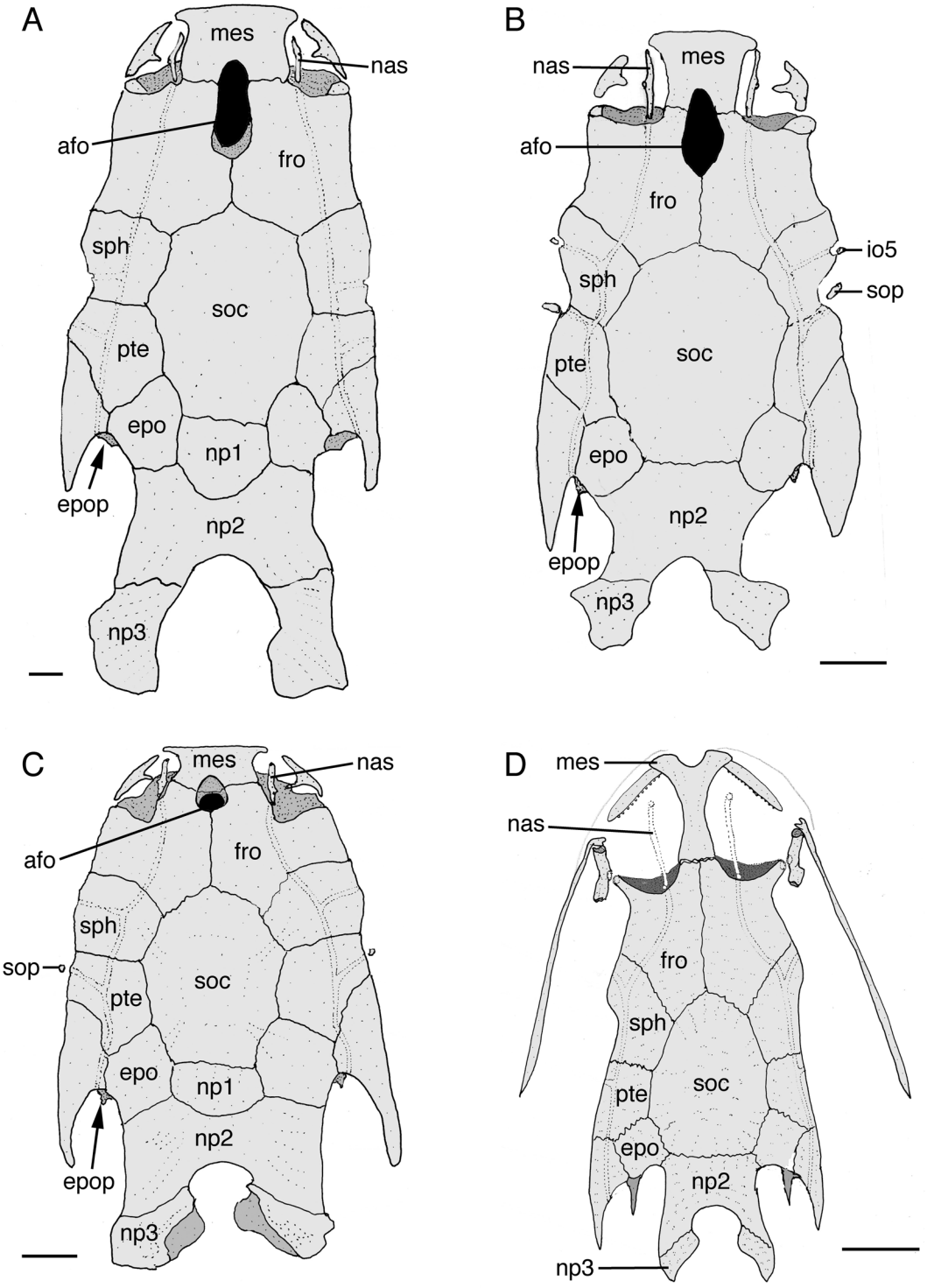
A
mes
nas
afo
fro
sph
soc
pte
epo
np1
epop
np2
np3
B
nas
mes
afo
fro
io5
sop
sph
soc
pte
epo
np2
epop
np3
C
mes
nas
afo
fro
sph
sop
soc
pte
epo
np1
np2
epop
np3
D
mes
nas
fro
sph
soc
pte
epo
np2
np3

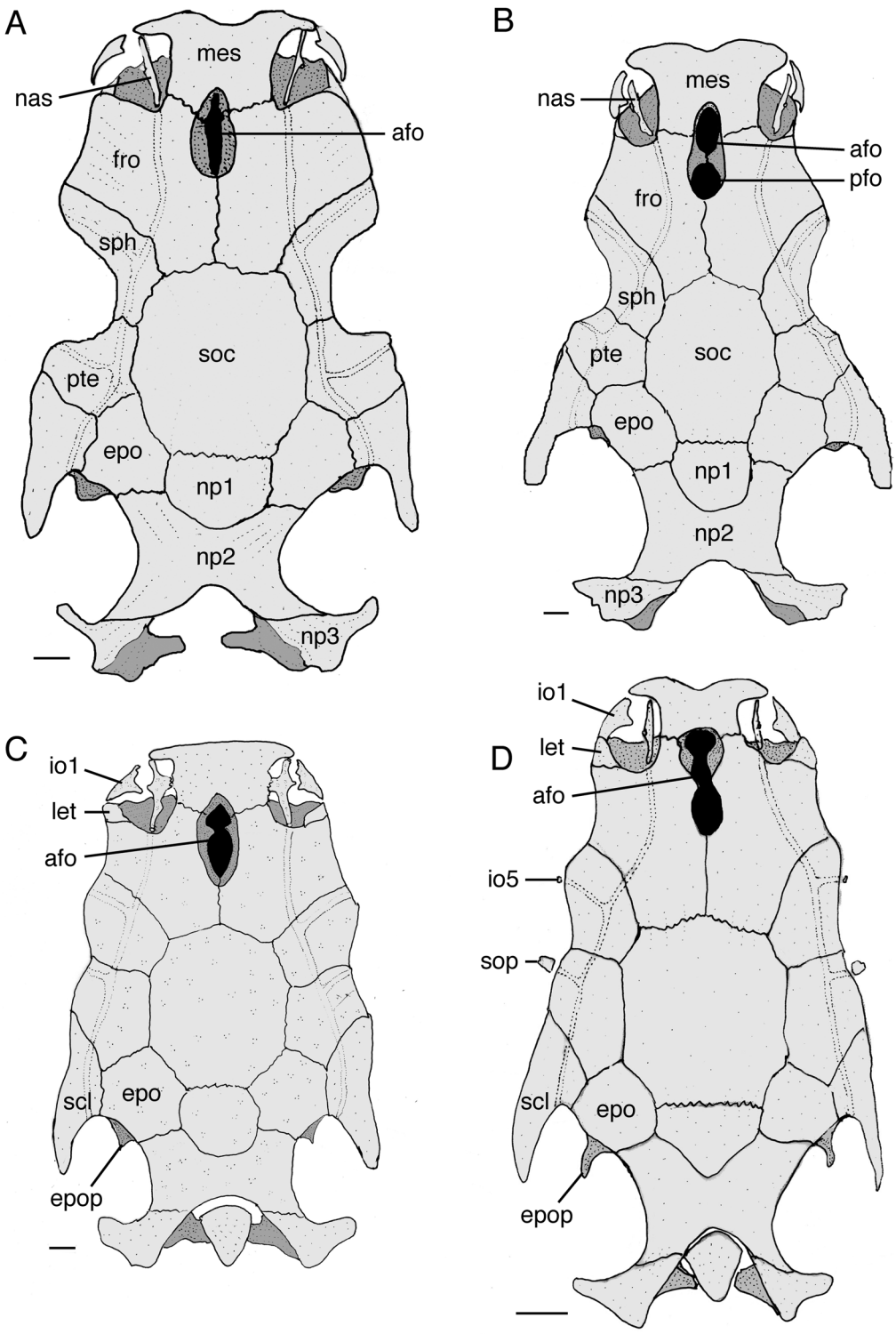
A
mes
nas
afo
fro
sph
soc
pte
epo
np1
np2
np3
B
mes
nas
afo
pfo
fro
sph
pte
soc
epo
np1
np2
np3
C
io1
let
afo
scl
epo
epop
D
io1
let
afo
io5
sop
scl
epo
epop

26. *Sphenotic and pterotic margin notch* (unordered; CI 1.0, RI 1.0). State 0: straight to slightly concave (Figs. 9C,D); state 1: concave (Fig. 9B); state 2: deeply concave (Fig. 9A), sphenotic barely constituting cranial roof (Ferraris, 1988: #N9; Soares-Porto, 1998: #7; Royero, 1999: #20; Akama, 2004: #34; Birindelli, 2014: #63; Calegari et al., 2019: #3552). State 1 is synapomorphic for *Glanidium*; state 2 exhibited by *Gephyromochlus leopardus*. Most centromochlin catfishes have the lateral margin of the cranial roof straight or slightly concave and involving the sphenotic and pterotic to accommodate a well-developed adductor mandibulae (Sarmento-Soares & Porto, 2006). In *Gephyromochlus leopardus,* the adductor mandibulae is extremely thick (Sarmento-Soares & Porto, 2006). The facial muscles also differ among *Gephyromochus*, *Glanidium* and the remaining centromochlins (see characters #131, #132).

27. *Posterior process on epiotic, size* (CI 1.0, RI 1.0). State 0: reduced or short (Figs. 8A,B, 9B); state 1: elongate (Fig. 8D; Ferraris, 1988: #N4; Curran, 1989: #3). In *Gelanoglanis*, the epiotic process is long and spine-like (Fig. 8D). Remaining centromochins have a relatively short epiotic process that in some cases barely emerges from the posterior edge of the skull.

28. *Infraorbital canal exit on sphenotic* (CI 0.50, RI 0.80). State 0: absent, sphenotic border smooth (Figs. 8C,D); state 1: notch present as distinct cavity in sphenotic bone allowing for last infraorbital ossicle attachment (Fig. 8B). The notch is present in *Centromochlus carolae, C. macracanthus, C. melanoleucus, C. musaicus, C. orca* and *C. schultzi*. The derived condition is only present in some species of *Centromochlus*, in which the exit of infraorbital canal is

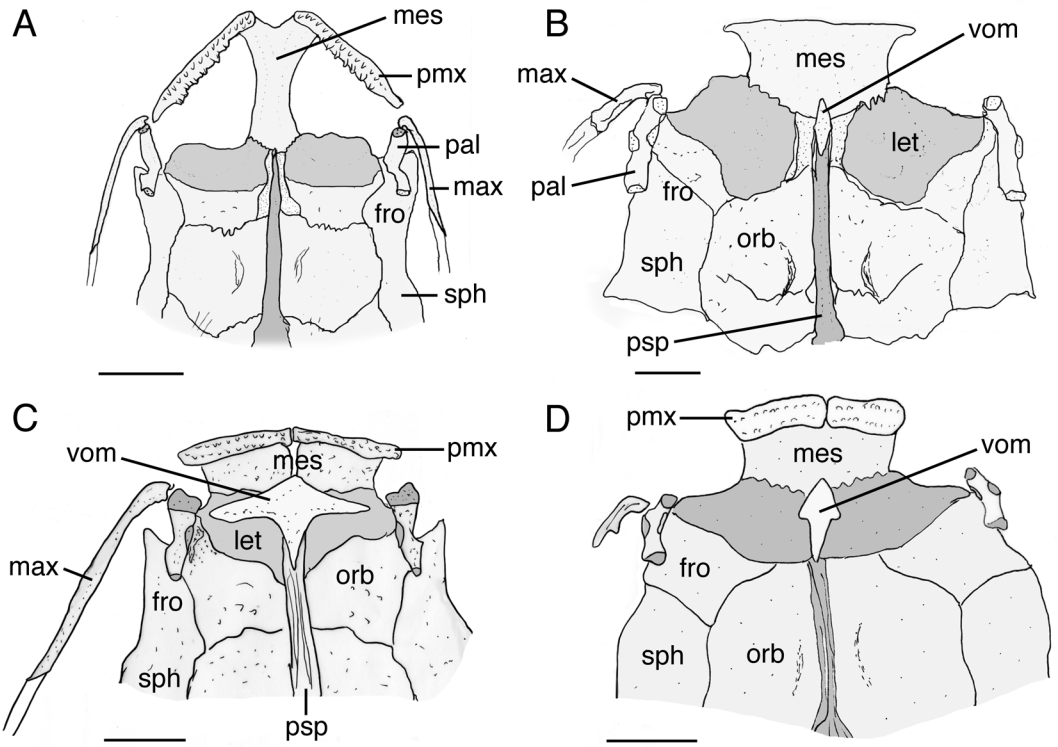

Fig. 10. (Above) Ventral view of anterior portion of neurocranium. A. *Gelanoglanis stroudi*, ANSP 142940, paratype, 24.8 mm SL. B. *Tatia romani,* MCNG 14896, 30.2 mm SL. C. *Centromochlus heckelii,* MZUSP 44128, 70.3 mm SL. D. *Tatia gyrina*, INPA 20971, 28.0 mm SL. Abbreviations: fro, frontal; let, lateral ethmoid; max, maxilla; mes, mesethmoid; orb, orbitosphenoid; pal, palatine; par, parasphenoid; pmx, premaxillary tooth patch; sph, sphenotic; vom, vomer. Scale bar =1 mm.

Fig. 9. (Page 102) Neurocranium in dorsal view: A. *Gephyromochlus leopardus*, ZMA 105.854, 34.8 mm SL, paratype. B. *Glanidium albescens*, MCNIP 1084, 23.9 mm SL. C. *Tatia intermedia*, MZUSP 47504, 40.0 mm SL. D. *Pseudotatia parva*, FMNH 57807, 35.0 mm SL. Abbreviations: afo, anterior fontanel; epo, epiotic; epop, epiotic process; fro, frontal; io1, first infraorbital; io5, posterior ossified infraorbital; let, lateral ethmoid; mes, mesethmoid; nas, nasal; np1, anterior nuchal plate; np2, middle nuchal plate; np3, posterior nuchal plate; pfo, posterior fontanel; pto, pterotic; scl, posttemporal-supracleitrum; soc, parietal-supraoccipital; sop, suprapreopercle; sph, sphenotic. Scale bar = 1 mm.

deeply marked in the sphenotic (Fig. 8B). Independent reduction or loss of notch acquired by the common ancestor of *C. existimatus* and *C. heckelii* (Fig. 8A).

29. *Vomer* (CI 1.0, RI 1.0). State 0: present (Figs. 10B, c); state 1: absent (Fig. 10A). The vomer is absent in *Gelanoglanis* (Ferraris 1988: #N11; Birindelli, 2014: #72; Calegari et al., 2019: #3572), a condition unique among catfishes (Fig. 10A).

30. *Vomer shape* (ordered; CI 1.0, RI 1.0). State 0: T-shaped with paired anterolateral processes (Fig. 10C); state 1: I-shaped with reduced anterolateral processes (Fig. 10D); state 2: lanceolate, lacking rostrolateral processes (Fig. 10B). State 1 present in *Tatia gyrina* and *T. meesi*; state 2 in *Tatia altae, T. perugiae* and *T. romani* (Soares-Porto, 1998: #11; Birindelli, 2014: #73; Calegari et al., 2019: #3573). Most catfishes have a T-shaped vomer with a distinct pair of rostrolateral processes (Lundberg, 1982). However, the vomer is shaped as an "I", with rudimentary lateral processes anteriorly in some auchenipterins such as *Ageneiosus* and *Tetranematichthys* (Britski, 1972; Ferraris, 1988; Walsh, 1990; Akama, 2004; Birindelli, 2014). Coded as inapplicable for *Gelanoglanis* which lacks a vomer (Fig. 10A).

Laterosensory system.—Characters 31–41 pertain to channels and ossifications associated with the cephalic laterosensory system.

31. *Nasal bone ossification* (CI 1.0, RI 1.0). State 0: present (Figs. 8A–C); state 1: absent, nasal canal not ossified (Fig. 8D; Calegari et al., 2019: #3511). Derived condition restricted to *Gelanoglanis* (Fig. 8D) wherein miniaturization and paedomorphic morphological features associated with reduction in body size involve changes in degree of development of the acoustic lateralis system (Soares-Porto et al., 1999; Calegari et al., 2014).

32. *Nasal bone shape* (CI 1.0, RI 1.0). State 0: tubular (Figs. 9A,B); state 1: plate-like (Fig. 9C; Soares-Porto, 1998: #5; Akama, 2004: #91, #93; Sousa, 2010: #20; Birindelli, 2014: #94; Calegari et al., 2019: #3512). A plate-like nasal bone with lateral flanges is a derived condition (Fig. 9C) present in *Tatia* clade A (*T. aulopygia*, *T. boemia*, *T. brunnea*, *T. caxiuanensis*, *T. caudosignata*, *T. dunni*, *T. galaxias*, *T. gyrina*, *T. intermedia*, *T. jaracatia*, *T. meesi*, *T. neivai*, *T. nigra* and *T. strigata*). Catfishes typically have a tubular nasal bone associated with the supraorbital canal, with a lateral branch that is variably ossified (Birindelli, 2014). Coded as inapplicable for *Gelanoglanis* which lacks nasal ossifications.

33. *Points of suture of nasal bone* (CI 1.0, RI 1.0). State 0: none, nasal structured as a free tube (Figs. 9A,B); state 1: sutured to mesethmoid (Fig. 9C). Nasal bone tightly attached to mesethmoid via suture is a derived condition exclusive to *Tatia* clade A (*T. aulopygia*, *T. boemia*, *T. brunnea*, *T. caxiuanensis*, *T. caudosignata*, *T. dunni*, *T. galaxias*, *T. gyrina*, *T. intermedia*, *T. jaracatia*, *T. meesi*, *T. neivai*, *T. nigra* and *T. strigata*). Coded as inapplicable for *Gelanoglanis* which lacks nasal ossifications.

34. *Lateral-line* (CI 0.50, RI 0.83). State 0: developed as a straight line (Fig. 11B); state 1: developed sinuously, at least anteriorly (Figs. 1A; 11A,E). State 1 in *Pseudotatia parva*, *Gelanoglanis*, *Centromochlus heckelii* and *C. existimatus* (Ferraris, 1988: #I12; Akama, 2004: #97; Birindelli, 2014: #115; Calegari et al., 2014). Members of Auchenipterinae, such as *Tocantinsia piresi*, exhibit a straight lateral line. However, in some auchenipterins the lateral line is sinuous, as in *Entomocorus gameroi* and *Liosomadoras oncinus* (Ferraris, 1988: #I12; Akama, 2004: #97). The lateral line canal as a straight tube along the horizontal myoseptum (Ferraris, 1988) is a condition observed in most Centromochlinae. The condition observed in *Gelanoglanis*, *C. heckelii* and *C. existimatus* is herein interpreted as synapomorphic, with independent acquisition in *Pseudotatia parva*. The sinuous lateral line on the anterior half of the body in *Pseudotatia parva* is extended until vertical through anal-fin origin, differing from the condition observed in *Gelanoglanis*, *C. heckelii* and *C. existimatus*, where sinuous lateral line is only anteriorly, until end of vertical through dorsal-fin origin.

35. *Length of infraorbital 1 ventral process* (CI 1.0, RI 1.0). State 0: short, free from orbital margin (Fig. 11D); state 1: long, composing anterior orbital margin (Figs. 11 A,B; Ferraris, 1988: #I2; Walsh, 1990: #13; Soares-Porto, 1998: #14; Akama, 2004: #29; Birindelli, 2014: #98; Calegari et al., 2019: #3516). State 1 found in *Gelanoglanis, Centromochlus carolae, C. musaicus* (Fig. 11B), *C. macracanthus*, *C. schultzi, C. orca*, *C. existimatus* and *C. heckelii* (Fig. 11A). The elongate ventral process of infraorbital 1 in *Centromochlus* may be associated with its large eye size. A long infraorbital 1 extended to anterior orbital margin is observed in doradids with large eyes (Higuchi, 1992: #A13, Sousa, 2010: #22, Birindelli, 2014: #97), and in auchenipterids (Britski, 1972, Soares-Porto, 1998). However, the tiny *Gelanoglanis* catfishes also have an elongate infraorbital 1 despite its small eyes. The association between eye size and infraorbital process elongation is speculative and needs further investigation. Coded as polymorphic for *T. reticulata* as both conditions are observed.

36. *Position of infraorbital 1 canal opening* (CI 0.50, RI 0.67). State 0: canal exits at ventral tip of infraorbital 1 (Fig. 11B,C); state 1: canal exits in middle of infraorbital 1 (Fig. 11A,D; Soares-Porto, 1998: #14). State 1 in *Centromochlus existimatus*, *C. heckelii* and *C. macracanthus* (Fig. 11A) and independently acquired in *Gephyromochlus leopardus* (Fig. 11D).

37. *Position of the opening of the infraorbital canal in the neurocranium* (CI 1.0, RI 1.0). State 0: the canal exits the neurocranium at the anterior portion of sphenotic (Fig. 11D); state 1: canal exits from middle to posterior portion of sphenotic (Fig. 11A). State 1 is present in *Centromochlus carolae, C. existimatus, C. heckelii, C. macracanthus, C. melanoleucus, C. musaicus, C. schultzi* and *C. orca*, the species with the largest eyes among centromochlins. Also present in *Gelanoglanis* and *Gephyromochlus leopardus*, in which infraorbital canal exits from the middle portion of the sphenotic. Ontogenetic evidence shows that the infraorbital canal tends to have a more posterior position on sphenotic as development occurs. In some species of Doradidae with a depressed head and large eyes, the posterior infraorbitals are

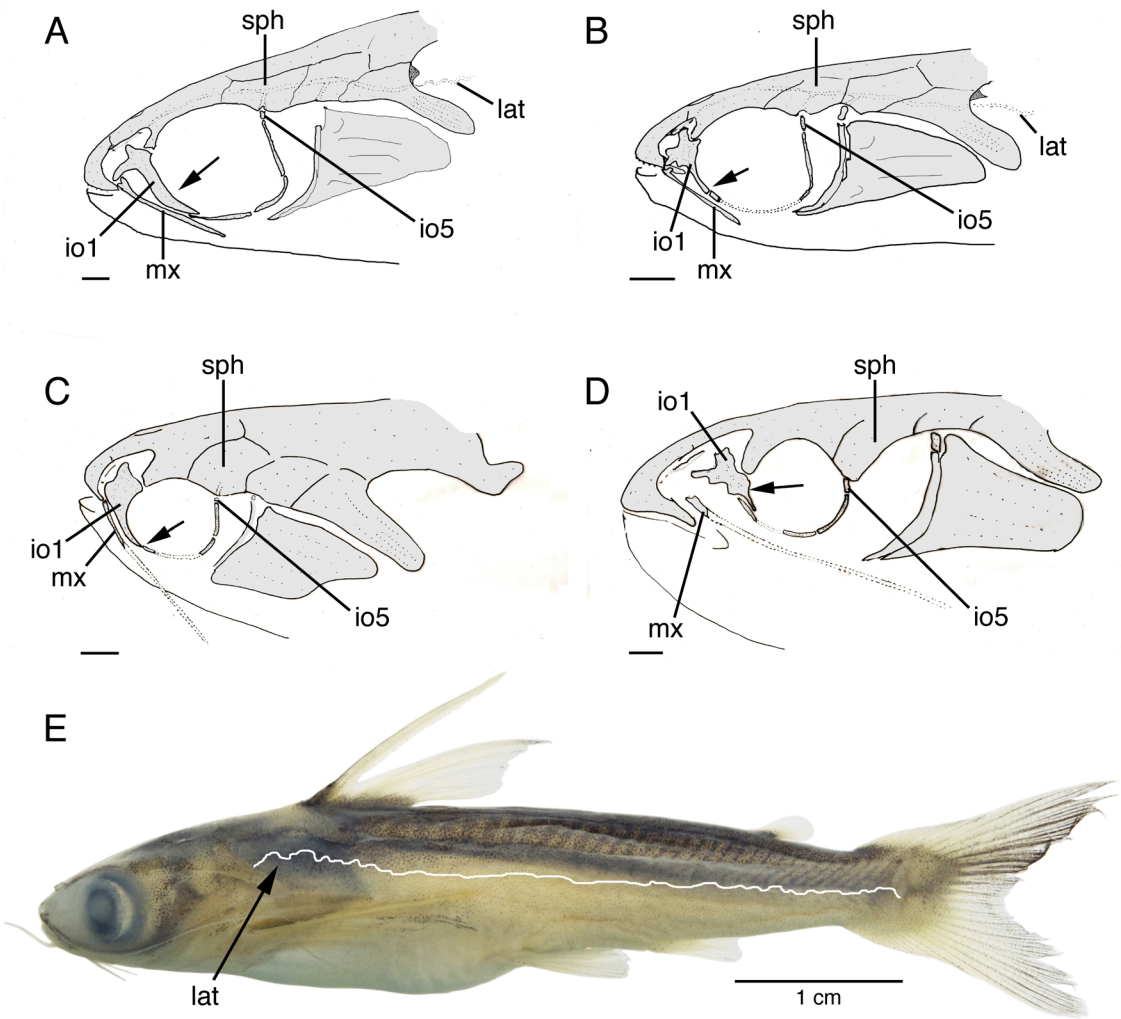

Fig. 11. Head in lateral view with detail of infraorbital canal bones. A. *Centromochlus heckelii*, MNRJ 12135, 50 mm SL. B. *Centromochlus musaicus*, MBUCV-V 17727, 26.8 mm SL paratype. C. *Tatia perugiae*, MZUSP 26684, 35.9 mm SL. D. *Gephyromochlus leopardus*, RMNH.PIS 28576, 71.2 mm SL, paratype. E. *Centromochlus existimatus*, ANSP 195385, 52.2 mm SL. Abbreviations: io1, first infraorbital; io5, posterior ossified infraorbital; mx, maxilla; sph, sphenotic. Short arrows indicate relative position of canal perforation on first infraorbital. Long arrow indicate sinous lateral line. Photo (E) by Mark Sabaj.

connected to the posterior portion of the sphenotic (Higuchi, 1992; Birindelli, 2014: #107). In centromochlin catfishes the derived condition is possibly due to a pelagic habit, a tendency observed in most *Centromochlus* and *Gelanoglanis* species, but not in *Gephyromochlus leopardus*.

38. *Ossification of infraorbital canal* (CI 1.0, RI 1.0). State 0: present (Figs. 8A–C); state 1: absent (Fig. 8D). Derived (reductive) state 1 present only in *Gelanoglanis* (Soares-Porto et al., 1999).

39. *Position of preopercle ossification relative to hyomandibula* (CI 0.50, RI 0.91). State 0: preopercle on lateral border of hyomandibula, hyomandibula border ends together with preopercular canal opening (Figs. 12D–F); state 1: preopercle on middle portion of hyomandibula, hyomandibula prolonged beyond preopercular canal opening (Figs. 12A–C). A preopercle shorter than the hyomandibula is a derived feature, synapomorphic for *Centromochlus*, *Gephyromochlus* and *Gelanoglanis* with a reversal in *C. orca*. In most auchenipterids, the preopercle canal exits lateral to tip of hyomandibula, a condition observed in *Tatia* and *Glanidium* (Figs. 12D–F). A reversal character state is observed for *Centromochlus orca* as the preopercle canal is uniquely short, differing from the condition in congeners (see Sarmento-Soares et al., 2016: fig. 4).

40. *Subpreopercle size* (CI 0.50, RI 0.67). State 0: relatively large, comparatively the same size as endopterygoid (Fig. 12F); state 1: vestigial, smaller than endopterygoid. In most centromochlin catfishes the subpreopercle corresponds to a small tubular ossification (Fig. 12C; Birindelli, 2014:#168). It is vestigial in *Tatia altae* and *T. perugiae* (see Soares-Porto, 1988: fig. 11), and a flattened tube in *Gelanoglanis stroudi and G. travieso* (Fig. 12C). A subpreopercle ossification reduced, smaller than the endopterygoid is synapomorphic for these species.

41. *Position of canal of mandibular ramus of laterosensory system* (CI 1.0, RI 1.0). State 0: within dentary bone (Fig. 12E); state 1: free from the dentary (Fig. 12C). Derived condition restricted to *Gelanoglanis* (Ferraris, 1988: #I10; Soares-Porto et al., 1999; Rengifo et al., 2008; Birindelli, 2014: #112; Calegari et al., 2019: #3524). Plesiomorphically among catfishes, each dentary contains a branch of the cephalic laterosensory system (e.g., Fig. 12E). A mandibular ramus free from the dentary is an uncommon feature in catfishes, but also found in the aspredinid *Aspredinichthys tibicen* (Cardoso, 2008: fig. 18). In *Gelanoglanis*, the mandibular canal is similarly free from the anguloarticular and dentary, a condition not reported for other auchenipterids or doradids. The absence or reduction of ossification in cephalic laterosensory system in *Gelanoglanis* are interpreted as distinct terminal conditions (#35, #41, #44) or may represent transitional features seen during the ontogeny of other species (#37).

Mandibular and hyoid arches.—Characters 42–52 pertain to the arrangement of teeth, suspensorium and hyoid bones. Although catfishes are unable to protrude their mouths like many other fishes, the gape of the mouth can expand greatly, mainly by lowering the hyoid apparatus (Gosline, 1973). In centromochlin catfishes, which are mainly invertivorous, grasping occurs between the premaxillary and dentary tooth patches, as additional tooth plates are seldom present on the palate. For each species, a particular morphology is exhibited in response to feeding.

42. *Number of rows of dentary teeth* (CI 0.50, RI 0.93). State 0: more than three rows of teeth; state 1: three or less rows. Having three or less rows of dentary teeth is a uniquely derived and unreversed synapomorphy for a monophyletic clade composed of *Centromochlus* and *Gelanoglanis*. Most catfishes have numerous small teeth arranged in several rows on the dentary (Berkovitz & Shellis, 2017). In *Centromochlus* and *Gelanoglanis* the dentary tooth patch has a few teeth. *Tatia gyrina* has few rows of dentary teeth (Soares-Porto, 1998: #1), interpreted as an independent acquisition relative to that of *Centromochlus* and *Gelanoglanis*

43. *Medial contact of premaxillary tooth patches* (CI 1.0, RI 1.0). State 0: present (Figs. 10C–D); state 1: absent, patches laterally displaced, widely separated (Fig. 10A; Ferraris, 1988: J20). Derived state found in *Gelanoglanis* and interpreted as a reductive state.

44. *Size of the maxilla* (ordered; CI 1.0, RI 1.0). State 0: maxillary bone smaller than the length of lateral ethmoid (Fig. 10B); state 1: maxillary bone about two-thirds length of lateral ethmoid (Fig. 10C); state 2: maxillary bone equals or surpasses length of lateral ethmoid (Figs. 8D, 10A). Elongation of maxillary bone found in *Centromochlus* (State 1) and *Gelanoglanis* (State 2). The transformational series is ordered as an exceptionally long palatine ossification is a neomorphic feature within centromochlin catfishes. Plesiomorphically among catfishes, the maxilla is a small element supporting the elastin cartilage of the maxillary barbel (Ghiot et al., 1984). In some Mochokidae (Vigliota, 2008: #33); Doradidae (Birindelli, 2014: #131) and Auchenipteridae (Ferraris, 1988: #J11; Soares-Porto, 1998: #2; Calegari et al., 2019: #3590) an elongated rod-like maxilla is the movable structure of the palatino-maxillary mechanism (Royero & Neville, 1997). The size of the maxillary is associated with movement of the maxillary barbel (see character #131) .

45. *Depth of coronoid process* (CI 1.0, RI 1.0). State 0: deep, mandible depth at coronoid process about one-third of mandible length (Fig. 12E); state 1: shallow, mandible depth at coronoid process about one-quarter of mandible length. Shallow mandible depth found in all species of *Centromochlus* and *Gelanoglanis* (Figs. 12A,B). Plesiomorphically among catfishes, there is a well formed dorsally directed coronoid process on the lower jaw where the dentary joins the angulo-articular (Vigliotta, 2008: #27). The coronoid process is absent or poorly formed in some Mochokidae (Vigliotta, 2008: #27) and absent in the auchenipterin *Asterophysus* (de Pinna, 1998: #50; Diogo, 2004: #400; Birindelli, 2014: #139). In some *Centromochlus* the posterodorsal portion of mandible is straight (Sarmento-Soares et al., 2017; Calegari et al., 2019: #3601).

46. *Position of the articulating facet for hyomandibula* (CI 0.33, RI 0.91). State 0: on sphenotic, pterotic and prootic; state 1: on sphenotic only (Mo, 1991: #21; Arratia, 1992: #35; Royero, 1999: #56; Britto, 2002: #181; Vigliotta, 2008: #10; Birindelli, 2014: #162; Calegari et al., 2019: #3619). Articulation facet for hyomandibula head limited to sphenotic in *Gelanoglanis* and independently acquired in *Tatia* Clade A species (*Tatia aulopygia*, *T. boemia*, *T. brunnea*, *T. caudosignata*, *T. caxiuanensis*, *T. dunni*, *T. galaxias*, *T. gyrina*, *T. intermedia*, *T. jaracatia*, *T. meesi*, *T. neivai*, *T. nigra* and *T. strigata*). A reversal occurs at the common ancestor of *Centromochlus* and persists in *C. melanoleucus, C. musaicus, C. carolae* and *C. orca*. In some basal lineages of catfishes, the hyomandibula inserts on the underside of the neurocranium between the sphenotic

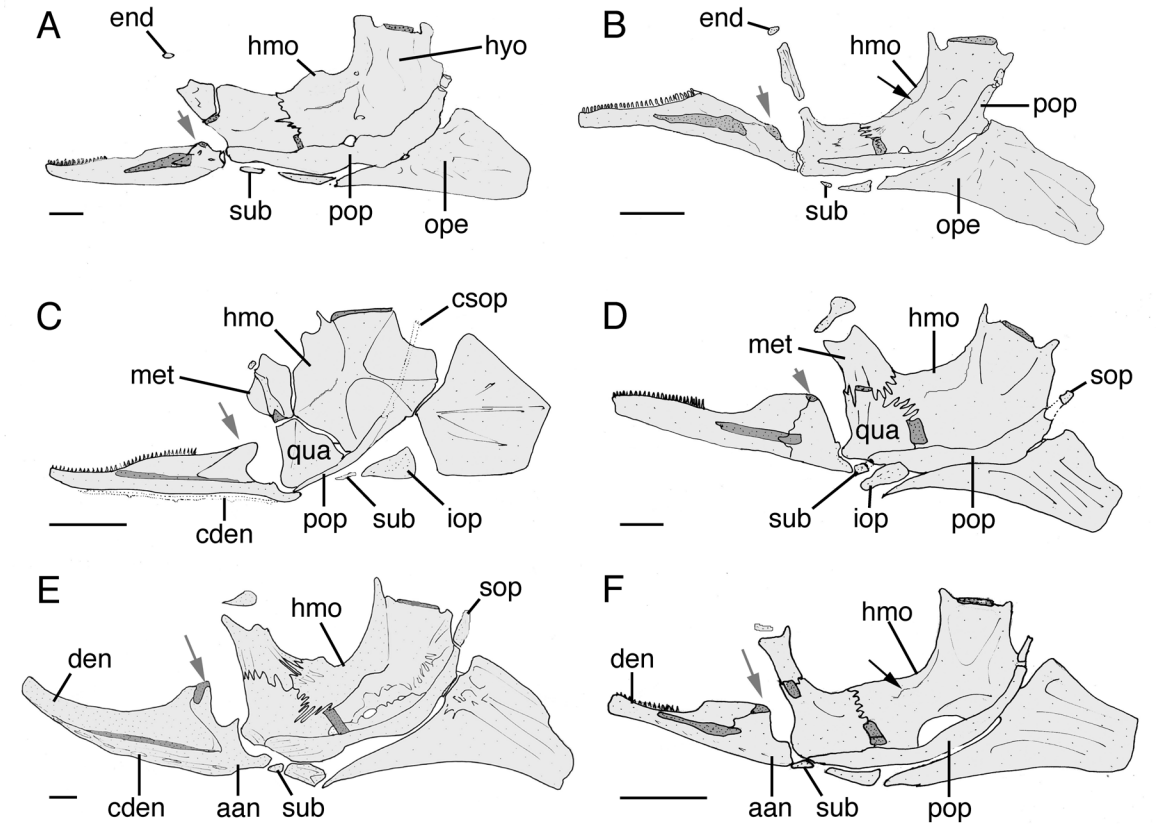

Fig. 12. Lateral view of left suspensorium. A. *Centromochlus heckelii*, MNRJ 12135, 50 mm SL. B. *Centromochlus musaicus* MBUCV-V-17727, paratype, 26.8 mm SL. C. *Gelanoglanis stroudi*, FMNH 83912, paratype, 24.6 mm SL. D. *Gephyromochlus leopardus*, RMNH. PIS 28576, paratype, 71.2 mm SL. E. *Glanidium botocudo*, MNRJ 32539, paratype, 82.0 mm. F. *Tatia brunnea*, RMNH.PIS 28571, 36,7 mm SL. Abbreviations: aan, angulo-articular; cden, dentary laterosensory canal; csop, suprapreopercular laterosensory canal; den, dentary; hyo, hyomandibula; hmo, hyomandibula membranous outgrowth; iop, interopercle; met, metapterygoid; end, endopterygoid; ope, opercle; pop, preopercle; qua, quadrate; sub, subpreopercle; sop, suprapreopercle. Black arrow: crest for the insertion of levator arcus palatini in the hyomandibula. Gray arrow: coronoid process. Scale bar = 1 mm.

and prootic (Vigliotta, 2008). Within Auchenipterinae, the hyomandibula articulates with the cranium via the sphenotic only in *Asterophysus*, *Auchenipterichthys*, *Auchenipterus*, *Entomocorus*, *Epapterus*, *Pseudepapterus*, *Trachelyopterichthys*, *Trachelyopterus* and *Trachycorystes* (Birindelli, 2014: #162).

47. *Levator arcus palatini insertion crest* (CI 0.33, RI 0.91). State 0: rounded; state 1: sharp (Fig. 12F; Sarmento-Soares & Porto, 2005). A sharp crest for insertion of muscle levator arcus palatini on the hyomandibula is found in Clade A *Tatia* (*T. aulopygia*, *T. boemia*, *T. brunnea*, *T. caxiuanensis*, *T. caudosignata*, *T. dunni*, *T. galaxias*, *T. gyrina*, *T. intermedia*, *T. jaracatia*, *T. meesi*, *T. neivai*, *T. nigra*, *T. strigata*) and also *T. altae*, *T. ferrarisi*, *T. meridionalis*, *T. perugiae*, *T. reticulata* and *T. romani*. The insertion of muscle levator arcus palatini on hyomandibula is rounded and weakly developed in most Auchenipteridae. A sharp crest for muscle attachment onto the hyomandibula also is observed in *Centromochlus musaicus* (Fig. 12B) and *C. carolae*, and coded as independent acquisition.

48. M*etapterygoid joint to quadrate and hyomandibula* (CI 0.50, RI 0.94). State 0: metapterygoid connected to both quadrate and hyomandibula (Figs. 12D,E); state 1: metapterygoid connected to quadrate only (Fig. 12F; Ferraris, 1988: #J3; (Arratia, 1992: #25; Soares-Porto, 1998: #12; Royero, 1999: #59; Britto, 2002: #189; Akama, 2004: #48; Birindelli, 2014: #164; Calegari et al., 2019: #3620). State 1 present in Clade A *Tatia* (*T. aulopygia*, *T. boemia*, *T. brunnea*, *T. caxiuanensis*, *T. caudosignata*, *T. dunni*, *T. galaxias*, *T. gyrina*, *T. intermedia*, *T. jaracatia*, *T. meesi*, *T. neivai*, *T. nigra*, *T. strigata*) and *Centromochlus carolae* and *C. musaicus*. Clade A *Tatia* plus the two species of *Centromochlus* share a similar suspensorium in which the conical metapterygoid is connected to quadrate only through dentate suture and/or cartilage (Figs. 12B,F). Polymorphisms regarding metapterygoid position were observed in *Tatia reticulata* and *T. romani*. In some individuals of *Tatia reticulata* and *T. romani* the metapterygoid is spatulate, joined to quadrate and hyomandibula, or sometimes conical, joined to quadrate only. For *Tatia reticulata* and *T. romani*, this feature was coded as polymorphic (0/1). The polymorphisms in suspensorium bones suggests that a conical metapterygoid is not a distinctive feature for *Tatia*, as was previously stated (e.g., Soares-Porto, 1998: #12). In most catfishes, including the majority of auchenipterids, the metapterygoid articulates with both the quadrate and hyomandibula (Britski, 1972), a condition observed here in *Glanidium*. Alexander (1965) considered the lack of contact between metapterygoid and hyomandibula as directly associated with the enlargement of the eye. We observed in other centromochlins with large eyes (e.g., some *Centromochlus*) a different solution to accommodate the eye, with the laminar expansion of the hyomandibula preventing contact with the metapterygoid (see character #47 below).

49. *Dorso-medial lamina of quadrate* (CI 0.50, RI 0.50). State 0: absent (Fig. 12D); state 1: present, interposed between metapterygoid and hyomandibula (Fig. 12A; Soares-Porto, 1998: #13). State 1 is a synapomorpy for the clade *Centromochlus existimatus* + *C. heckelii* and independently acquired by *C. orca*. A laminar projection of the hyomandibula was observed in some auchenipterins including species of *Ageneiosus* and *Tetranematichthys* (Ferraris, 1988: #J2; Soares-Porto, 1998: #13; Walsh, 1990: #1; Royero, 1999: #55, #59; Akama, 2004: #47; Birindelli, 2014: #163), and is interpreted as independent acquisition from the condition in *Centromochlus*.

50. *Endopterygoid shape* (CI 0.33, RI 0.75). State 0: comma-shaped (Figs. 12D-F); state 1: rounded (Figs.11A–C; Vigliotta, 2008: #44; Calegari et al., 2019: #3621). A rounded entopterygoid is herein hypothesized to have evolved three times in Centromochlinae, being synapomorphic for *Gelanoglanis* (Fig. 12C), *Centromochlus carolae* + *C. musaicus* (Fig. 12B), and *C. existimatus* + *C. heckelii* (Fig. 11A). The entopterygoid (= mesopterygoid of Soares-Porto, 1988) corresponds to a sesamoid ossification ligamentously connected with the neurocranium in most catfishes (Arratia, 1992: #20–21; Vigliotta, 2008: #44; Birindelli, 2014: #165).

51. *Hyomandibula passage for trigeminofacial nerve* (CI 1.0, RI 1.0). State 0: single opening; state 1: double opening. (Birindelli, 2014: #161). A double opening is synapomorphic for the clade composed of *Glanidium catharinensis, G. ribeiroi* and *G. melanopterum*. In most catfishes there is a single opening in the hyomandibula for the passage of the hyomandibular branch of the trigeminofacial nerve. Two openings were reported in auchenipterins with robust, depressed heads: *Trachelyopterus coriaceus*, *T. galeatus*, and *Trachycorystes trachycorystes* (Royero, 1999: #60; Akama, 2004: #55). The trigeminofacial passage through the hyomandibula is either single or double in specimens of *Glanidium cesarpintoi*, and therefore coded as polymorphic (0/1).

52. *Width of hyomandibula laminar outgrowth* (CI 1.0, RI 1.0). State 0: wide (Figs. 12D–E); state 1: narrow (Fig. 12F). A wide hyomandibula laminar outgrowth is the plesiomorphic state observed in centromochlin

catfishes. The derived state, a narrow hyomandibula laminar outgrowth, is synapomorphic for Clade A *Tatia* (*T. aulopygia*, *T. boemia*, *T. brunnea*, *T. caxiuanensis*, *T. caudosignata*, *T. dunni, T. galaxias, T. gyrina, T. intermedia, T. jaracatia, T. meesi, T. neivai, T. nigra,* and *T. strigata*). All Clade A *Tatia* have a complex quadrate (sensu Arratia, 1992), and a narrow hyomandibula outgrowth is associated with the arrangement of suspensorium bones. Scored as polymorphic (0/1) in *Centromochlus carolae, C. musaicus,* and *Tatia altae, T. perugiae, T. reticulata* and *T. romani*.

Opercular bones.—Characters 53–54 pertain to opercular series and associated bones.

53. *Suprapreopercle* (CI 1.0, RI 1.0). State 0: present (Figs. 12A,B); state 1: absent (Fig. 12C; Lundberg, 1970: #70; Britski, 1972: #21; Britto, 2002: #196; Birindelli, 2014: #167; Calegari et al., 2019: #3623). State 1 exclusive to *Gelanoglanis*. In most centromochlin catfishes, the position of suprapreopercular ossicle is dorsal to the hyomandibula-opercle joint and anterior to opercle. Being present in all Auchenipteridae and absent in Doradidae (Britski, 1972: 21), the absence of suprapreopercle ossification is interpreted as a secondary loss in *Gelanoglanis*. Although associated to an elongation of the dorsal portion of the preopercle, resulting in shortening of suprapreopercle (Soares-Porto, 1998: 15), such an association was not confirmed in the current study. Coded as polymorphic for *Tatia perugiae* (0/1).

54. *Suprapreopercle size* (CI 1.0, RI 1.0). State 0: long, comparatively longer than the hyomandibular facet to cranium (Fig. 12E); state 1: short, shorter than the neighboring hyomandibular facet to cranium (Fig. 12B). Suprapreopercle reduced in the clade formed by *Gephyromochlus*, *Gelanoglanis*, *Centromochlus* and *Tatia*. A tendency towards suprapreopercle reduction was observed in most Centromochlinae. Inapplicable (-) for *Gelanoglanis stroudi*, *G. nanonocticolus*, *G. travieso* and *G. pan*, as no suprapreopercle is present.

Hyoid arch.—Characters 55–57 pertain to hyoid bar and urohyal on anterior portion of hyobranchial skeleton.

55. *Laminar expansion of urohyal* (CI 1.0, RI 1.0). State 0: present (Fig. 13C); state 1: absent (Figs. 12A,B; Birindelli, 2014: #169). Laminar expansion absent in *Tatia, Centromochlus, Gelanoglanis* and *Gephyromochlus*. The urohyal possesses lateral wing-like expansions in most catfishes, as a triangular shape in dorsal view (Lundberg, 1982; Arratia & Schultze, 1990).

56. *Size of urohyal ventral process* (CI 1.0, RI 1.0). State 0: small, ventral process shorter than urohyal (Fig. 13B); state 1: long, ventral process longer than urohyal (Fig. 13C; Sarmento-Soares & Martins-Pinheiro, 2013). *Glanidium* is unique among centromochlin catfishes in having a large robust process on the urohyal. Ontogenetic series reveals the urohyal tends to become thick with development. Ferraris (1988), Walsh (1990), and Birindelli (2014) referred to a distinctively long laminar projection of the urohyal in *Tetranematichthys* and some *Ageneiosus*

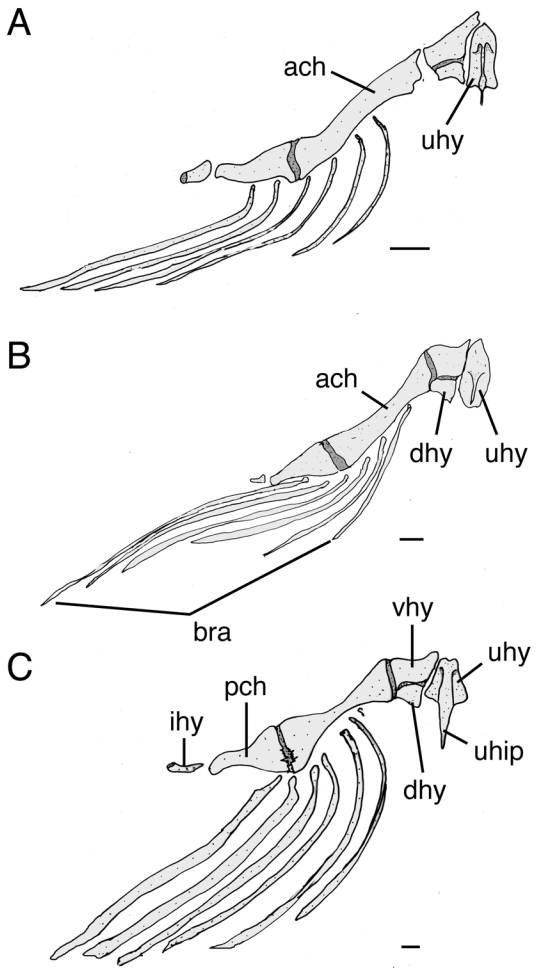

Fig. 13. Ventral view of right hyoid arch. A. *Centromochlus macracanthus*, MZUSP 52924, 58.0 mm SL. B. *Tatia perugiae*, MCNG 21691, 29.4 mm SL. C. *Glanidium albescens* MCNIP 1084, 23.9 mm SL. Abbreviations: ach, anterior ceratohyal; bra, branchiostegal rays; dhy, dorsal hypohyal; ichc, interceratohyal cartilage; ihy, interhyal; pch, posterior ceratohyal; vhy, ventral hypohyal; uhy, urohyal; uhyp, urohyal ventral process. Scale bar = 1 mm.

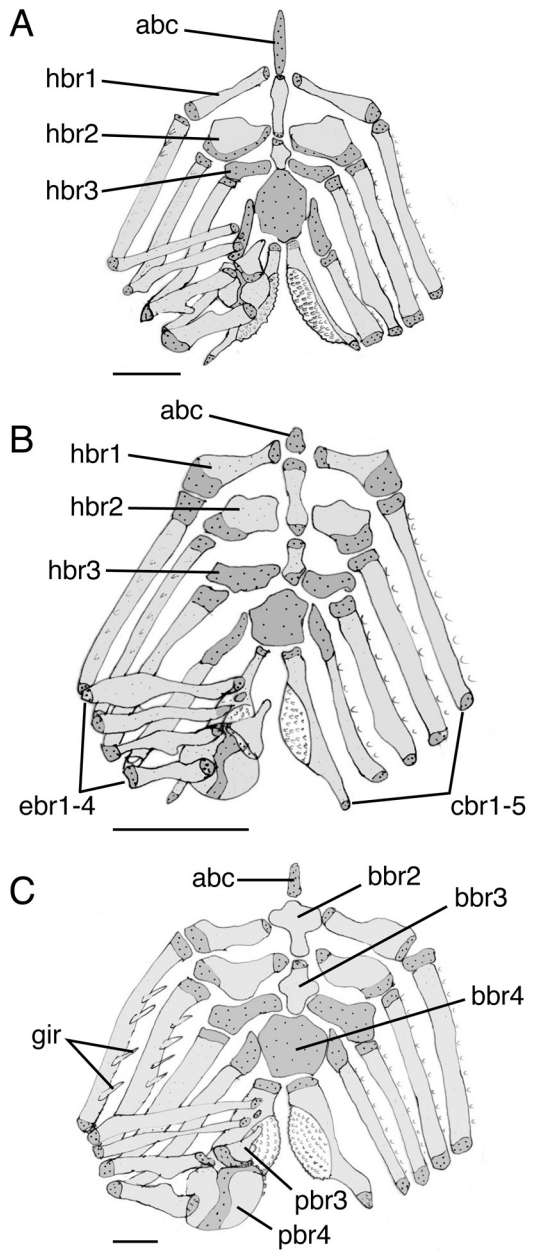

Fig. 14. Branchial arches in dorsal view. A. *Centromochlus heckelii*, MZUSP unnumbered, 76.8 mm SL. B. *Tatia britskii*, MZUSP 43251, 34.5 mm S, paratype, 35.9 mm SL. C. *Glanidium botocudo*, MNRJ 32539, 82.0 mm SL, paratype. Abbreviations: abc, anterior basibranchial cartilage; bbr2, basibranchial 2; bbr3, basibranchial 3; bbr4, basibranchial 4; cbr1-5, ceratobranchials 1 to 5 (anterior to posterior); ebr1-4, epibranchials 1 to 4 (anterior to posterior); gir, gill rakers; hbr1-3, hypobranchials 1 to 3; pbr3, pharyngobranchial 3; pbr4, pharyngobranchial 4. Scale bar = 1 mm.

species. The condition in both *Tetranematichthys and Ageneiosus* is superficially similar to that of *Glanidium*, but the urohyal is bifurcated (vs. pointed in *Glanidium*). Differences in the urohyal ventral process were observed between species, and a much-elongated sharpened process is observed in *Glanidium botocudo* relative to its congeners (Sarmento-Soares & Martins-Pinheiro, 2013). In *Glanidium botocudo,* the urohyal ventral process is longer than the central portion (vs. shorter than central portion in remaining congeners). In the remaining Centromochlinae, the urohyal process is small, acutely pointed, shortly projected from central portion.

57. *Interhyal size* (CI 1.0, RI 1.0). State 0: short, shorter than dorsal hypohyal height (Fig. 13B); state 1: elongated, longer than dorsal hypohyal height (Fig. 13A). Interhyal elongated in *Centromochlus existimatus, C. heckelii, C. macracanthus* and *C. schultzi* and herein hypothesized as synapomorphic for that clade.

Branchial arches.—Characters 58–62 pertain to branchial arches and associated bones. As typical respiratory organs in fishes, each branchial arch consists of cartilaginous or bony skeletal parts surrounded by respiratory epithelium and blood vessels (Rojo, 1991). The arrangement of bony plates of dermal origin, coupled with toothed faces on the fifth ceratobranchial and fourth pharyngobranchial, exhibits little variaton among centromochlin catfishes. Branchial arch characters #58–#60 were coded as missing data (?) for *Tatia marthae* and *Pseudotatia parva*.

58. *Length of anterior basibranchial cartilage* (CI 1.0, RI 1.0). State 0: elongate (Fig. 14A); state 1: short (Fig. 14B). The basibranchial cartilage is the anteriormost element of the branchial series. It is usually elongate in auchenipterid catfishes, but reduced to a short cartilage in species of *Tatia*.

59. *Shape of basibranchial 2* (CI 1.0, RI 1.0). State 0: cylindrical, elongate; state 1: flattened dorsoventrally, spatulate (Fig. 14C). Most catfishes exhibit cylindrical and elongate basibranchials (Arratia, 1987; Vigliota, 2008: #50). A flattened and spatulate basibranchial 2 is synapomorphic for *Glanidium*.

60. *First hypobranchial shape* (CI 1.0, RI 1.0): State 0: discoid (Fig. 14C); state 1: cylindrical (Fig. 14A; Higuchi, 1992: #A46; Birindelli, 2014: #191). In most catfishes, the first two hypobranchials are discoid (Higuchi, 1992). A cylindrical, tubular first hypobranchial is uniquely observed in *Centromochlus*, *Gelanoglanis* and *Gephyromochlus*.

61. *Gill rakers size* (CI 0.50, RI 0.83). State 0: gill rakers short or rudimentary (Fig. 14B); state 1: gill rakers robust (Fig. 14C; Birindelli, 2014: #183). Gill rakers in *Glanidium* are robust, with space between adjacent rakers greater than their length; condition independently acquired in *Gephyromochlus leopardus*. In most catfishes, such as Diplomystidae, Doradidae and Aspredinidae, gill rakers are small and ossified (Cardoso, 2008). In most Auchenipterinae gill rakers are long and ossified, whereas most centromochlins exhibit rudimentary gill rakers. Coded as inapplicable for *Gelanoglanis*, which lacks gill-rakers.

62. *Number of rows of gill rakers on branchial arches* (CI 1.0, RI 1.0): State 0: one or two rows; state 1: none (Calegari et al., 2019: #3635). Most auchenipterids have two rows of gill-rakers on the branchial arches. In centromochlins, one row of short rakers is observed in most species. In *Gelanoglanis*, all branchial arches are without gill rakers. Adapted from Birindelli (2014: #181, #182).

Axial skeleton.—Characters 63–69 pertain to anterior vertebrae and ribs.

63. *Size of transformator process of tripus* (CI 1.0, RI 1.0): State 0: well developed and firmly attached to swim bladder; state 1: reduced, loosely connected to swim bladder wall (Fig. 15C). The transformator process of tripus is distinctively reduced and loosely attached to the tunica externa of the swim bladder in *Glanidium catharinensis* and *G. melanopterum*. Such a condition resembles that reported for *Trachelyichthys decaradiatus* by Britski (1972: 20). In doradid and other auchenipterid catfishes the transformator process of the tripus is straight and firmly attached to the tunica externa of swim bladder (Bridge & Haddon, 1892: 160; Britski, 1972: 19; Ferraris, 1988: #V2; Royero, 1999: #73; Akama, 2004: #69; Birindelli, 2014: #203).

64. *Shape of disc (Mullerian ramus) on parapophysis of fourth vertebra* (CI 0.50, RI 0.75). State 0: Müllerian ramus round, broad, spoon-shaped, on side of swim bladder (Fig. 14C); state 1: conical, projecting into lumen of swimbladder (Figs. 15A,B; Britski, 1972: Soares-Porto, 1998: #16; Curran, 1989: #17; Birindelli, 2014: #206; Calegari et al., 2019 #3660). The mullerian ramus is conical and projects into the swimbladder lumen in *Centromochlus carolae*, *C. musaicus, C. orca*, *C. heckelii, C. existimatus*, *C. schultzi* and *C. macracanthus*.

65. *Size of disc (Mullerian ramus) on parapophysis of fourth vertebra* (unordered; CI 1.0, RI 1.0). State 0: parapophysis diameter same width as basioccipital (Fig. 15C); state 1: parapophysis diameter half the width of basioccipital; state 2: parapophysis diameter one-fourth of basioccipital width (Fig. 15D; Calegari et al., 2019 #3661). The parapophysis diameter is half the width of bassioccipital in *Tatia gyrina, T. meesi* and *T. caxiuanensis*. The parapophysis diameter is one-fourth the width of bassioccipital in species of *Gelanoglanis* (Fig. 15D). In some of the smaller-sized centromochlins such as *Tatia gyrina, T. meesi*, *T. caxiuanensis* and *Gelanoglanis* the Müllerian ramus disc is reduced in size. In the small-sized doradid *Physopyxis* (Sousa, 2010: #46) and in large-sized species of the auchenipterin *Ageneiosus*, the disc of the Müllerian ramus is compact, reduced in size (Britski, 1972: 20; Ferraris, 1988: #V7; Walsh, 1990: #23; Higuchi, 1992: #A52; Royero, 1999: #74; Akama, 2004: #67).

66. *Size of parapophysis of fifth vertebra* (CI 1.0, RI 1.0). State 0: same size as parapophysis of sixth vertebra; state 1: smaller than parapophysis of sixth vertebra (Fig. 15A; Ferraris, 1988: #V11). Most catfishes have the parapophysis of the fifth vertebrae moderate in size, similar to those of subsequent vertebrae (de Pinna, 1996). The parapophysis of the fifth vertebra in most doradids and auchenipterids is somewhat reduced in size (Bridge & Haddon, 1892: 230; Regan, 1911; Alexander, 1965: 111; Britto, 2002: #233; Diogo, 2004: #138;Vigliotta, 2008: #80; Birindelli, 2014: #211; Calegari et al., 2019: #3665). Extreme reduction is unique to *Centromochlus, Gephyromochlus* and *Gelanoglanis*.

67. *Ornamentation of the parapophysis of sixth vertebra* (CI 1.0, RI 1.0). State 0: absent; state 1: present. The parapophysis of the sixth vertebral centrum is smooth in centromochlin catfishes except for *Tatia jaracatia* and *T. neivai*. In those two species, the parapophysis of sixth vertebrae is ornamented as a rough surface that adheres to the swim-bladder capsule.

68. *Opening of the aortic passage* (CI 0.50, RI 0.85). State 0: ventrally opened (Fig. 15C) state 1: partial closure of aortic passage (Fig. 15B); state 2: ventrally covered by superficial ossification (Fig. 15E; Birindelli, 2014: #226). State 1 in some *Centromochlus* species such as *C. existimatus*, *C. heckelii*, and *C. orca*. State 2 in Clade B *Tatia*: *Tatia altae, T. ferrarisi, T. meridionalis, T. perugiae, Tatia reticulata,* and *T. romani* (Fig. 15E). Although variation in the ventral superficial ossification with partial closure of aorta was reported by Birindelli (2014: #216) as a polymorphic feature for both *Centromochlus* and *Tatia,* we observed distinctions among species.

69. *Position of posterior ribs* (CI 1.0, RI 1.0). State 0: ribs attached to consecutive vertebrae; state 1: vertebral centra

without ribs followed by rib-bearing vertebra (Soares-Porto, 1998: #17; Sarmento-Soares & Martins-Pinheiro, 2008). Among catfishes, the ribs are sequential, each placed on consecutive vertebrae. A vertebra without ribs between rib-bearing vertebrae is uniquely derived feature for *Tatia boemia*, *T. neivai* and *T. jaracatia*.

Dorsal fin and supports.—Characters 70–81 pertain to dorsal fin and supporting bones.

70. *Anterior nuchal plate* (CI 0.20, RI 0.80): State 0: present (Figs. 9A–D); state 1: absent (Figs. 8B,D; Akama, 2004: #32, #40; Sousa, 2010: #54; Birindelli, 2014: #228, #231, Calegari et al., 2019: #3670). Most auchenipterids, doradids and some mochokids have a well-formed nuchal shield, considered herein to be composed of the anterior, middle and posterior (paired) nuchal plates (Vigliota, 2008; Birindelli, 2014).

The anterior nuchal plate is absent in *Gelanoglanis stroudi*, *G. nanonocticolus*, *G. travieso*, *G. pan, Centromochlus carolae, C. melanoleucus, C. musaicus, C. schultzi, C. orca, C. macracanthus, Tatia ferrarisi, T. meridionalis, T. romani, T. marthae, T. bockmanni, T. britskii, T. concolor, T. punctata* and *T. simplex*. Interpreted as a reversal in Clade A *Tatia* containing *T. aulopygia*, *T. boemia*, *T. brunnea*, *T. caxiuanensis*, *T. caudosignata*, *T. dunni*, *T. galaxias*, *T. gyrina*, *T. intermedia*, *T. jaracatia*, *T. meesi*, *T. neivai*, *T. nigra* and *T. strigata*. A reversal also defines the clade *Centromochlus existimatus* plus *C. heckelii*. The only centromochlin polymorphic for the presence or absence of an anterior nuchal plate is *Tatia reticulata* (0/1).

71. *Suture between parieto-supraoccipital and middle nuchal plate* (CI 0.25, RI 0.84). State 0: absent; state 1: present (Figs. 8B,D; Britski, 1972: 27; Ferraris, 1988: #D1 and D3; Walsh, 1990: #4; Soares-Porto, 1998: #9; Royero, 1999: #26; Birindelli, 2014: #229, Calegari et al., 2019: #3672). Suture between parieto-supraoccipital and middle nuchal plate is considered synapomorphic for *Gephyromochlus*, *Gelanoglanis*, *Centromochlus* and *Tatia* with two reversals. Suture between parieto-supraoccipital and middle nuchal plate present in *Gelanoglanis stroudi*, *G. nanonocticolus*, *G. travieso*, *G. pan, Centromochlus carolae, C. melanoleucus, C. musaicus, C. schultzi, C. orca, C. macracanthus, Tatia ferrarisi, T. meridionalis, T. romani, T. marthae, T. bockmanni, T. britskii, T. concolor, T. punctata* and *T. simplex*. Interpreted as a reversal in Clade A *Tatia* containing *Tatia aulopygia*, *T. boemia*, *T. brunnea*, *T. caxiuanensis*, *T. caudosignata*, *T. dunni*, *T. galaxias*, *T. gyrina*, *T. intermedia*, *T. jaracatia*, *T. meesi*, *T. neivai*, *T. nigra* and *T. strigata*. Another reversal defines the clade *Centromochlus existimatus* + *C. heckelii* (Figs. 9C). For *Tatia altae*, *T. perugiae*, *Tatia boemia*, *T. neivai* and *T. dunni*, this character condition was coded as inapplicable (0/1), as asymmetry in shape of middle nuchal plate was observed (Sarmento-Soares & Martins-Pinheiro, 2008: fig. 11), but the anterior plate was always present on the posterior cranial roof.

72. *Shape of posterior nuchal plate* (CI 1.0, RI 1.0). State 0: laterally recurved (Figs. 9A-D); state 1: lateral margin straight (Fig. 8A; Ferraris, 1988: #D4). Straight lateral margin present in *Centromochlus existimatus* and *C. heckelii*. In most auchenipterid catfishes, the posterior nuchal plate is ventrolaterally expanded (wing-like) with posteroventral portion attached to infranuchal ligament connected to first rib (Britski, 1972). No other centromochlin species have such a large posterior nuchal plate as in *C. existimatus* and *C. heckelii*. Both species are conservative in the possession of a large posterior nuchal plate, as all examined specimens have the same condition.

73. *Dorsal-fin spinelet* (CI 1.0, RI 1.0). State 0: present; state 1: absent. (Vari & Calegari, 2016: fig. 3; (Britto, 2002: #288; Birindelli, 2014: #235; Calegari et al., 2019: #3681). A previously unreported reduced feature shared by *G. varii* and *G. nanonocticolus* is the loss of the dorsal-fin spinelet, which is present and bears a large pair of ventral process in all auchenipterids, including other *Gelanoglanis* (Vari & Calegari, 2016).

74. *Spinous unbranched rays of dorsal fin* (CI 0.5, RI 0.5). State 0: present; state 1: absent. (Calegari et al., 2019: #3684). The anterior dorsal-fin ray is soft (not spinous) in *Gelanoglanis nanonocticolus* and *G. travieso* (Fig. 2C). In Centromochlinae the dorsal fin is usually composed of a spinelet, a spine and subsequent branched rays. *Gelanoglanis stroudi* has a robust dorsal-fin spine with well developed serrae along its posterior margin (Bohlke, 1980; Calegari et al., 2014). A dorsal-fin spine also is present in type specimens of *Gelanoglanis pan* from the upper Tapajós.

Fig. 15. (Page 113) Ventral view of anterior vertebrae and associated bones. A. *Centromochlus heckelii*, MZUSP 8336, 62.0 mm SL. B. *Centromochlus orca*, INPA 35086, 54.1 mm SL, paratype. C. *Glanidium catharinensis*, MZUSP 9308, 103.2 mm SL. D. *Gelanoglanis stroudi*, FMNH 83912, 24.6 mm SL. E. *Tatia perugiae*, MCNG 21691, 28.2 mm SL. Abbreviations: aor, channel for aorta passage; boc, basioccipital; cve, complex vertebra; np3, posterior nuchal plate; osu, os suspensorium; pv4, parapophysis of fourth vertebra; pv5, parapophysis of fifth vertebra; pv6, parapophysis of sixth vertebra; rib, pleural rib; scl, trans-scapular process of posttemporal-supracleithrum; tri, tripus. Arrow indicates transformator process of tripus. Scale bar = 1 mm.

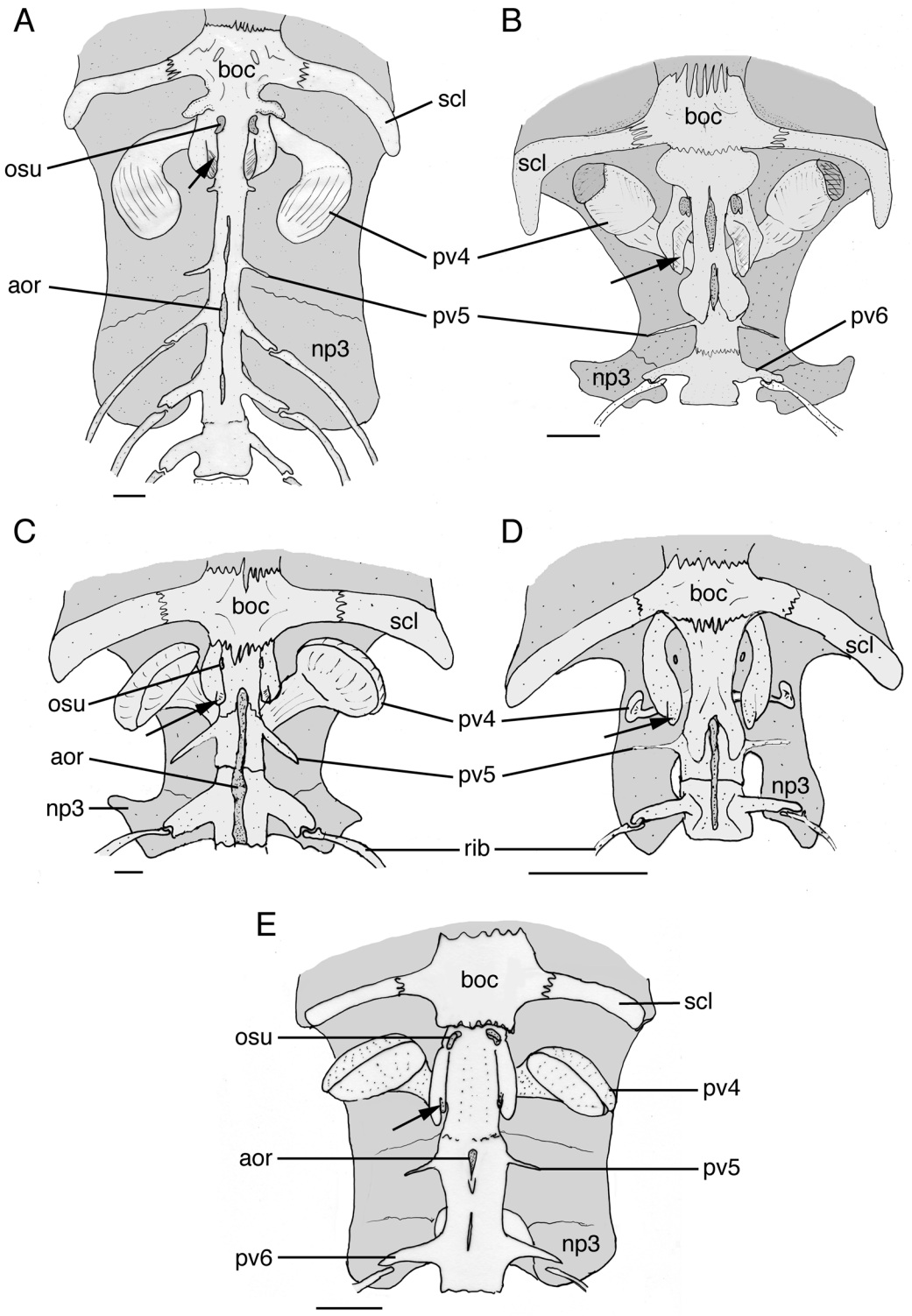
A
boc
scl
osu
pv4
aor
pv5
np3
B
boc
scl
pv6
np3
C
boc
scl
osu
pv4
aor
pv5
np3
rib
D
boc
scl
np3
E
boc
scl
osu
pv4
aor
pv5
np3
pv6

75. *Serrations on distal tip of anterior margin of dorsal-fin spine* (CI 0.5, RI 0.0). State 0: distinct (Figs. 16A,C,E); state 1: rudimentary (Fig. 16D). The dorsal-fin spine has rudimentary serrations along the anterior border in *Tatia romani* and *T. meridionalis*. Rudimentary serrations are herein distinguished from distinct ones, differing from Calegari et al. (2019: #3689) who considered serrations present even when rudimentary. Coded as inapplicable for *Gelanoglanis nanonocticolus* and *G. travieso* as these taxa do not have a spinous dorsal-fin ray, and for *Glanidium* as the spine margin is smooth along distal tip.

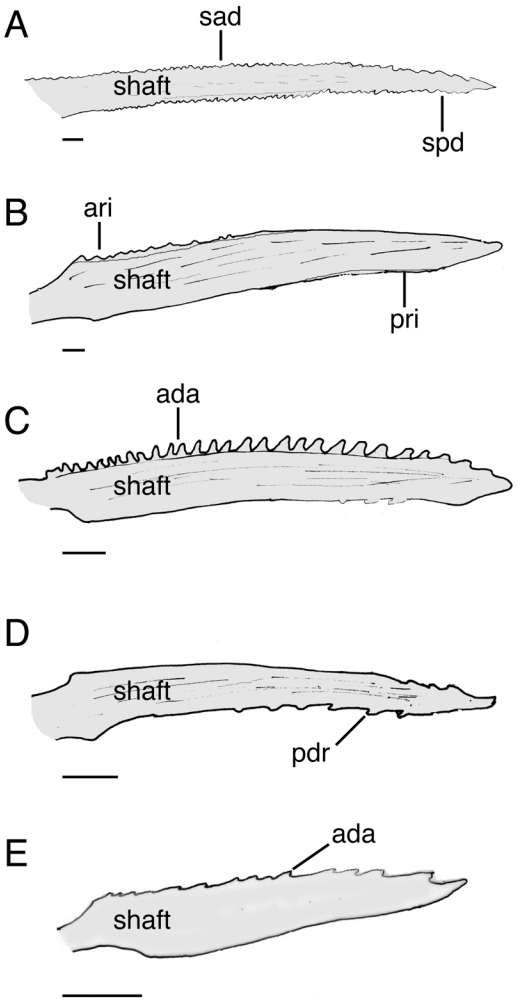

Fig. 16. Dorsal-fin spine. A. *Centromochlus heckelii*, MPEG 4977, 83.5 mm SL. B. *Glanidium botocudo*, MNRJ 32539, 82.0 mm SL. C. *Tatia perugiae*, MZUSP 26684, 35.9 mm SL. D. *Tatia romani*, MCNG 14896, 29.0 mm SL. E. *Tatia britskii*, MZUSP 115271, 39.2 mm SL. Abbreviations: ada, anterior serrations antrorse; sad, small anterior serrations; ari, anterior ridge; pdr, posterior serrations retrorse; spd, small posterior serrations; pri, posterior ridge; shaft, spine shaft. Scale bar = 1 mm.

76. *Shape of serrations on proximal end of anterior margin of dorsal-fin spine* (CI 1.0, RI 1.0). State 0: anterior proximal margin of dorsal spine with lanceolate serrations (Fig. 16C); state 1: with small undulations imparting rugose surface (Fig. 16B); state 2: smooth margin (Fig. 16D). State 1 is synapomorphic for *Glanidium*. Coded as inapplicable for *Gelanoglanis nanonocticolus* and *G. travieso*, as these taxa do not have a spinous dorsal-fin ray, and for *Tatia romani* and *T. meridionalis* as the spine margin is smooth proximally.

77. *Texture of serrations on posterior border of dorsal-fin spine* (CI 0.17, RI 0.55). State 0: posterior margin smooth; state 1: small, blunt serrations in a longitudinal groove along posterior margin (Fig. 16A). State 1 found in *Centromochlus*. Coded as inapplicable for *Gelanoglanis nanonocticolus* and *G. travieso* as these taxa do not have a spinous dorsal-fin ray.

78. *Size of serrations on distal tip of posterior margin of dorsal-fin spine* (CI 0.50, RI 0.86). State 0: small serrations on distal posterior margin; state 1: well-formed retrorse serrations on distal posterior margin of dorsal-fin spine (Fig. 16C; Royero, 1987; Royero, 1999: #79; Akama, 2004: #130; Birindelli, 2014: #245). The serrations are well-formed and retrorse in Clade B *Tatia* (*T. altae, T. ferrarisi, T. meridionalis, T. perugiae, T. reticulata, T. romani*) and independently acquired in *Gephyromochlus leopardus*. Coded as inapplicable for *Gelanoglanis nanonocticolus* and *G. travieso* as these taxa do not have a spinous dorsal-fin ray. Also coded as inapplicable for *Centromochlus* as the entire spine is serrated posteriorly (i.e., serrations not limited to distal margin). The presence of serrations on the posterior face of the dorsal-fin spine is highly variable among catfishes. Plesiomorphically among catfishes, as in the Diplomystidae, the posterior margin of the dorsal spine is without any conspicuous serrations (Arratia, 1987). Although in some Doradidae and Auchenipterinae, including *Liosomadoras oncinus*, the posterior margin of the dorsal spine has well-formed and pointed serrae. In others, such as *Pseudotatia parva* and *Tocantinsia piresi*, the posterior border is smooth.

79. *Dorsal-fin spine lateral surface* (CI 1.0, RI 1.0). State 0: with ridges and grooves (Fig. 16A-D); state 1: smooth (Fig. 16E). The entire lateral surface of dorsal-fin spine is smooth in *Tatia bockmanni*, *T. britskii* and *T. simplex*. Most centromochlin species have lateral surface of spine coarsely textured with patterns of ridges and grooves.

80. *Dorsal-fin spine size* (CI 1.0, RI 1.0). State 0: moderately developed, dorsal-fin spine length 30% or less of standard length (SL); state 1: well developed, dorsal-fin spine length about 35 to 40% SL. Well-developed dorsal-fin spine synapomorphic for the clade consisting of *C. existimatus*, *C. heckelii* and *C. macracanthus* (Soares-Porto, 1998: #23; Birindelli, 2014: #238). Coded as inapplicable for *Gelanoglanis nanonocticolus* and *G. travieso*, species lacking a spinous dorsal fin.

81. *Number of branched dorsal-fin rays* (CI 1.0, RI 1.0). State 0: six to eight; state 1: four to five. Four to five branched dorsal fin rays is synapomorphic for Centromochlinae (Britski, 1972: 29; Akama, 2004: #128; Birindelli, 2014: #237; Calegari et al., 2019: #3678). Most centromochlins have five branched dorsal-fin rays, but some individuals of *Tatia punctata* exceptionally have four. *Pseudotatia parva* has six branched dorsal-fin rays. Among catfishes, the number of branched dorsal-fin rays is quite variable, but phylogenetically informative for certain groups, including Auchenipteridae. Some auchenipterins, such as *Entomocorus*, *Pseudepapterus*, *Spinipterus*, *Trachelyopterus*, *Trachycorystes* also have five branched dorsal-fin rays (Birindelli, 2014: #237). Most species of the Auchenipteridae and Doradidae have six branched dorsal-fin rays (Birindelli, 2014).

Paired fins.—Characters 82–92 pertain to the pectoral and pelvic fins and the support structures of the former.

82. *Size of coracoid process* (CI 1.0, RI 1.0). State 0: long, surpassing pectoral-fin base (Fig. 17A,B); state 1: small, comparatively shorter than pectoral-fin base. A small coracoid process is diagnostic for *Tatia* (Fig. 17C). Within the Auchenipterinae, the coracoid process is long, extending well beyond the posterior extremities of the dorsal processes of the cleithrum (Vigliotta, 2008; Birindelli, 2014). A posterior coracoid process comparatively shorter than anal-fin base in *Tatia* is interpreted as a new development.

83. *Humeral spine size* (unordered; CI 0.67, RI 0.89). State 0: moderately developed, length of humeral spine 15–25% SL (Fig. 2F); state 1: weakly developed, length of humeral spine 12.0–14.4% SL; state 2: reduced, length of humeral spine less than 12.0% SL. The humeral spine (posterior cleithral process) is weakly developed in *Tatia dunni, T. brunnea, T. caudosignata* and *T. nigra* (State 1), and extremely reduced in *Gelanoglanis* (State 2). In most Auchenipteridae the posterior cleithral process is moderately developed (Poll, 1971; Vigliotta, 2008: #54; Birindelli, 2014: #266). The scarcely developed posterior cleithral process in *Gelanoglanis* is a larval characteristic (Lundberg et al., 2004).

84. *Size of postcleithrum dorsal process* (CI 0.7, RI 0.9). State 0: comparatively shorter or same length as first unbranched pectoral-fin ray; state 1: comparatively longer than first unbranched pectoral-fin ray. Dorsal process of the postcleithrum is elongate, longer than first unbranched pectoral-fin ray in *G. varii* and *G. nanonocticolus* (Vari & Calegari, 2016)

85. *Exposure of posterior coracoid process* (CI 1.0, RI 1.0). State 0: covered by thick skin (Fig. 17C); state 1: covered by thin skin, externally visible (Fig. 17A). Coracoid externally visible in *Centromochlus heckelii, C. existimatus, C. macracanthus* and *C. schultzi*. In auchenipterins with elongate bodies such as *Pseudotatia*, *Auchenipterus*, *Epapterus* and *Pseudepapterus* the posterior coracoid process is elongated, extending well beyond base of pectoral-fin rays, but not visibly exposed (Soares-Porto, 1998: #21; Ferraris & Vari, 1999; Ferraris & Vari, 2000; Vari & Ferraris, 2006; Birindelli, 2014: #270, #272). An

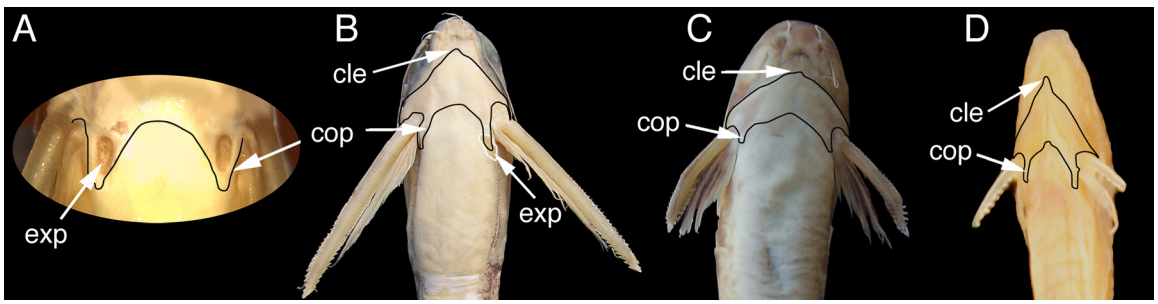

Fig. 17. Ventral view of pectoral girdle with contours outlined in black. A. *Centromochlus existimatus*, INPA 40662, 59.0 mm SL. B. *Centromochlus macracanthus*, MZUSP 30605, paratype, 71.8 mm SL. C. *Tatia brunnea*, AMNH 74441, 80.9 mm SL. D. *Gelanoglanis stroudi*, FMNH 83911, 23.0 mm SL. White arrows indicates anteriormost extent of cleithrum and posterior process of cleithrum. Abbreviations: cle, cleithrum joint angle; cop, coracoid process; exp, exposed coracoid externally visible.

externally visible posterior coracoid process is uniquely derived for the clade containing *Centromochlus heckelii, C. existimatus, C. macracanthus* and *C. schultzi*, and attains a largely exposed area in *C. existimatus* (Fig. 17A).

86. *Third pectoral-fin radial* (CI 1.0, RI 1.0). State 0: present; state 1: absent. The third pectoral-fin radial is absent in *Gelanoglanis stroudi*, *G. nanonocticolus*, *G. travieso* and *G. pan*. In most Auchenipteridae, the second and third proximal radials of the pectoral fin are enlarged distally and support several rays (Ferraris, 1988: #P10; Walsh, 1990: #6; Royero, 1999: #90; Akama, 2004: #115; Birindelli, 2014: #255; Calegari et al., 2019: # 3698). In *Gelanoglanis*, the pectoral fin is reduced, with four or five rays, and the third proximal radial is missing.

87. *Serrations on anterior margin of pectoral-fin spine* (CI 0.50, RI 0.75). State 0: present (Fig. 18A); state 1: absent (Fig. 18C). The anterior margin of the pectoral fin-spine is serrated and uniquely derived for the clade composed of *Gephyromochlus leopardus, Gelanoglanis* and *Centromochlus*. In *Centromochlus*, the character is reversed and serrations are present on the anterior margin at some point during ontogeny (Fig. 18C). Among basal catfishes, including Diplomystidae, the anterior margin of the pectoral spine is keeled, but without serrations (Arratia, 1987). However, in doradids and auchenipterins *Tocantinsia* and *Pseudotatia*, the anterior margin of the pectoral spine has well-developed serrations. Some auchenipterins such as *Ageneiosus, Auchenipterus, Epapterus, Pseudauchenipterus, Pseudepapterus, Tetranematichthys,* and *Trachelyopterus coriaceus* lack serrations on the anterior face of the pectoral-fin spine (Ferraris, 1988: #P7; Soares Porto, 1998: #20; Royero, 1999: #88; Walsh, 1990: #34; Akama, 2004: #107; Birindelli, 2014: #257; Calegari et al., 2019: #3702). The character was coded inapplicable for *Gelanoglanis nanonocticolus* as the first pectoral-fin ray is a filamentous simple ray instead of the stout spine of congeners.

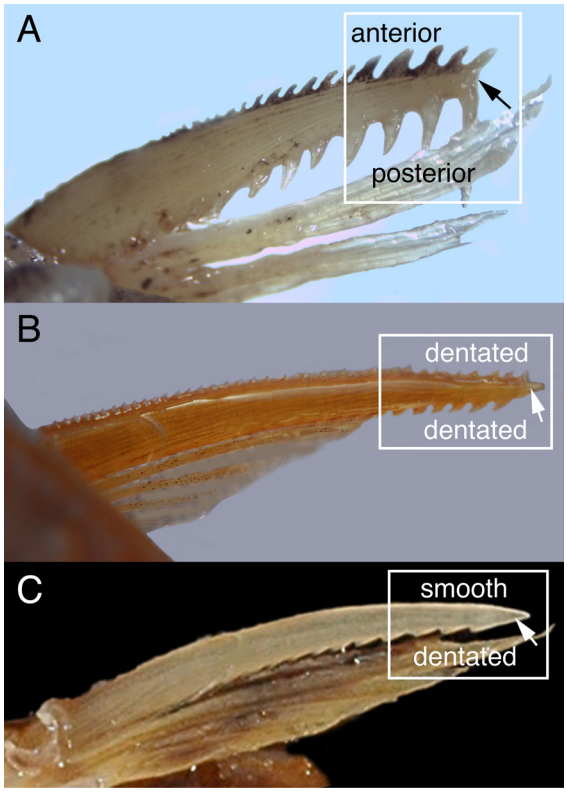

Fig. 18. Pectoral-fin spine. A. *Glanidium albescens*, MCNIP 1084. B. *Centromochlus musaicus*, MCNG 21796, 50.8 mm SL. C. *Gephyromochlus leopardus*, ZMA 102 233, 100.0 mm SL. Right spine in dorsal view with directional terms and position of serrations. White arrow indicates spine tip.

88. *Shape of tip of pectoral-fin spine shaft* (CI 1.0, RI 1.0). State 0: bifurcated, with fin-spine segments distal to spine shaft tip (Fig. 18A); state 1: tip pointed, formed by last anterior serration (Figs. 18B,C). The tip of pectoral-fin spine shaft is non-bifurcated and synapomorphic for the clade composed of *Gephyromoclus*, *Centromochlus* and *Gelanoglanis*. Coded as inapplicable for *Gelanoglanis nanonocticolus* as the first pectoral-fin ray is a filamentous simple ray instead of the stout spine of congeners.

89. *Grooves on pectoral-fin spine shaft* (CI 1.0, RI 1.0). State 0: present (Fig. 18A); state 1: absent (Fig. 18C). The grooves on pectoral-fin spine shaft are absent and synapomorphic for the claded composed of *Gephyromoclus, Centromochlus*, *and Gelanoglanis*. The character was coded inapplicable for *Gelanoglanis nanonocticolus* as the first pectoral-fin ray is a filamentous simple ray instead of the stout spine of congeners.

90. *Anterior distal serrations on pectoral-fin spine edge* (CI 0.50, RI 0.75). State 0: present (Fig. 18A); state 1: absent (Fig. 18C). Anterior distal serrations on pectoral-fin spine absent and synapomorphic for the *Centromochlus*, *Gephyromoclus* plus *Gelanoglanis* clade, but reversed in *Centromochlus*, as a short ridge on anterior distal edge is observed (Fig. 18B). The presence or absence of serrations along the anterior margin of the pectoral spine is phylogenetically informative for groups within the Siluriformes (Vigliotta, 2008: #59). The character is coded inapplicable for *Gelanoglanis nanonocticolus* as the first pectoral-fin ray is a filamentous simple ray instead of the stout spine of congeners.

91. *Number of posterior serrations on pectoral-fin spine* (CI 1.0, RI 1.0). State 0: 6–20 serrations (Fig. 19G); state 1: 25–45 serrations (Fig. 19C). State 1 is synapomorphic for *Centromochlus*. In *Centromochlus*, the spine has numerous, retrorse posterior serrations. Although posterior serrations are irregularly spaced in some adult *C. schultzi*, the serrations are numerous, regularly spaced and oriented retrorsely in small specimens. Coded as inapplicable for *Gelanoglanis nanonocticolus* as the first pectoral-fin ray is a filamentous simple ray instead of the stout spine of congeners. Also coded as inapplicable for *Gephyromochlus leopardus* as posterior border has long sharp serrae instead of small serrations (Fig. 17C).

92. *Pelvic-fin margin* (CI 0.50, RI 0.25). State 0: rounded; state 1: pointed (Ferraris, 1988: #PV5). The pelvic fin margin is pointed in *Centromochlus existimatus* (anterior unbranched ray long with subsequent rays progressively shorter). Condition is similar to *Gelanoglanis nanonocticolus*, but in that species the pointed pelvic fin is due to sexual dimorphism (Fig. 4) and independently acquired. In the remaining centromochlins, as in most Doradoidea, a the pelvic fin margin is rounded with the unbranched ray almost the same length as subsequent ones.

Anal fin and supports.—Characters 93–115 pertain to the arrangements and variation of rays and supports

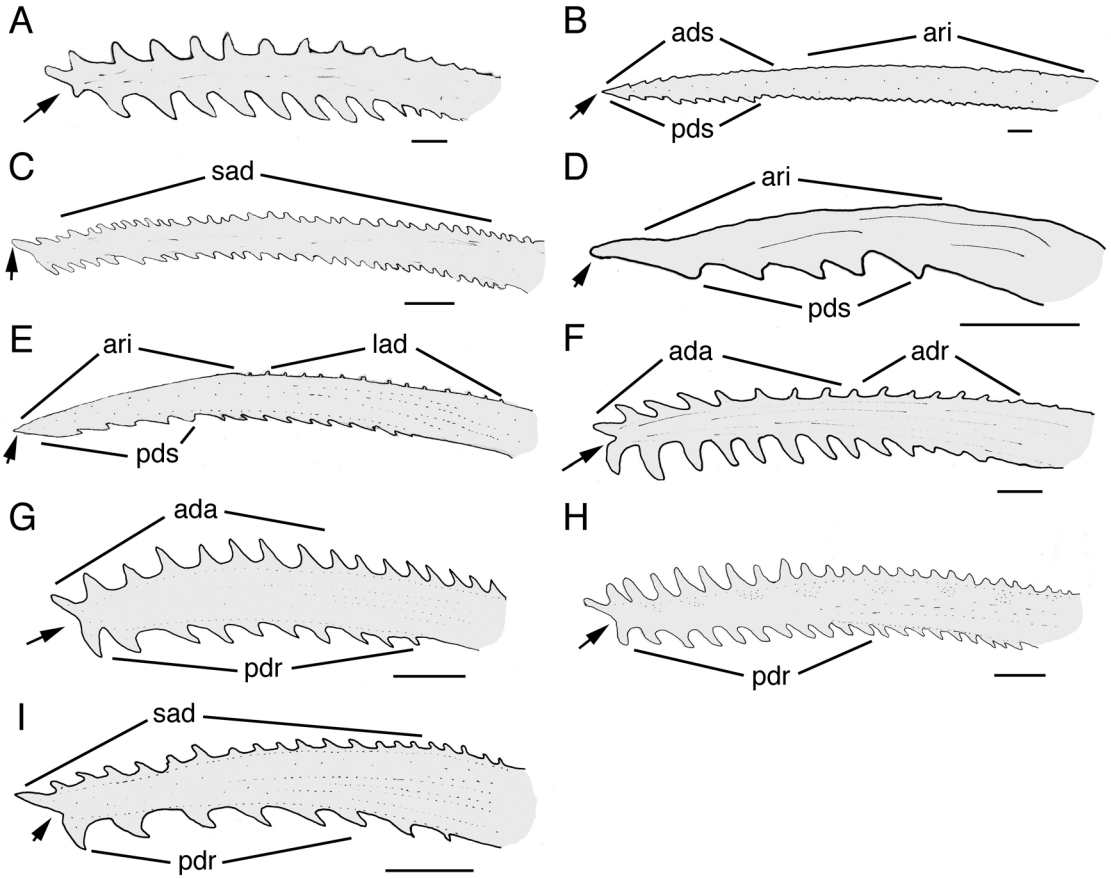

Fig. 19. Pectoral-fin spine. A. *Pseudotatia parva*, FMNH 70580, 47.2 mm SL, holotype, photo by M.W. Littmann. B. *Centromochlus heckelii*, MPEG 4977, 83.5 mm SL. C. *Centromochlus musaicus*, ANSP 160656, 57.0 mm SL. D. *Gelanoglanis stroudi*, FMNH 83912, 24.6 mm SL, paratype. E. *Gephyromochlus leopardus*, ZMA 102 233, 100.0 mm SL. F. *Glanidium albescens*, MBML 11230, 23.1 mm SL. G. *Tatia aulopygia*, MZUSP 31075. H. *Tatia punctata*, RMNH 26495, 45.0 mm SL, holotype. I. *Tatia perugiae*, MZUSP 31880, 28.2 mm SL. Abbreviations: ada, anterior serrations antrorse; ads, anterior distal serrae; ari, anterior ridge; lad, Small clusters of low anterior serrations; pdr, posterior serrations retrorse; pds, posterior distal serrae; pri, posterior ridge; sad, small anterior serrations; spd, small posterior serrations. Arrow indicate distal pectoral fin spine shaft tip. Scale bar = 1 mm.

observed during maturity. In species with no availability of mature specimens for examination, the following features are usually coded as missing data, with the exception of meristic characters.

93. *Direction of anal-fin proximal radials in adult males* (CI 1.0, RI 1.0). State 0: in transverse orientation to vertebral axis (Birindelli, 2014: 470 fig. 18c); state 1: aligned nearly parallel to vertebral axis (Figs. 20B; 21A,B; Ferraris, 1988: #A5, #A6; Soares-Porto, 1998: #28; Akama, 2004: #133, #152; Birindelli, 2014: #289). The oblique anal-fin rays in males is diagnostic for the subfamily Centromochlinae. The anal-fin proximal radials in mature males of all Centromochlinae are oblique and posteriorly oriented relative to the body axis (Soares-Porto, 1998: #28; Royero, 1999: #132; Akama, 2004: #147; Birindelli, 2014: #288; Calegari et al., 2019: #3738). State 0 in *Pseudotatia parva*. In Auchenipterinae, the anal-fin proximal radials in mature males are oriented transversely to vertebral axis.

94. *Partial fusion of proximal radials in modified anal fin of adult males* (CI 1.0, RI 1.0). State 0: absent, proximal radials independent; state 1: proximal radials partially or completely connected to each other (Figs. 20B; 21A,B). The proximal radials of the anal fin are independent in *Pseudotatia parva*. The proximal radials of the anal fin are partially or completely connected in *Gelanoglanis*, *Glanidium*, *Gephyromochlus leopardus* and young *Tatia* and *Centromochlus*. This character is diagnostic for Centromochlinae, with differences among included genera (Ferraris, 1988: #A7; Soares-Porto, 1998: #30; Royero, 1999: #139; Akama, 2004: #153; Birindelli, 2014: #291; Calegari et al., 2019: #3739). In mature males of *Glanidium,* the anterior proximal radials are fused and the posterior ones are usually sutured through its middle portion (Fig. 20A). Such a condition was observed in mature males of *Gephyromochlus* and all species of *Glanidium*.

95. *Complete fusion of proximal radials in modified anal fin of adult males* (CI 1.0, RI 1.0). State 0: anterior proximal radials fused, posterior ones joined but not fused (Fig. 21A); state 1: anterior and posterior proximal radials fused (Fig. 21B; Soares-Porto, 1998: #30)). In mature males of *Tatia*, *Centromochlus* and *Gelanoglanis,* the proximal radials are completely fused, indicating a progressive change towards complete fusion of elements in remaining centromochlins. In auchenipterins, the proximal radials are not sutured together in mature males.

96. *Length* of *anal-fin rays in mature males* (CI 0.67, RI 0.95). State 0: long, length of anal-fin rays more than 8% SL; state 1: short, length of anal-fin rays less than 7% SL (Figs. 20B,C; Soares-Porto, 1998: #27; Soares-Porto et al., 1999; Sarmento-Soares & Martins-Pinheiro, 2008: 498; Birindelli, 2014: #290). Anal-fin rays short in Clade A *Tatia* (i.e., *T. aulopygia*, *T. boemia*, *T. brunnea*, *T. caxiuanensis, T. caudosignata*, *T. gyrina, T. meesi*, *T. dunni, T. galaxias,*

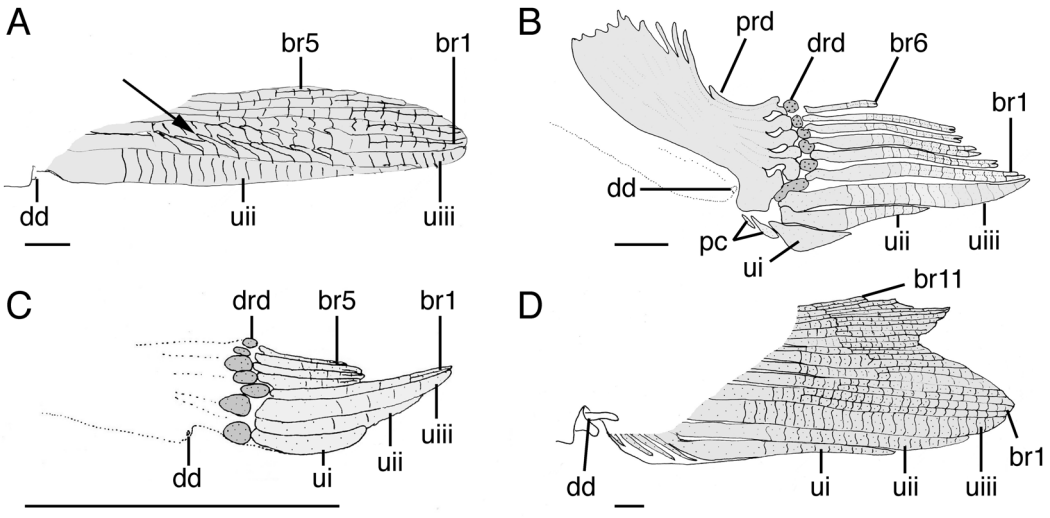

Fig. 20. Anal-fin rays. A. *Centromochlus heckelii*, INPA 10967, 108.7 mm SL. B. *Tatia meridionalis*, MBML 5616, 46.2 mm SL. C. *Gelanoglanis nanonocticolus* MZUSP 28308, paratype. D. *Gephyromochlus leopardus*, ZMA 102 233, 34.8 mm SL. Abbreviations: br, branched ray (numbered accordingly); dd, deferent duct; drd, distal radial; pc, procurrent rays; prd, proximal radial; ui, unbranched first ray; uii, unbranched second ray; uiii, unbranched third ray. Arrow indicates retrorse curved segment. Scale bar = 1.0 mm.

T. intermedia, T. jaracatia, T. neivai, T. nigra, and *T. strigata*). The small anal fin in *Gelanoglanis* is interpreted as an independent acquisition relative to Clade A *Tatia*.

97. *Thickness of anal-fin rays in mature males* (CI 1.0, RI 1.0). State 0: anterior rays as thick as posterior ones; state 1: anterior rays thicker than posterior ones (Figs. 20–21). The derived state is synapomorphic and diagnostic for Centromochlinae.

98. *Reduction of anal-fin rays in adult males* (unordered; CI 0.67, RI 0.67). State 0: all rays similar in size (Figs. 20A,B); state 1: four rays reduced (Figs. 20C,D); state 2: two rays reduced (Fig. 21C). Four anal fin rays are reduced in *Gephyromochlus leopardus*, and this condition is independently acquired in *Gelanoglanis nanonocticolus* and *G. pan*. Two anal fin rays are reduced in *Tatia aulopygia* and *T. strigata*. In centromochlin catfishes, only mature males of *Gephyromochlus* and *Tatia* have a notch in anterior border of anal fin as a result of reduction of rays in mature males. In *Gephyromochlus leopardus,* branched rays 4–7 are shortened, while in *Gelanoglanis nanonocticolus* and *G. pan* the second to fifth branched rays are reduced. In *Tatia strigata,* the second and third branched rays are reduced, and in *T, aulopygia* the fourth and fifth branched rays are reduced.

99. *Number of segments on third unbranched anal-fin ray of males* (CI 1.0, RI 1.0). State 0: same number of segments in males and females; state 1: more segments in males. There are more segments in males than in females in *Glanidium* (Fig. 20D). In the remaining auchenipterids, females have the same number of segments as males.

100. *Number of unbranched anal-fin rays* (CI 1.0, RI 1.0). State 0: three; state 1: two. Centromochlins exhibit three unbranched anal-fin rays, except *Centromochlus heckelii*, *C. existimatus* and *C. macracanthus*, which have only two (Fig. 20A).

101. *Number of branched anal-fin rays* (unordered; CI 0.50, RI 0.80). State 0: eight or more (Figs. 19D, 20A); state 1: seven; state 2: six (Fig. 19A,B); state 3: five (Fig. 20C). State 0 found in *Glanidium*. This character condition evolved in four steps. State 1 is synapomorphic for the clade composed of *Gelanoglanis*, *Centromochlus* and *Tatia* (step 1). A reversal is observed in *Gephyromochlus leopardus* (step 2). State 2 is acquired in *Gelanoglanis nanonocticolus* (step 3) and common ancestor of *C. existimatus* + *C. heckelii* (step 4). Ambiguities were evaluated using ACCTRAN. Centromochlin catfishes usually have reduced number of 5–8 branched anal-fin rays, exceptionally 11 in *Gephyromochlus leopardus*. Most species of *Tatia* have seven rays, whereas six rays is common in *Tatia perugiae, T. reticulata, T. romani, T. ferrarisi* and *T. meridionalis*. Most auchneipterins have more than eight anal-fin rays (Ferraris, 1988: #A2; Walsh, 1990: #29; Royero, 1999: #93; Akama, 2004: #132; Birindelli, 2014: #287) including *Pseudotatia parva* with more than 15 rays.

102. *Size of first anterior distal radial on modified male anal fin* (CI 1.0, RI 1.0). State 0: anterior first distal radial as large as posterior distal radials; state 1: anterior first distal radial much larger than posterior ones (Fig. 20B). State 1 observed in *Tatia altae, T. ferrarisi, T. meridionalis, T. perugiae,* and *T. romani*. In centromochlin catfishes, the distal radial cartilages supporting anal fin are somewhat similar in size, with the posterior ones becoming progressively smaller. The exceptionally larger anterior first distal radial is a derived feature in *Tatia altae, T. ferrarisi, T. meridionalis, T. perugiae,* and *T. romani*.

103. *Spines on segments of first branched anal-fin ray of mature males* (CI 1.0, RI 1.0). State 0: segments not spinous anteriorly; state 1: spinous anteriorly (Fig. 20B, Ferraris, 1988: #A11; Soares-Porto, 1998: #37; Royero, 1999: #134, #135, #137; Birindelli, 2014: #310). The presence of retrorse spines on segments of first branched anal-fin ray of mature males is synapomorphic for a clade composed of *Tatia aulopygia*, *T. boemia*, *T. brunnea*, *T. caudosignata*, *T. dunni, T. galaxias, T. intermedia, T. jaracatia, T. neivai, T. nigra,* and *T. strigata*. In *Tatia caxiuanensis,* some specimens have segments with small retrorse spines and some not; coded as polymorphic for this feature.

104. *Position of spines on segments of anterior anal-fin rays of mature males* (CI 0.50, RI 0.75). State 0: spines absent from posterior margin of segments (Figs. 20C–D); state 1: retrorse curved spines along posterior margin, forming a sharp keel (Fig. 20A; Ferraris, 1988: #A9; Soares-Porto, 1998: #38; Royero, 1999: #134, #136; Akama, 2004: #157; Birindelli, 2014: #293). State 1 found in *Centromochlus heckelii* and *C. existimatus*, and independently acquired in *Tatia altae, T. perugiae*, and *T. romani*.

105. *Spines on segments along anterior margin of third unbranched anal-fin ray of mature males* (CI 0.50, RI 0.91). State 0: absent; state 1: present (Fig. 20B; Ferraris, 1988: #A11; Soares-Porto, 1998: #37, #39; Royero, 1999: #134, #135, #137; Akama, 2004: #155, #156; Birindelli, 2014: #294). State 1 synapomorphic for a clade composed of *Tatia aulopygia*, *T. boemia*, *T. brunnea*, *T. caudosignata*, *T. dunni, T. galaxias, T. intermedia, T. jaracatia, T. neivai, T. nigra*, and *T. strigata*; independently acquired in *T. caxiuanensis*.

106. *Arrangement of rays on tip of modified anal-fin rays of mature males* (CI 0.50, RI 0.95). State 0: all rays converging towards tip; state 1: two rays, the first and third unbranched rays, converging towards the tip (Fig. 21B; Ferraris, 1988: #A10). The first and third unbranched ray converge towards tip in *Tatia*. Condition independently acquired in *Gelanoglanis nanonocticolus*.

107. *Serrations on distal segments of third unbranched anal-fin ray of mature males* (CI 1.0, RI 1.0). State 0: absent; state 1: present (Fig. 21A; Akama, 2004: #155, #156; Birindelli, 2014: #310). The presence of serrations is diagnostic for a clade composed of *Glanidium ribeiroi*, *G. melanopterum* and *G. catharinensis*. During maturity in these species of *Glanidium*, the third unbranched ray, and sometimes the second, have the distal segments of the anterior rays with a rough, serrated margin.

108. *Number of procurrent rays on modified anal fin of mature males* (CI 0.28, RI 0.75). State 0: one; state 1: two (Fig. 20B); state 2: usually three procurrent rays, rarely four or five. There are two procurrent rays on the modified anal fin of mature males in *Tatia altae*, *T. ferrarisi*, *T. meridionalis*, *T. perugiae*, *T. reticulata* and *T. romani*. There are more than two procurrent rays on the modified anal fin of mature males in *Gephyromochlus* and *Glanidium*. State 2 also observed in *Pseudotatia parva*. There is only one procurrent ray on the modified anal fin of mature males in *Tocantinsia piresi*.

109. *Fleshy tegumentary keel on anterior margin of modified anal fin of mature males* (CI 1.0, RI 1.0). State 0: absent; state 1: present during final phase of male maturity (Fig. 21C. State 1 in *Tatia aulopygia*, *T. brunnea, T. caudosignata*, *T. dunni*, *T. galaxias*, *T. intermedia, T. nigra,* and *T. strigata*. The presence of a tegumentary keel was recognized as polymorphic (0/1) for *T. neivai* and *T. gyrina* species.

110. *Vestigial rays at posterior end of anal fin* (CI 1.0, RI 1.0). State 0: absent; state 1: present (Fig. 21D; Soares-Porto, 1998: #36). Sixth and/or seventh branched anal-fin rays are vestigial in Clade C *Tatia*: *T. concolor, T. bockmanni, T. britskii, T. punctata, T. simplex,* and *T. marthae*.

111. *Fusion of segments on first unbranched anal-fin ray* (CI 0.50, RI 0.94). State 0: segments not fused; state 1: segments fused (Figs. 20B, 21B,C; Soares-Porto, 1998: #33; Sarmento-Soares & Martins-Pinheiro, 2008: 498; Birindelli, 2014: #298). The segments are fused in a variety of *Tatia*, such as *T. altae, T. aulopygia*, *T. boemia, T. caxiuanensis*, *T. ferrarisi, T. galaxias, T. gyrina, T. intermedia, T. jaracatia, T. meesi, T. meridionalis, T. perugiae, T. neivai, T. caudosignata*, *T. reticulata, T. romani* and *T. strigata*. The character is coded as polymorphic for *Tatia brunnea* and *T. dunni* wherein both conditions are present.

112. *Thickness of last unbranched anal-fin ray of mature males* (CI 1.0, RI 1.0). State 0: width of last unbranched anal-fin ray equal to preceding ray; state 1: width of last unbranched anal-fin ray much larger than first branched ray (Fig. 20B; Soares-Porto, 1998: #34). State 1 is diagnostic for a clade composed of *Tatia altae*, *T. ferrarisi*, *T. meridionalis*, *T. perugiae,* and *T. romani*. The character is coded as polymorphic (0/1) for *Tatia reticulata*.

113. *Connective tissue enclosure of first, second and third anal-fin unbranched rays of mature males* (CI 1.0, RI 1.0). State 0: first three unbranched rays of anal fin of mature males loosely attached to each other; state 1: first three unbranched rays of the anal fin of mature males tightly attached to form a rigid anterior fin margin. State 1 is synapomorphic for the clade composed by *Tatia brunnea*, *T. caudosignata*, *T. dunni*, and *T. nigra*. Ferraris (1988: #A14) associated the rigid fin margin to the transfer of sperm.

114. *Muscle inclinator anales in nuptial males* (CI 1.0, RI 1.0). State 0: in separate bundles (Fig. 21E); state 1: conjoined, packed into a single bundle with mixed fibers (Fig. 21F). A voluminous muscle *inclinator anales* is modified in nuptial males of *Tatia,* permitting anal fin rotational movements to a transverse position during maturity. The muscle *inclinator anales* arises in the fascia between the skin and the hypaxial body musculature. It usually inserts between the bases of the anal-fin rays, distal to the insertions of the *erectores* and *depressores anales* (Winterbottom, 1974). *Tatia* is the only centromochlin catfish with *inclinatores anales* that are well developed anteriorly with mixed fibers. In these catfishes, nuptial males curve and fold the modified anal fin during reproduction.

115. *Muscle erectores anales in anal fin of sexually mature males* (CI 1.0, RI 1.0). State 0: arranged as parallel bundles along proximal radials (Fig. 21E); state 1: conjoined, as compacted muscle bundles, permitting anal-fin rays to be arranged into a tube during reproduction (Fig. 21F). In most Auchenipteridae, the muscle *erector anales* is arranged as parallel muscle bundles along the proximal radials of the anal fin with tendinous insertions on the anterolateral base of rays. A

compaction of *erector anales* fibers is synapomorphic for a subgroup of clade A *Tatia* composed of *T. aulopygia, T. brunnea, T. caudosignata*, *T. dunni, T. galaxias, T. intermedia, T. nigra* and *T. strigata*. The muscle *erectores anales* allows the manipulation of the anal fin to form a tube through which sperm can transfer. Ferraris (1988: #A14) reported the arrangement of anal fin rays in a tube and associated it with rigid anterior unbranched rays (Character #111 herein). We observed the anal fin of some specimens bent laterally with rays forming a tube (Fig. 21F; Sarmento-Soares & Martins-Pinheiro, 2008: fig. 39b).

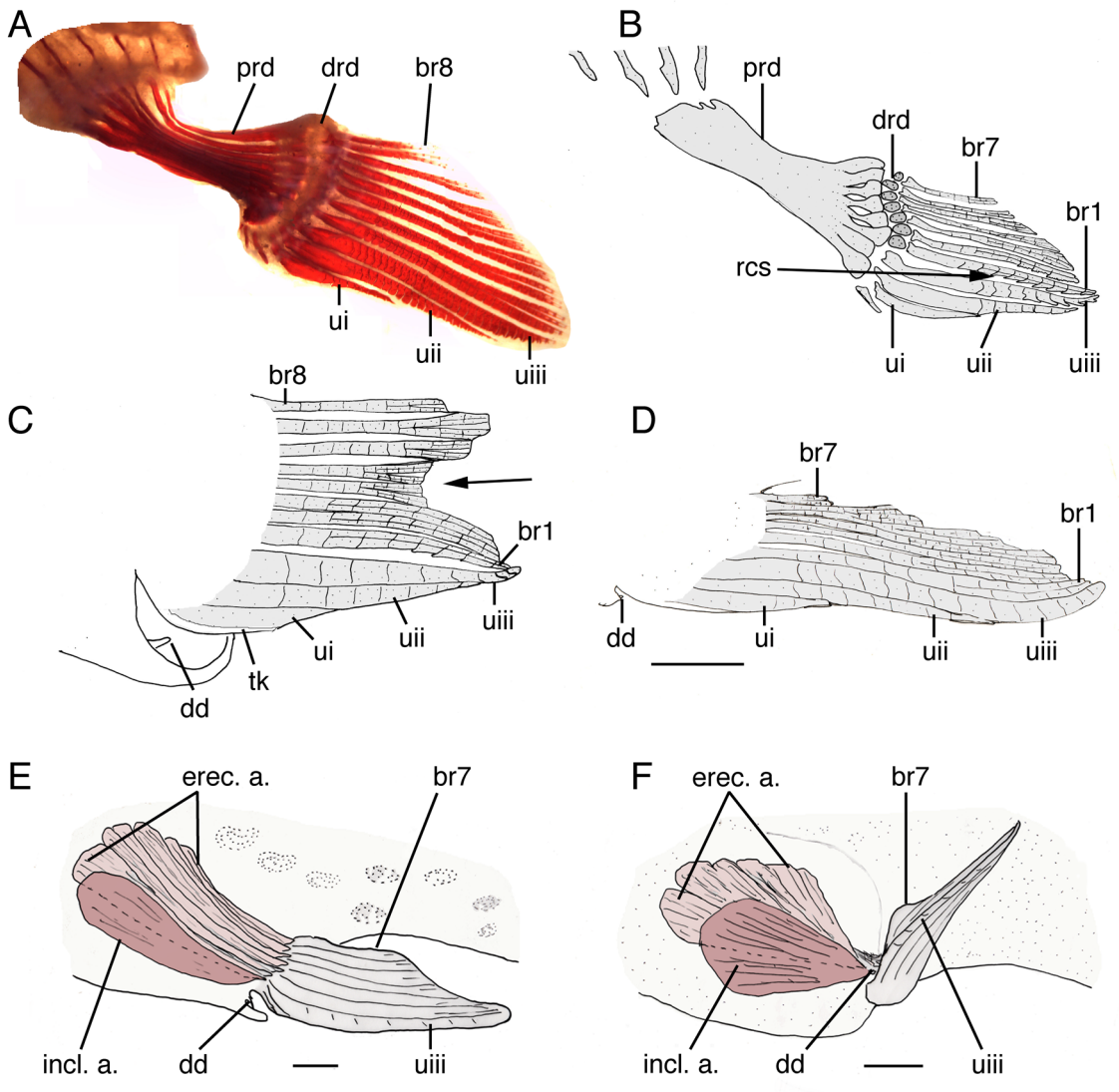

Fig. 21. Anal-fin rays (A-D) plus anal-fin erectors and inclinators muscles (E-F). A. *Glanidium catharinensis*, MZUSP 9308, 103.2 mm SL. B. *Tatia intermedia*, RMNH 26199, 50.0 mm SL. C. *T. aulopygia*, INPA 11080, 104.6 mm SL. D. *T. punctata*, RMNH 26495, 45.0 mm SL, holotype. E. *Centromochlus schultzi*, UNT 16340, 98.2 mm SL. F. *Tatia galaxias*, MCNG 15001, 28.3 mm SL. Abbreviations: br1, branched ray one; br7, branched ray seven; br8, branched ray eight; dd, deferent duct; drd, distal radial; erec. a. erectors anales; hs, hemal spines; incl. a., inclinators anales; prd, proximal radial; rr, rudimentary rays; tk, tegumentary keel; ui, unbranched first ray; uii, unbranched second ray; uiii, unbranched third ray. The hypaxials, posterior inclinators anales, and depressors anales removed. Short arrow indicates ray shortening. Long arrow indicates retrorse curved segment (rcs). Scale bar = 1 mm.

Pelvic and anal fin supports.—Characters 116–118 pertain to pelvic- and caudal-fin related structures.

116. *Number of pelvic-fin branched rays* (CI 1.0, RI 1.0). State 0: six; state 1: five. Six rays in Auchenipterinae. Five rays in Centromochlinae. The pelvic-fin ray count in the Centromochlinae is herein interpreted as a derived feature relative to that in the Auchenipterinae.

117. *Ventral process on hypurapophysis* (CI 1.0, RI 1.0). State 0: absent (Fig. 22B); state 1: present (Fig. 22A; Ferraris, 1988: #C5; Akama, 2004: #139; Birindelli, 2014: #304; Calegari et al., 2019: #3748). State 1 in species of *Centromochlus*. In most Auchenipteridae, the hypurapophysis and secondary hypurapophysis together form a low arch with no projection. In *Centromochus existimatus* and *C. heckelii,* for example, a conspicuous ventral process is visible as a directed spur on the hypurapophysis. Besides *Centromochlus*, such a process was observed in auchenipterins with pelagic habits such as *Auchenipterus*, *Entomocorus*, *Epapterus*, and *Pseudepapterus* (Ferraris, 1988: #C5; Akama, 2004: #139; Birindelli, 2014: #304, fig. 66a).

118. *Length of caudal-fin lobes in mature males* (CI 1.0, RI 1.0). State 0: lobes of same length; state 1: upper lobe longer than lower lobe. Adapted from Ferraris (1988: #C6) and Soares-Porto (1998: #24). Among catfishes, the shape of the caudal fin is highly variable, but phylogenetically informative for some groups, including Centromochlinae. In most centromochlins, the caudal-fin lobes are the same size in both males and females. However, mature males of *Tatia aulopygia, T. boemia, T. brunnea, T. caudosignata*, *T. dunni, T. galaxias, T. intermedia, T. jaracatia, T. neivai, T. nigra,* and *T. strigata* exhibit an elongated upper caudal-fin lobe, which is herein hypothesized as synapomorphic for the clade composed of these species.

Mandibular muscles and associated head bones.—Characters 119–132 pertain to some cranial muscles, mandibular muscles and associated head bones. Much variation was observed in the mandibular muscles of centromochlin catfishes, especially in the adductor mandibulae muscle complex. Regarding centromochlins, specimen dissection was unavailable for *Gelanoglanis stroudi*, *G. nanonocticolus*, *G. travieso, G. pan, Tatia altae*, *T. ferrarisi*, *T. concolor, T. marthae*, and *T. punctata*.

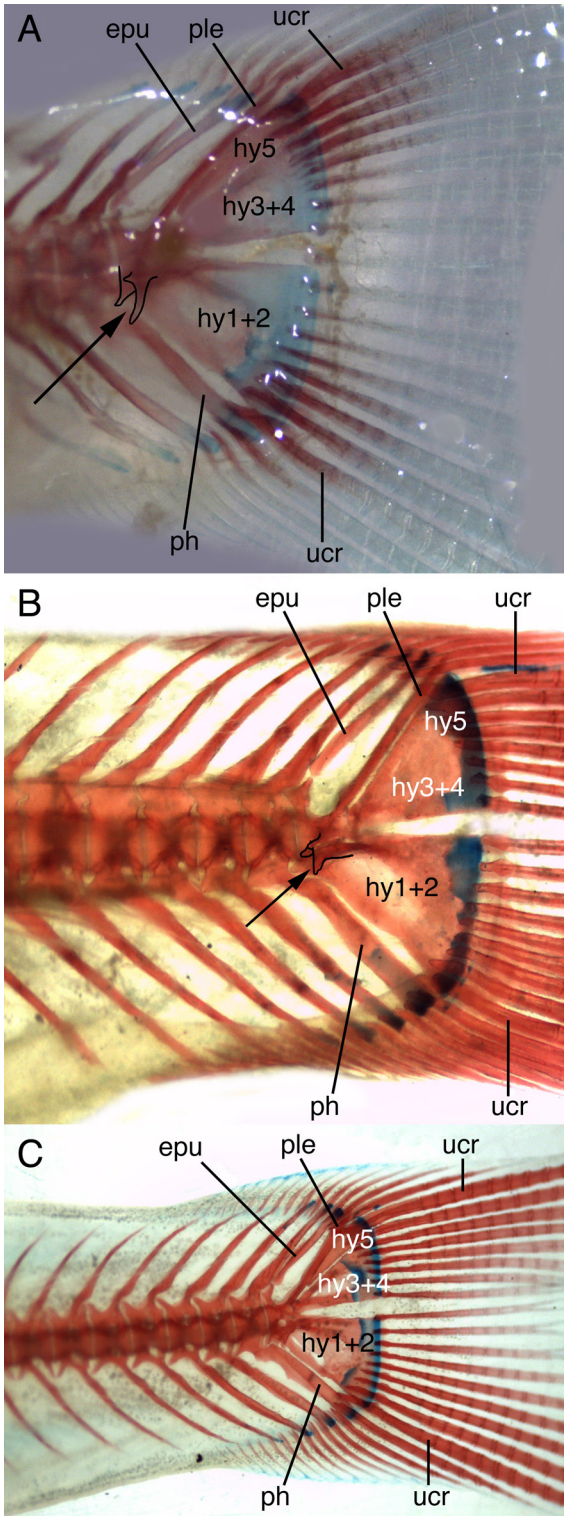

Fig. 22. (Right) Caudal-fin skeleton in lateral view. A. *Centromochlus macracanthus*, MZUSP 30619, 42.0 mm SL, paratype. B. *Tatia perugiae*, MZUSP 26684, 35.9 mm SL. C. *Glanidium bockmanni*, MZUSP 82351, 48.0 mm SL. Abbreviations: hy1+2, hypurals 1 to 2; hy3+4, hypurals 3 to 4; hy5, hypural 5; epu, epural; ph, parhypural; ple, pleurostyle; ucr, dorsal and ventralmost principal unbranched caudal-fin rays. Arrow indicates ventral process (elongate spur) of hypurapophysis. Scale bar = 10 mm.

119. *Muscular fibers at insertion of pars rictalis of adductor mandibulae (AM)* (CI 1.0, RI 1.0). State 0: *Pars rictalis* fibers mixed with *AM pars substegalis* at muscle insertion (Fig. 24A-C); state 1: fibers individualized from *AM pars substegalis* at muscle insertion (Fig. 23C). State 1 in *Centromochluls schultzi*, *C. heckelii*, *C. existimatus* and *C. macracanthus*. The *AM pars rictalis* corresponds to a thin muscle part ventral to *AM pars malaris* (Fig. 23C). The condition of an individualized section, without fibers mixed with *AM pars substegalis*, is uniquely observed in this centromochlin clade. The plesiomorphic condition is a voluminous thick muscle, with fibers mixed with *AM pars substegalis*. Among the species examined for myological characters, the most robust *AM pars rictalis* was observed in *Gephyromochlus leopardus*. In this species, the *pars rictalis* fibers are mixed with those of the *pars substegalis* at the muscle insertion (interpreted herein as plesiomorphic).

120. *Adductor mandibulae, pars malaris sections* (CI 1.0, RI 1.0). State 0: two muscle sections (Fig. 24A); state 1: single muscle section (Fig. 23A). Subdivision into two separate sections was observed in all species of *Glanidium*. A single section of the *pars malaris* of *adductor mandibulae* is found in *Centromochlus*, *Gephyromochlus* and available *Tatia*. The *adductor mandibulae pars malaris* corresponds in state 1 to a single muscle block much compressed medially near eye rim and limited dorso-rostrally by *levator arcus palatini* (Fig. 23B).

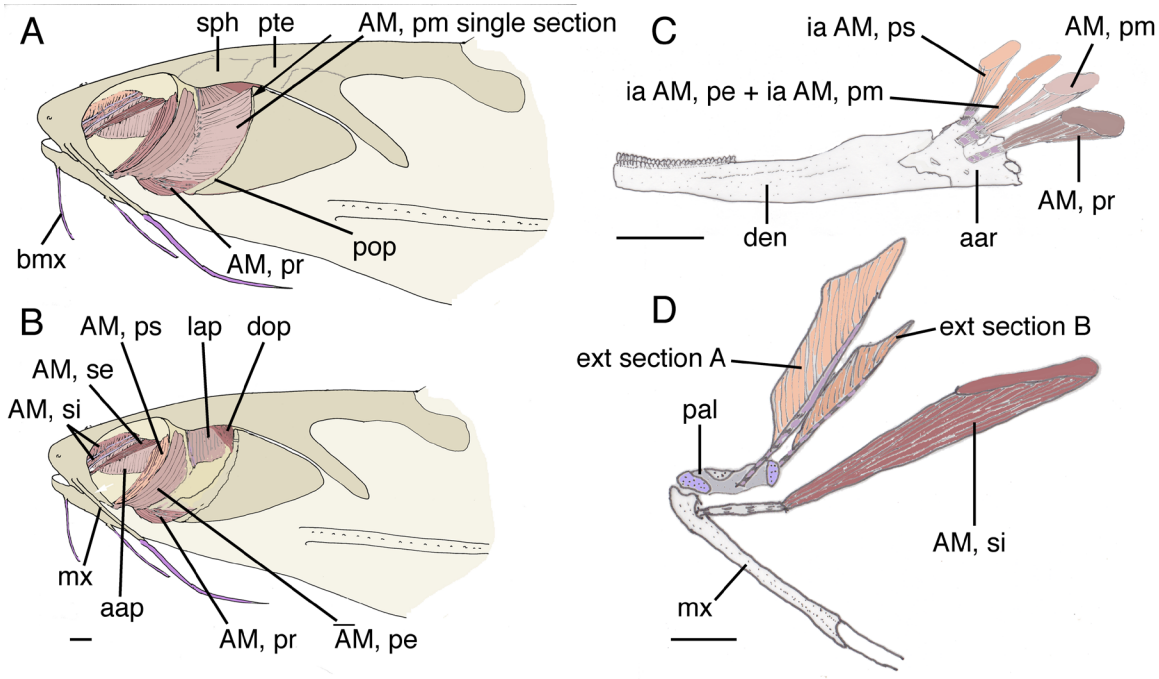

Fig. 23. Head muscles in *Centromochlus*. A. *Centromochlus existimatus*, INPA 40662, 59.0 mm SL, muscles after removal of skin. B. *Centromochlus existimatus*, INPA 40662, 59.0 mm SL, muscles after removal of adductor mandibulae pars rictalis and pars malaris. C. *Centromochlus heckelii*, MNRJ 12130, 60.0 mm SL, detail of the lower jaw in mesial view indicating the insertion parts of adductor mandibulae muscle sections. D. *Centromochlus heckelii*, MZUSP 44128, 72.2 mm SL, detail of the autopalatine and maxilla, indicating the insertion of muscles adductor mandibulae pars stegalis interna and extensor tentaculi. Abbreviations: AM, pe, adductor mandibulae, pars epistegalis; AM, pm single section, adductor mandibulae, pars malaris organized in a single muscle section; AM, pr, adductor mandibulae, pars rictalis; AM, ps, adductor mandibulae, pars substegalis; AM, se, adductor mandibulae, pars stegalis externa; AM, si, adductor mandibulae, pars stegalis interna; aar, anguloarticular; den, dentary; dop, muscle dilatator operculi; ext, extensor tentaculi sections A and B; hyo, hyomandibula; ia AM ps, intersegmental aponeurosis adductor mandibulae pars substegalis; ia AM pe+ ia AM pm, intersegmental aponeurosis adductor mandibulae pars epistegalis plus pars malaris in a single insertion; lap, muscle levator arcus palatini; lmbc, lateral mental barbel core; mx, maxilla; mbc, mental barbel core; mxbc, maxillary barbel core; pal, autopalatine; pop, preopercle; sop, suprapreopercle; sph, sphenotic; pte, pterotic. White arrow indicates position of infraorbital 1. Black arrow indicates origin of adductor mandibulae, pars rictalis on hyomandibula. Scale bar = 1 mm.

121. *Origin of adductor mandibulae pars malaris* (CI 1.0, RI 1.0). State 0: sphenotic and pterotic (Fig. 24A); state 1: preopercle (Fig. 23A; Birindelli, 2014: #51). Position at preopercle is coded as derived (State 1) and present in all examined centromochlins except *Glanidium*. In the Auchenipterinae and remaining catfishes examined, the *adductor mandibulae* originates on the lateral border of the cranium formed by the sphenotic and pterotic (Fig. 24A).

122. *Origin of adductor mandibulae pars substegalis* (CI 1.0, RI 1.0). State 0: superficial, on hyomandibula and quadrate with longest fibers on border of hyomandibula, not reaching cranial roof (Fig. 23C: AM, ps); state 1: deep, on hyomandibula and quadrate with longest fibers on sphenotic, orbitosphenoid and pterosphenoid (Fig. 24B). State 1 is synapormorphic for a clade composed of *Glanidium catharinensis*, *G. melanopterum* and *G. ribeiroi* in which the *AM. pars substegalis* is hypertrophied.

123. *Position of intersegmental aponeurosis (IA) at insertion of adductor mandibulae pars epistegalis* (CI 1.0, RI 1.0). State 0: insertion on medial face of mandibula at Meckelian fossa (Fig. 24C); state 1: insertion on lateral face of mandibula, at angulo-articular (Fig. 23C). State 1 in *Centromochlus musaicus*, *C. orca*, *C. existimatus*, *C. heckelii*, *C. macracanthus* and *C. schultzi*. Having a intersegmental aponeurosis (IA) thinner and laterally placed on mandibula is synapomorphic for *Centromochlus*.

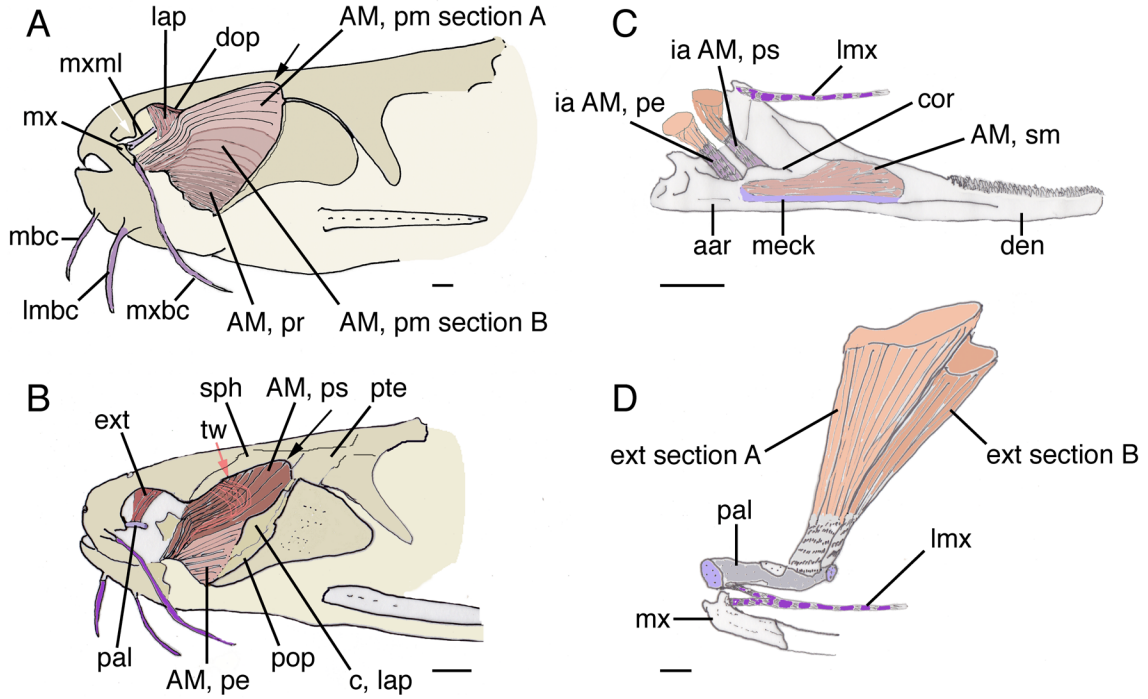

Fig. 24. Head muscles in *Glanidium*. A. *Glanidium ribeiroi*, MNRJ 27963, 98.5 mm SL, after removal of skin. B. *Glanidium melanopterum*, MNRJ 16262, 110.5 mm SL, after removal of adductor mandibulae pars rictalis and pars malaris. C. *Glanidium melanopterum*, MNRJ 16262, 110.5 mm SL, detail of left lower jaw in medial view indicating the insertion parts of pars epistegalis, pars substegalis and segmentum mandibularis. D. *Glanidium melanopterum*, MNRJ 16262, 110.5 mm SL, detail of the autopalatine and maxilla, indicating the insertion of muscle extensor tentaculi (ext), sections a and b. Abbreviations: AM, pe, adductor mandibulae, pars epistegalis; AM, pm, adductor mandibulae, pars malaris; AM, pr, adductor mandibulae, pars rictalis; AM, ps, Adductor Mandibulae, pars substegalis; AM, se, adductor mandibulae, pars stegalis externa; AM, si, adductor mandibulae, pars stegalis interna; AM, sm, adductor mandibulae, segmentum mandibularis; aar, angulo-articular; cor, coronoid process; dop, muscle dilatator operculi; hyo, hyomandibula; lap, muscle levator arcus palatini; lmbc, lateral mental barbel core; lmx, maxillary ligament; mx, maxilla; mbc, mental barbel core; mxbc, maxillary barbel core; meck, meckelian cartilage; mxml, maxilo-mandibular ligament; pal, palatine; pop, preopercle; sop, suprapreopercle; tw, twisted fibers at origin of adductor Mandibulae, pars substegalis; Red arrow, position of twisted fibers at adductor mandibulae, pars substegalis. White arrow indicates position of infraorbital 1. Black arrow indicates origin of adductor mandibulae, pars rictalis on cranium. Scale bar = 1 mm.

124. *Fibers at origin of adductor mandibulae pars substegalis* (CI 1.0, RI 1.0). State 0: fibers parallel to each other at origin; state 1: fibers twisted at origin (Fig. 24B). The *pars substegalis* is a thick muscle with twisted fibers (state 1) uniquely observed in *Glanidium catharinensis* and *G. melanopterum*. The twisted fibers are visible on medial muscle bundles (Fig. 24B). In other centromochlins, the *pars substegalis* is attached to the cranial roof through parallel fibers only.

125. *Position of adductor mandibulae (AM) segmentum mandibularis* (CI 1.0, RI 1.0). State 0: *AM, segmentum mandibularis* on medial surface of dentary (Fig. 24C); state 1: *AM segmentum mandibularis* oriented caudally onto angulo-articular (Fig. 25C). State 1 found in *Tatia aulopygia*, *T. intermedia* and *T. strigata*.

126. *Insertion of levator arcus palatini* (CI 0.50, RI 0.94). State 0: dorsal to *AM pars malaris*; state 1: between *AM pars malaris* and *AM pars epistegalis,* visible below skin (Fig. 25D); state 2: *Levator arcus palatini* sided but not intersected between muscle sections (Fig. 23A). State 1 synapomorphic for *Tatia aulopygia, T. intermedia, T. caxiuanensis*, *T. galaxias, T. gyrina, T. meesi* and *T. strigata*. In these species the *levator arcus palatini* is intersected between *AM pars malaris* and *AM pars epistegalis*. State 2 in *Centromochlus* where the *levator arcus palatini* is below skin and on dorso-lateral face of hyomandibula.

127. *Medial crest on opercle for insertion of dilatator operculi* (CI 1.0, RI 1.0). State 0: antero-medial border of opercle flattened, without an elevated area for muscle attachment; state 1: antero-medial border concave, with a prominent crest for muscle insertion. State 1 synapomorphic for *Glanidium*. Originating from the dorsolateral region of the orbitosphenoid and lateral margin of the frontal, the muscle *dilatator operculi* passes lateral to the *levator arcus palatini* and suprapreopercle, but medial to the *adductor mandibulae pars malaris*.

128. *Keel on parasphenoid for attachment of adductor arcus palatini* (CI 1.0, RI 1.0). State 0: no keel; state 1: sharp crest forming a keel for muscle attachment on parasphenoid. Keel for muscle attachment present in *Centromochlus musaicus*, *C. existimatus, C. heckelii*, *C. macracanthus, C. orca* and *C. schultzi*. In state 0, cranial roof is not keeled at *adductor arcus palatini* origin and muscle spreads over the orbitosphenoid, pterosphenoid and parasphenoid. A cranial ventral keel is associated with a pelagic lifestyle, being present in auchenipterids with large eyes such as *Auchenipterus*. Adapted from N17 of Ferraris (1988) and Birindelli (2014: #78) regarding cranial ventral keel, and from Sarmento-Soares & Porto (2006) regarding muscle section.

129. *Shape of extensor tentaculi* (CI 1.0, RI 1.0). State 0: trapezoidal (Fig. 24D); state 1: pinnate (Fig. 23D). State 1 synapomorphic for *Centromochlus musaicus*, *C. existimatus, C. heckelii*, *C. macracanthus, C. orca* and *C. schultzi*. Usually originating only from the ventrolateral regions of the lateral ethmoid and orbitosphenoid, *extensor tentaculi* with pinnate arrangement of muscle fibers is uniquely derived and synapomorphic for *Centromochlus*.

130. *Ligament on adductor mandibulae pars stegalis interna* (CI 0.50, RI 0.92). State 0: muscle bundle present, no ligament (Fig. 23D); state 1: muscle replaced by a ligament for barbel adduction (Figs. 24C-D: lmx). State 1 found in *Glanidium albescens, G. botocudo, G. catharinensis, G. cesarpintoi, G. melanopterum* and *G. ribeiroi*. Interpreted as independent acquisition in *Tatia T. aulopygia*, *T. brunnea*, *T. caudosignata*, *T. dunni*, *T. galaxias*, *T. intermedia* and *T. nigra*. Ligament named as a muscle *retractor tentaculi* derivation due to its insertion on the maxilla (Sarmento-Soares & Porto, 2006). The term *retractor tentaculi* was avoided following the recommendation of Datovo & Vari (2014) regarding homologies of the muscle with the corresponding muscle section of other teleosts.

131. *Abduction of the maxillary barbel* (CI 1.0, RI 1.0). State 0: over the lateral ethmoid flange anteroposteriorly, promoting limited lateral movement (Sarmento-Soares & Porto, 2006: fig. 11); state 1: wide range of rotational movements (Sarmento-Soares & Porto, 2006: fig. 12). State 1 synapomorphic for a clade composed of *Centromochlus musaicus, C. carolae, C. orca, C. existimatus, C. heckelii, C. macracanthus* and *C. schultzi*. The maxillary barbel in Auchenipteridae performs vertical movements (Ferraris, 1988: #J12; Akama, 2004: #60; Birindelli, 2014: #13, fig. 7). This assumption is based on the maxillary bone's articulatory facet with the palatine, and also on the palatine's articulatory facet with the lateral ethmoid, but a biomechanical study is lacking for these catfishes. A biomechanical study performed with the African catfish *Clarias gariepinnus* asserts sliding movements (Adriaens and Verraes, 1996), and inspired us to manipulate barbels in dissected specimens to check performance. Aquarium observations on *Centromochlus heckelii* confirm a wide range of barbel movements relative to other centromochlins, such as *Tatia intermedia* (LMSS, pers. obs). The performance of movements during abduction

of maxillary barbel in a select group of *Centromochlus* (*Centromochlus musaicus, C. carolae, C. orca, C. existimatus, C. heckelii, C. macracanthus, C. schultzi*) reveals a wide array of movements when compared to remaining centromochlins. Among Centromochlinae, wide rotational movements of maxillary barbels are uniquely observed in these *Centromochlus*.

132. *Insertion position of levator operculi* (CI 1.0, RI 1.0). State 0: onto medial crest on opercle; state 1. onto dorsomedial crest on opercle (Sarmento-Soares & Porto, 2006: fig. 10). Muscle inserts along medial face of opercle in its posterodorsal region. In some Auchenipteridae, a bony crest is present on the posterodorsal portion of the hyomandibula, where the muscle *levator operculi* is inserted (Lundberg, 1970; Sarmento-Soares & Porto, 2006; Birindelli, 2014; Calegari et al., 2019). Size of crest is distinctive among species. A prominent longitudinal crest is synapomorphic for a clade composed of *Glanidium cesarpintoi*, *G. botocudo* and *G. albescens*.

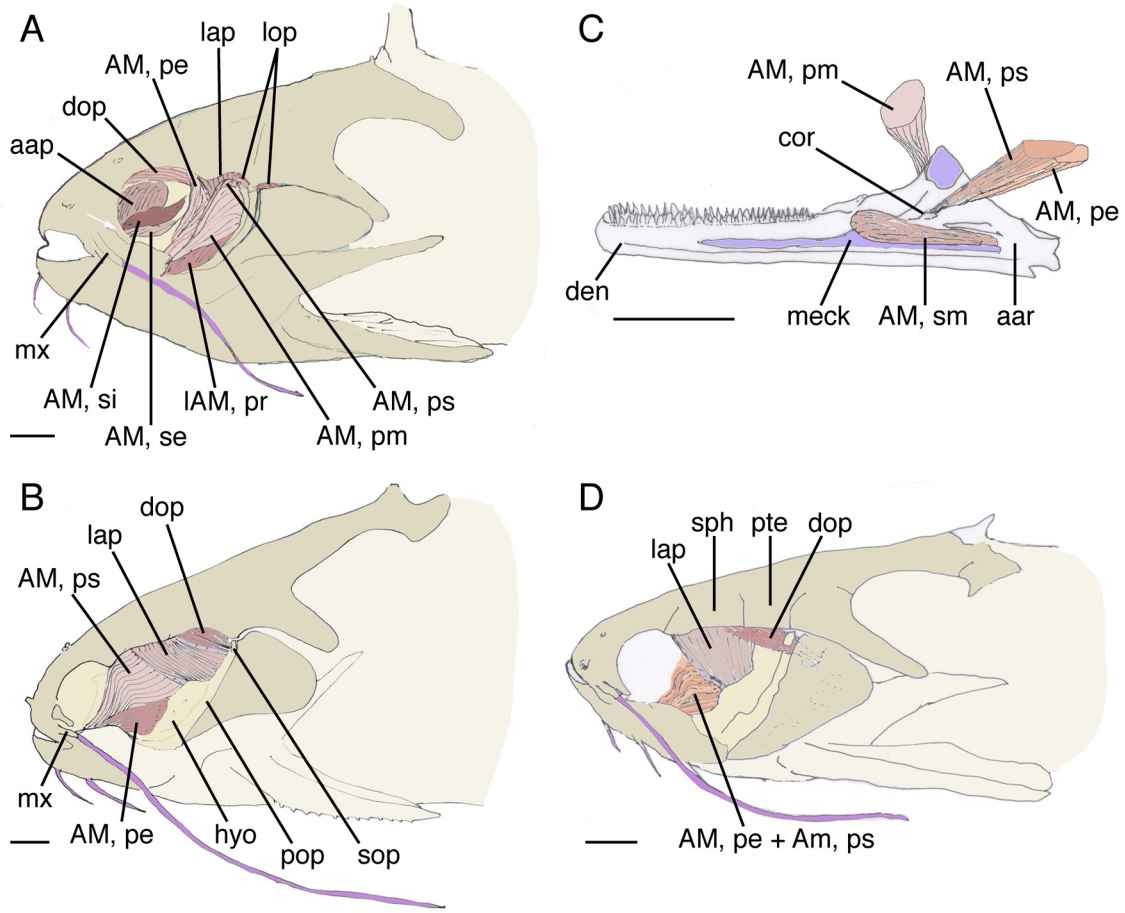

Fig. 25. Head muscles in *Tatia*. A. *Tatia intermedi*a, INPA 11076, 84.7 mm SL, after removal of skin. B. *Tatia romani*, MCNG 14896, 29.8 mm SL, after removal of adductor mandibulae pars rictalis and pars malaris. C. *Tatia romani*, MCNG 14896, 29.8 mm SL, detail of right lower jaw in mesial view indicating the insertion parts of pars epistegalis, pars substegalis and segmentum mandibularis. D. *Tatia gyrina*, INPA 20971, 27.2 mm SL, after removal of adductor mandibulae pars rictalis and pars malaris. Abbreviations: AM, pe, adductor mandibulae, pars epistegalis; AM, pe+ AM, ps, adductor mandibulae, pars epistegalis mixed to pars substegalis; AM, pm, adductor mandibulae, pars malaris; AM, pr, adductor mandibulae, pars rictalis; AM, ps, adductor mandibulae, pars substegalis; AM, se, adductor mandibulae, pars stegalis externa; AM, si, adductor mandibulae, pars stegalis interna; AM, sm, adductor mandibulae, segmentum mandibularis; aar, angulo-articular; cor, coronoid process; dop, muscle dilatator operculi; hyo, hyomandibula; lap, muscle levator arcus palatini; mx, maxilla; meck, meckelian cartilage; pop, preopercle; sop, suprapreopercle; sph, sphenotic; pte, pterotic. White arrow indicates position of infraorbital 1. Scale bar = 1.0 mm.

CLASSIFICATION

Centromochlinae Bleeker 1862

This subfamily is well supported as a monophyletic clade (Ferraris, 1988; Soares-Porto, 1998; Birindelli, 2014). Centromochlinae is diagnosed by the following seven exclusive characters: female urogenital papilla with a flap (#12: 0>1); position of urogenital opening in males, opening emerging from skin flap near antero-distal margin of anal fin (#15: 0>1); number of branched dorsal-fin rays, five (#81: 0>1); orientation of anal-fin proximal radials in adult males, oblique, aligned nearly parallel to vertebral axis (#93: 0>1); partial fusion of proximal radials in modified anal fin of adult males (#94: 0>1); thickness of anal-fin rays in mature males, anterior rays thicker than posterior ones (#97: 0>1); and pelvic fin with five branched rays (#116: 0>1).

Included genera.—*Centromochlus*, *Gelanoglanis*, *Gephyromochlus*, *Glanidium* and *Tatia*.

Remarks.—The tribes Gelanoglanini, Centromochlini, Glanidiini and Pseudotatiini proposed by Calegari et al. (2019) are dismissed. Unlike Calegari et al. (2019), we do not consider *Pseudotatia parva* to be a member Centromochlinae.

Centromochlus Kner 1857

Genus diagnosed by three exclusive characters: ventrolateral position of eye socket (#2: 0>1); sphenotic notched for the exit of infraorbital canal (#28: 0>1); and posterior serrations along pectoral-fin spine numerous, 25–45 (#91: 0>1). Support for the monophyly of *Centromochlus* (eight species) is moderate (Bremer support 3; Bootstrap 70; Table 2; Figs. 26, 27).

Included species.—*Centromochlus heckelii* (type species), *C. melanoleucus* n. comb., *C. carolae* n. comb., *C. musaicus* n. comb., *C. orca, C. existimatus, C. macracanthus* n. comb., and *C. schultzi* n. comb.

Remarks.—*Balroglanis* was originally described as a subgenus of *Centromochlus* by Grant (2015) and elevated to genus by Calegari et al. (2019) for three species: *B. schultzi, B. macracanthus* and *B. carolae*. Those species represent a paraphyletic assemblage in our analysis. Therefore *Balroglanis* Grant (2015) is herein synonymized with *Centromochlus* (Table 1). Likewise, we consider the *Centromochlus* subgenus *Sauronglanis* Grant (2015) to be a synonym to *Centromochlus*. *Sauronglanis* was not considered in Calegari et al. (2019). Grant (2015) assigned four species to subgenus *Sauronglanis*. In the current study, three of those species are valid in *Centromochlus* (*C. musaicus*, *C. carolae*, *C. melanoleucus*) and the fourth is valid in *Tatia* (*Tatia marthae*).

Glanidium Lütken 1874

Genus diagnosed by the following eight characters, six of them exclusive: concave notch on margin of sphenotic and pterotic (#26: 0>1, exclusive); long ventral process of urohyal, longer than urohyal (#56: 0>1, exclusive); basibranchial 2 flattened dorsoventrally, spatulate (#59: 0>1, exclusive); gill rakers robust (#61: 0>1, also in *Gephyromochlus leopardus*); anterior margin of dorsal spine with small undulations, surface rugose (#76: 0>1, exclusive); third unbranched anal-fin ray in males with more segments than in females (#99: 0>1, exclusive); *dilatator operculi* inserted on a prominent crest at concave antero-medial border of opercle (#127: 0>1, exclusive); and *adductor mandibulae pars stegalis interna* replaced by a ligament for barbel adduction (#130: 0>1, also in *Tatia*). *Glanidium* is a well supported genus (Bremer support 8; Bootstrap 100; Table 2) composed of two sister clades, each with three species (Figs. 26, 27).

Included species.—*Glanidium albescens* (type species), *G. botocudo*, *G. ribeiroi*, *G. melanopterum*, *G. cesarpintoi* and *G. catharinensis*.

Gephyromochlus Hoedeman 1961

Monotypic genus diagnosed by the following four characters, one of them exclusive: deeply concave notch on margin of sphenotic and pterotic (#26: 0>2, exclusive); canal posterior opening on middle of infraorbital 1 process (#36: 0>1, also present in *Centromochlus existimatus*, *C. heckelii* and *C. macracanthus*); gill rakers robust (#61: 0>1, also in *Glanidium*) and modified anal-fin with margin notched (#98: 0>1, also in *Gelanoglanis nanonocticolus* and *G. pan*).

Included species.—*Gephyromochlus leopardus* (type species).

Gelanoglanis Böhlke 1980

Genus diagnosed by the following twenty characters, 15 of them exclusive: wide sinuous mouth gape (#0: 0>1, exclusive); posterior nare opening enlarged, with well-developed lamellae in large rosette (#1: 0>1, exclusive); eye less than 10% HL (#3: 0>1, exclusive); one pair of

chin barbels (#10: 0>1, exclusive); rostral margin of mesethmoid deeply constricted and with lateral cornua (#21: 0>1, exclusive); epiotic with sharply pointed, elongate, posteriorly directed spinous process (#27: 0>1, exclusive); vomer absent (#29: 0>1, exclusive); nasal channel free, no ossified bone present (#31: 0>1, exclusive); lateral line sinuous at least anteriorly (#34: 0>1, also present in *Centromochlus heckelii* and *C. existimatus*); non-ossified infraorbital (#38: 0>1); mandibular ramus canal of laterosensory system free from dentary (#41: 0>1, exclusive); premaxillary tooth patches laterally displaced, widely separated (#43: 0>1, exclusive); length of maxilla more than 60% length of palatine (#44: 1>2, exclusive); entopterygoid reduced to small round bone (#50: 0>1, also present in *Centromochlus musaicus*, *C. carolae*, *C. heckelii* and *C. existimatus*); suprapreopercle ossicle absent (#53: 0>1, exclusive); branchial arches without gill rakers (#62: 0>1, exclusive); parapophysis of fourth vertebra (Mullerian ramus disc) reduced (#65: 0>2, exclusive, unordered); posterior cleithral process (humeral spine) scarcely developed (#83: 0>, also reduced in *Tatia dunni, T. brunnea, T. caudosignata* and *T. nigra*); third pectoral-fin radial absent (#86: 0>1, exclusive); length of anal fin in mature males less than 7% SL (#96: 0>1, exclusive). *Gelanoglanis* is a very well supported genus (Bremer support 22; Bootstrap 100; Table 2) including two sister clades of two and three species, respectively (Figs. 26, 27).

Included species.—Gelanoglanis stroudi (type species)*, G. nanonocticolus, G. travieso, G. pan* and *G. varii*.

Tatia Miranda Ribeiro 1911

Genus diagnosed by the following five features, three of them exclusive: urogenital opening in females slit-like (#14: 0>1, also present in *C. existimatus* and *C. heckelii*); anterior basibranchial cartilage narrow (#58: 0>1, exclusive); coracoid process small, shorter than pectoral fin base (#82: 0>1, exclusive); modified anal-fin rays with the third unbranched and first branched rays converging to pointed tip (#106: 0>1, also in *Gelanoglanis nanonocticolus*); *inclinator anales* in mature males permitting anal fin rotational movement to a transverse position (#114: 0>1, exclusive). *Tatia* is a moderately supported genus (Bremer support 3; Bootstrap 91; Table 2) including twenty six species in three clades that form a trichotomy (Figs. 26, 27).

Included species.—Tatia intermedia (type species)*, T. aulopygia*, *T. boemia, T. brunnea*, *T. caudosignata, T. dunni, T. galaxias, T. jaracatia, T. neivai, T. nigra, T. strigata, T. gyrina, T. caxiuanensis, T. meesi*. *T. perugiae, T. altae, T. meridionalis* n. comb., *T. ferrarisi* n. comb., *T. romani, T. reticulata, T. concolor, T. simplex*, *T. punctata*, *T. marthae, T. bockmanni* n. comb. and *T. britskii* n. comb.

Remarks.—We consider the two subgenera proposed by Grant (2015) and elevated by Calegari et al. (2019), *Ferrarissoaresia* and *Duringlanis*, to be synonyms of *Tatia*, the most species-rich genus in Centromochlinae. Some species of *Tatia* are respresented only by type material or by few specimens in collections. The limited availability of specimens makes it difficult to code characters for phylogenetic analysis. We adopted a conservative perspective by keeping *Tatia* as a large assemblage composed of three monophyletic clades, A, B and C.

Tatia Clade A

This clade is diagnosed by five characters, three of which are exclusive. Members of Clade A have the nasal bone sutured to mesethmoid (#33: 0>1, exclusive); hyomandibula articulating facet through sphenotic only (#46: 0>1, also in *Gelanoglanis stroudi*, *G. nanonocticolus*, *G. travieso, G. varii* and *G. pan*); metapterygoid conical, with little or no laminar projection (#48: 0>1, exclusive, polymorphic in some *Centromochlus* and *Tatia* Clade B); hyomandibula deeply notched (#52: 0>1, also in some *Centromochlus* and *Tatia* Clade B); and anal fin in mature males extremely short, longest rays less than 5% SL (#96: 0>1, exclusive). With 14 species, *Tatia* Clade A is well supported in the present analysis (Bremer support 5; Table 2).

Included species.—Tatia intermedia, T. aulopygia, *T. boemia, T. brunnea*, *T. caudosignata*, *T. dunni, T. galaxias, T. jaracatia, T. neivai, T. nigra, T. strigata, T. gyrina, T. caxiuanensis* and *T. meesi*.

Remarks.—Most of the derived characters supportive of *Tatia* Clade A are based on features proposed in Sarmento-Soares & Martins-Pinheiro (2008).

Tatia Clade B

This clade is diagnosed by the two features, one of them exclusive: the aortic canal covered ventrally by superficial ossification (#68: 0>2, exclusive); and the posterior margin of dorsal spine with well-formed retrorse serrae (#78: 0>2, also in *Gephyromochlus leopardus*).

Included species.—Tatia perugiae, T. altae, T. meridionalis, T. ferrarisi, T. romani and *T. reticulata*.

Remarks.—Within *Tatia* Clade B, the cladistic analysis revealed that *Tatia perugiae* and *T. altae* are sister species and closely related to *T. romani*. Ferraris (1988) similarly included *Centromochus perugiae* and *C. altae* in his unnamed "Genus A". *Tatia* Clade B includes species assigned to *Ferrarissoaresia* (*T. ferrarisi*, *T. meridionalis*), *Duringlanis* (*T. altae, T. perugia, T. romani*) and *Tatia* (*T. reticulata*) by Calegari et al. (2019). As a result, we treat *Duringlanis* and *Ferrarissoaresia* as junior synonyms of *Tatia*.

Tatia Clade C

The monophyly of *Tatia* Clade C is supported a single exclusive character: modified anal fin in mature males with sixth and/or seventh branched fin rays rudimentary (#110: 0>1, exclusive).

Included species.—*Tatia concolor, T. simplex*, *T. punctata*, *T. marthae, T. bockmanni* and *T. britskii*.

Remarks.—Tatia Clade C needs further investigation. Most of the features evaluated for included species represent symplesiomorphies. The limited material available in collections impedes a more detailed investigation of these catfishes.

DISCUSSION

Phylogenetic implications.—Auchenipteridae is composed of two monophyletic clades, Auchenipterinae and Centromochlinae (Ferraris, 1988; Soares-Porto, 1998; Akama, 2004; Birindelli, 2014; Calegari et al., 2019). In the current study, seven synapomorphies support the monophyly of Centromochlinae. *Glanidium* is recovered sister to all other members of Centromochlinae, corroborating previous analyses (Soares-Porto, 1998; Birindelli, 2014). Six exclusive characters support a monophyletic clade within Centromochlinae composed of *Gephyromochlus* sister to *Gelanoglanis* + *Centromochlus*. *Gephyromochlus leopardus* was long placed in *Glanidium* due to its morphological resemblance to other members of that genus (Ferraris, 1988; Soares-Porto, 1998; Sarmento-Soares & Martins-Pinheiro, 2013). Species of *Glanidium* and *Gephyromochlus leopardus* are the only large-sized centromochlins, almost reaching about 200 mm in SL. Other characteristics common to both taxa include numerous branched anal-fin rays (>8), and modified male anal fin without spines. *Glanidium* and *Gephyromochlus leopardus* also share a deeply concave cranial border, first noticed by Ferraris (1988: #N9), and later assumed to be synapomorphic by Soares-Porto (1998: #7), Royero (1999: #20), Akama (2004: #34) and Birindelli (2014: #63). Myology suggests that this concavity is variable and not synapomorphic among these taxa. The similarity in the notched margin on sphenotic and pterotic bones (see character #26) is considered convergent between *Glanidium* and *Gephyromochlus leopardus*. The partial fusion of proximal radials in modified anal fin of adult males (see character #94) also is considered independently evolved in both *Gephyromochlus* and *Glanidium*. Characters such as the number of anal-fin unbranched rays and first branched ray enlarged and elongated in dimorphic male, assumed distinctive for *Glanidium*, are shared by other centromochlin taxa and herein considered plesiomorphic (see characters #101, #106).

Gelanoglanis is diagnosed by 20 derived features, 15 of them exclusive to the genus. Some of these are paedomorphic (reductive) characters, including reduction in fin-ray counts, and reduction of ossification in laterosenrory channel (characters #35, #41, #44). The interpretation of some of these reductive characters is based on ontogeny (vs. terminal condition in fully developed individuals), and may add clues to the investigation of centromochlin evolution. The paedomorphic nature of *Gelanoglanis* was previously recognized by Soares-Porto et al. (1999) and Calegari et al. (2014).

The taxonomic history *Centromochlus* and *Tatia* is highly intertwined, and the composition of these two genera is still under dispute. Mees (1974) assigned most species of *Centromochlus* known at that time to *Tatia* based on the modified anal fin and morphological similarities in external appearance. Uncertainties regarding the distinction between *Centromochlus* and *Tatia* were pointed out by Britski (1972) who suggested their synonymy based on cranial roof morphology and sexually dimorphic features. The recognition of differences in the modified anal fin of dimorphic males helped establish the generic limits of *Centromochlus* and *Tatia* (Ferraris, 1988). Ferraris (1988) separated the 15 species of *Tatia* known at the time into three groups, *Tatia* and unnamed genera A and B. Soares-Porto (1998) transferred to *Centromochlus* most of the species previously allocated to *Tatia* based on anal-fin ray arrangement and the suspensorium bones. *Tatia* was taxonomically revised by Sarmento-Soares & Martins-Pinheiro (2008) who added three new species, but conceded that the inclusion of some species remained problematic. The dubious

Fig. 26. (Page 130) Optimization of characters in one of the most parsimonious trees. Optimization was obtained through TNT and visualized by Winclada. Character number displayed above each hashmark (black boxes indicate synapomorphies/ autapomorphies; white box homoplasies). Number of each character state change below each branch (0,1,2) according to character description. Names of taxa as discussed in text.

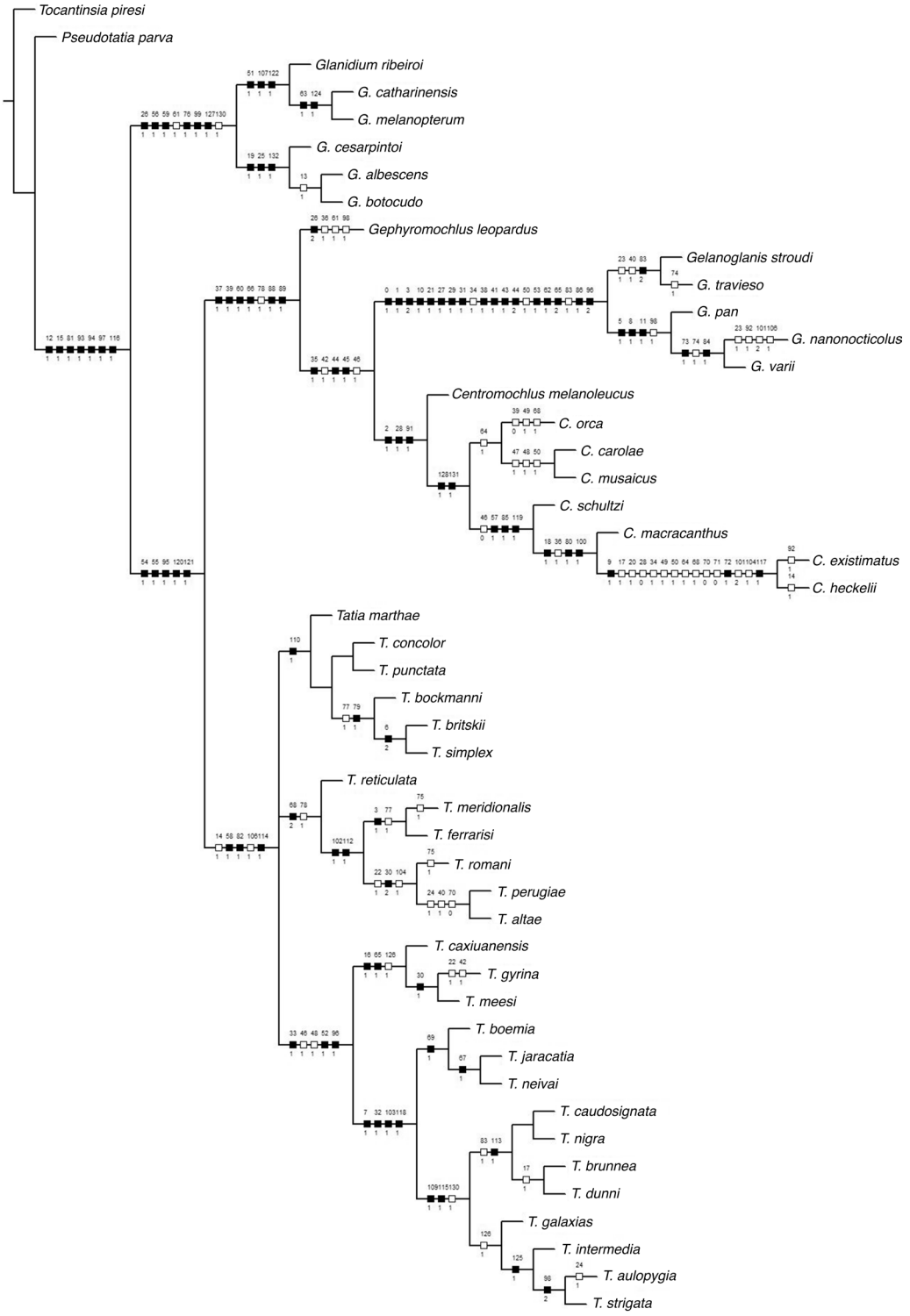
Tocantinsia piresi
Pseudotatia parva
Glanidium ribeiroi
G. catharinensis
G. melanopterum
G. cesarpintoi
G. albescens
G. botocudo
Gephyromochlus leopardus
Gelanoglanis stroudi
G. travieso
G. pan
G. nanonocticolus
G. varii
Centromochlus melanoleucus
C. orca
C. carolae
C. musaicus
C. schultzi
C. macracanthus
C. existimatus
C. heckelii
Tatia marthae
T. concolor
T. punctata
T. bockmanni
T. britskii
T. simplex
T. reticulata
T. meridionalis
T. ferrarisi
T. romani
T. perugiae
T. altae
T. caxiuanensis
T. gyrina
T. meesi
T. boemia
T. jaracatia
T. neivai
T. caudosignata
T. nigra
T. brunnea
T. dunni
T. galaxias
T. intermedia
T. aulopygia
T. strigata

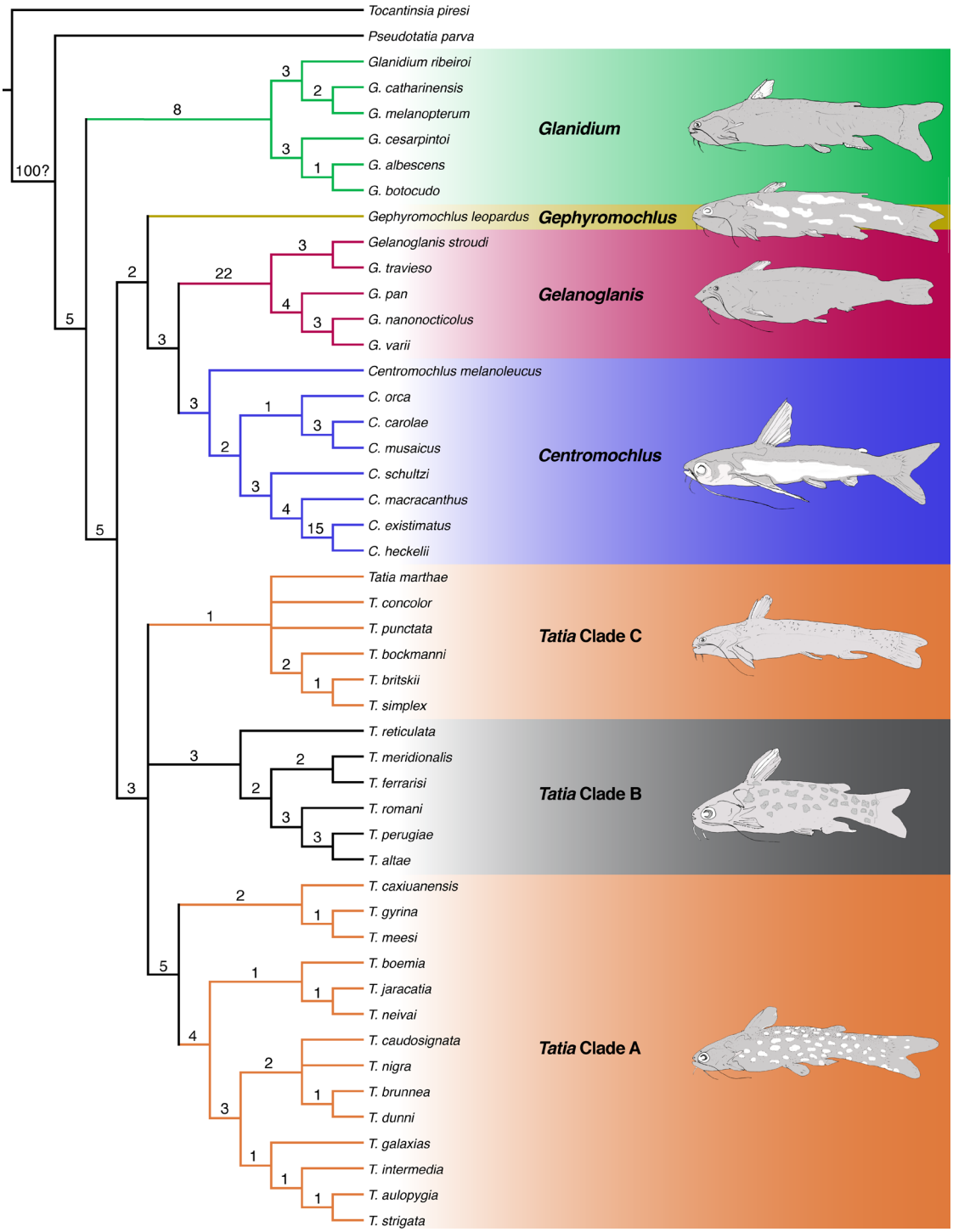

Fig. 27. Consensus tree of phylogenetic relationships in Centromochlinae (Auchenipteridae) obtained through TNT. Node values correspond to Bremer support. Names of taxa as discussed in text.

position of *Tatia musaica* led Sarmento-Soares et al. (2017) to consider *Tatia* as a paraphyletic assemblage. *Tatia musaica* was originally described in *Tatia* (Royero, 1992), removed to *incertae sedis* in Centromochlinae by Sarmento-Soares & Martins-Pinheiro (2008); re-assigned to *Tatia* by Vari & Ferraris (2013) and then transferred to *Centromochlus* (*Sauronglanis*) *musaicus* by Grant (2015). Sarmento-Soares et al. (2017) and Calegari et al. (2019) restored the original placement of Royero's species in *Tatia*. Here we return the species to *Centromochlus* (i.e., *C. musaicus*). The recent descriptions of new species of *Centromochlus* and *Tatia* in the absence of a expanded phylogenetic analysis prompted the current reappraisal of centromochlin catfishes.

In our analysis, *Tatia* is monophyletic based on five derived features and composed of three clades (A, B, and C) in a basal trichotomy. Species assigned to *Balroglanis* (*B. carolae, B. macracanthus, B. schultzi*) or *Tatia* (*T. melanoleuca, T. musaica, T. orca*) by Calegari et al. (2019) are here transferred to *Centromochlus*, and *Balroglanis* is not supported as a monophyletic subunit within that genus. Features associating some of these species with *Tatia* in previous studies (e.g., caudal peduncle deep, >12% of SL, with middorsal keel posterior to the adipose fin) were hypothesized as synapomorphic for a subgroup within *Tatia*. Structures in *Tatia musaica* and *T. carolae*, such as adductor arcus palatini origin at a crest on parasphenoid (#128) and abduction movement of the maxillary barbell (#131), remove these species to *Centromochlus*.

In their combined analysis of morphological and molecular data for Auchenipteridae, Calegari et al. (2019) included *Pseudotatia parva* in Centromochlinae, but lacked molecular data for *P. parva*. Birindelli (2014) previously assigned *P. parva* to Auchenipterinae based on his phylogenetic analysis of morphological data. Our analysis included only one species of Auchenipterinae (designated as the outgroup), and therefore did not adequately test the placement of *P. parva*. Nevertheless, we consider *P. parva* to be a member of the subfamily Auchenipterinae. The monophyly of the Auchenipterinae is supported by having urogenital tube opening at the tip of anterior anal-fin rays in males, a sinusoidal lateral line, and an accessory cartilage present between third and fourth basibranchials (Birindelli & Zuanon, 2012; Birindelli, 2014). In *Pseudotatia parva,* the urogenital tube opens at the tip of anterior anal-fin rays in males, a condition unique to Auchenipterinae. In Centromochlinae, the urogenital tube opens at base of anal fin. Additionally, a sinuous lateral line is observed in *P. parva*. Most Centromochlinae lack a sinusoidal lateral line (see character #34).

Biogeographic Implications.—Freshwater fish diversity is associated with the geological history of the river basins (Lundberg et al., 1998). Vicariance via a barrier such as a waterfall is commonly used to explain divergence within species groups, and historical watershed connections are commonly used to infer to dispersal between adjacent river basins (Albert & Carvalho, 2011). *Glanidium* is endemic to Atlantic coastal drainages of eastern and southern Brazil from the mouth of the rio São Francisco to the state of Rio Grande do Sul. The Serra do Espinhaço, a north-south mountain chain spanning Bahia and Minas Gerais states, represents an important divide between the ancient São Francisco and younger coastal drainages (Sarmento-Soares & Martins-Pinheiro, 2013). Allopatric speciation seems to account for differentiation between *Glanidium albescens* in the São Francisco, and its sister species, *G. botocudo*, in younger coastal rivers (Sarmento-Soares & Martins-Pinheiro, 2013). The westward erosive retreat of the eastern margin of the South American continental platform promoted the capture of upland streams draining the Brazilian Shield by lowland coastal river systems (Ribeiro, 2006). Those captures would allow for the transfer of upland fishes to coastal river systems.

Centromochlins of the Amazonian lowlands include *Centromochlus*, *Gelanoglanis* and *Tatia*. In the Guyana Shield uplands, *Gephyromochlus*, *Centromochlus*, *Gelanoglanis* and *Tatia* are present. Some species are distributed in both the Amazonian floodplain and along the Guyana shield. Small-sized species from the Guyana Shield such as as *Tatia reticulata*, *T. gyrina,* and *T. meesi,* as well as *T. caxiuanensis* from northeastern Pará state, form a group sister to a large clade containing lowland species of the Amazon, Paraná-Paraguay and upper Uruguay systems. Upper Amazon species of *Tatia* are related to each other.

The biogeographic patterns of Amazonian fishes distinguished by Dagosta & de Pinna (2019) indicate that South American lowlands taxa occupy the lower altitudes of cis-Andean South America. Centromochlinae catfishes such *Tatia intermedia* and *T. aulopygia* exemplify such a pattern; those fishes live in the lowland floodplains of the Amazon and/or Madeira rivers. Lowlands are generally inhabited by widely distributed taxa living in sympatry and less susceptible to extinction, resulting in a high accumulation of species (Dagosta & de Pinna, 2017). The widespread lowland species of *Centromochlus* (e.g., *C. heckelii* and *C. existimatus*) and *Tatia* (e.g., *T. intermedia* and *T. aulopygia*) have a broad distribution resulting from dispersion along fluvial valleys. The Guyana Shield is inhabited by several species with restricted distributions, some of which are rheophilic and occupy lotic environments. The centromochlins *Tatia meesi*, *Centromochlus carolae* and *C. musaicus* are not necessarily rheophilic, but

reported to inhabit riffles and possibly require oxygenated waters to survive. The less vagile fishes and can serve as models for studies of historical biogeography (Cardoso & Montoya-Burgos, 2009; Lujan & Armbruster, 2011).

KEY TO GENERA OF CENTROMOCHLINAE

1. Large sinuous mouth, extending past vertical through eye; opening for posterior nare large, olfactory rosette well developed; eye small, diameter less than 4% HL; one pair of chin barbels …….....*Gelanoglanis*

1'. Short straight mouth, not reaching vertical through eye; opening for posterior nare small, olfactory rosette normally developed; eye medium to large, diamter greater than 6% HL; two pairs of chin barbels.....2

2. Latero-posterior margin of sphenotic distinctly concave (Figs. 9A,B); 8 to 11 (rarely 7) branched anal-fin rays; male modified anal fin with 20 to 43 segments along third unbranched ray ……...……. 3

2'. Latero-posterior margin of sphenotic straight to slightly concave (Fig. 9C,D); 5 to 7 (rarely 8) branched anal-fin rays; male modified anal fin with 6 to 15 segments along third unbranched ray …….....……..…… 4

3. Anterior margin of pectoral spine rugose or with very small serrations, tip of spine pungent (Fig. 18C, 19E); 10 or 11 branched anal-fin rays...…….....*Gephyromochlus*

3'. Anterior margin of pectoral spine with well-formed serrations, tip of spine bifurcate (Fig. 18A, 19F); 8 or 9 branched anal-fin rays.....*Glanidium*

4. Mesethmoid short (compact), maximum width up to two times medial length; posterior nuchal plate reduced and curved (Fig. 8C); eye diameter less than 25% HL; three unbranched rays on male modified anal fin (Fig. 20B); color pattern spotted or reticulated.....*Tatia*

4'. Mesethmoid generally longer, maximum width less than 1.5 times medial length; posterior nuchal plate large and straight (Fig. 8A); eye diameter ≥25% HL; two unbranched rays on male modified anal fin (Fig. 20A); color greyish with wavy pattern or contrasting colors.....*Centromochlus*

ACKNOWLEDGEMENTS

We thank our colleagues at INMA for their assistance, particularly M. M. C. Roldi, Juliana P. Silva, L. Tonini, S. Recla, R. L. Betzel and A. Serpa. For loans, exchange of specimens and/or courtesies extended during visits to their institutions we thank M. H. Sabaj (ANSP), S. A. Schaefer (AMNH), B. Chernoff (FMNH), C. L. DoNascimiento (IAvH), C. Taylor (INHS), L. Rapp and R. Leitão (INPA), L. Sousa (LIA), R. Royero (MBUC-V), D. Taphorn (MCNG), L. R. Malabarba, B. Calegari, R. E. Reis, E. Pereira (MCP), P. A. Buckup, M. R. Britto, C. Moreira (MNRJ), A. Clistenes, P. R. D. Lopes (MZFS), A. Akama, W. Wosiacki (MPEG), J. L. Birindelli, L. Shibatta, O. Shibatta, R. H. C. Nascimento (MZUEL), H. A. Britski, O. T. Oyakawa, A. Datovo, M. Gianetti, M. Pastana (MZUSP), C. Pavanelli (NUP), R. de Ruiter (RMNH), F.Raynner (UFOPA); P. Lucinda, C. Chamon (UNT), C. J. Ferraris Jr; S. Raredon, T. Griswold, and the late R. P. Vari (USNM). We acknowledge C. J. Ferraris Jr, K. Luckenbill, S. Raredon for images and radiographs and the All Catfish Species Inventory Project and California Academy of Sciences (CAS) Ichthyology Type Image base for availability of images. We are indebted to C. J. Ferraris Jr, J. L. O. Birindelli, M. Arce H., M. H. Sabaj, M. R. Britto and P. Lucinda, for further comments and suggestions on manuscript draft. We are also grateful to C. B. M. Alves, J. L.O. Birindelli, S. Grant, L. Montag, L. Sousa, and N. Lujan for making their images of live fishes available. We are indebted to L. Montag, N. Milani, R. de Ruiter, C. B. M. Alves, J. L. O. Birindelli, M. W. Littmann, L. M. Sousa, F. Cabeceira and California Academy of Sciences (CAS) database for some images of specimens in present study; thanks also to K. Luckenbill for improvements to figures. Thanks to B. B. Calegari, F. C. P. Dagosta, F. C. T. Lima, J. L.O. Birindelli and S. Grant for exchange of ideas regarding auchenipterid catfishes. We are grateful to P. Goloboff for clarifying ideas about rooting the analysis using TNT computer program. Study funded by Conselho Nacional de Desenvolvimento Científico e Tecnológico (CNPq) (proc. 471963/2013-5) and PCI-E1 grant 465023/2014-2 (to LMSS). Comparative material from rio Xingu made available by iXingu Project (NSF DEB-12578113; PI M. H. Sabaj).

LITERATURE CITED

Adriaens D., and W. Verraes. 1996. Ontogeny of cranial musculature in *Clarias gariepinus* (Siluroidei: Clariidae): the adductor mandibulae complex. Journal of Morphology, 229:255–269.

Akama, A. 2004. Revisão sistemática dos gêneros *Parauchenipterus* Bleeker, 1862 e *Trachelyopterus* Valenciennes, 1840 (Siluriformes, Auchenipteridae). Unpublished Ph. D. Dissertation, Universidade de São Paulo, São Paulo, 375 p.

Albert, J.S., and T.P. Carvalho. 2011. Neogene Assembly of Modern Faunas, p. 119–136 *In:* J.S. Albert and R.E. Reis (eds.). Historical biogeography of Neotropical freshwater fishes. University of California Press, Berkeley.

Alexander, R.M. 1965. Structure and function in the catfish. Journal of Zoology, 148: 88–152.

Arce H., M., R.E. Reis, A.J. Geneva and M.H. Sabaj. 2013. Molecular phylogeny of thorny catfishes (Siluriformes: Doradidae). Molecular Phylogenetics and Evolution, 67: 560–577.

Arratia, G., and H.P. Schultze. 1990. The urohyal: development and homology within osteichthyans. Journal of Morphology, 203: 247–282.

Arratia, G. 1987. Description of the primitive family Diplomystidae (Siluriformes, Teleostei, Pisces): morphology, taxonomy and phylogenetic implications. Bonner Zoologische Monographien, 24: 1–120.

Arratia, G. 1992. Development and variation of the suspensorium of primitive catfishes (Teleostei: Ostariophysi) and their phylogenetic relationships. Bonner Zoologische Monographien, 32: 1–149.

Arratia, G. 2003. Catfish Head Skeleton, an overview, p. 3–46 *In:* Arratia, G., B. G. Kapoor, M. Chardon and R. Diogo (eds.). Catfishes. Science Publishers, Enfield.

Berkovitz, B., and P. Shellis, 2017. The teeth of non-Mammalian Vertebrates. Elsevier, London, 331 p.

Birindelli, J.L.O., and J. Zuanon. 2012. Systematics of the Jaguar catfish genus *Liosomadoras* Fowler, 1940 (Auchenipteridae: Siluriformes). Neotropical Ichthyology, 10: 1–11.

Birindelli, J.L.O. 2014. Phylogenetic relationships of the South American Doradoidea (Ostariophysi: Siluriformes). Neotropical Ichthyology, 12: 451–564.

Bleeker, P. 1862-1863. Atlas ichthyologique des Indes Orientales Néêrlandaises, publié sous les auspices du Gouvernement colonial néêrlandais. Tome II. Siluroïdes, Chacoïdes et Hétérobranchoïdes. Amsterdam.

Böhlke, J.E. 1980. *Gelanoglanis stroudi*: A new catfish from the Rio Meta system in Colombia (Siluriformes, Doradidae, Auchenipterinae). Proceedings of the Academy of Natural Sciences of Philadelphia, 132: 150–155.

Bremer, K. 1994. Branch support and tree stability. Cladistics, 10: 295–304.

Bridge, T.W., and A.C. Haddon. 1892. Contributions to the anatomy of fishes. II. The air-bladder and weberian ossicles in the Siluridae. Phylosophical Transactions of the Royal Society of London, series B, 84: 65–333.

Britski, H.A. 1972. Sistemática e evolução dos Auchenipteridae e Ageneiosidae (Teleostei, Siluriformes). Unpublished Ph. D. Dissertation, Universidade de São Paulo, São Paulo, 142 p.

Calegari, B.B., R.P. Vari and R.E. Reis. 2019. Phylogenetic systematics of the driftwood catfishes (Siluriformes: Auchenipteridae): a combined morphological and molecular analysis. Zoological Journal of the Linnean Society, 20: 1–113.

Calegari, B.B., R.E. Reis and R.P. Vari. 2014. Miniature catfishes of the genus *Gelanoglanis* (Siluriformes: Auchenipteridae): monophyly and the description of a new species from the upper rio Tapajós basin, Brazil. Neotropical Ichthyology, 12: 699–706.

Cardoso, A.R. 2008. Filogenia da família Aspredinidae Adams, 1854 e revisão taxonômica de Bunocephalinae Eigenmann and Eigenmann, 1888 (Teleostei: Siluriformes: Aspredinidae). Unpublished Ph.D. dissertation, Pontifícia Universidade Católica do Rio Grande do Sul, Porto Alegre, 259 p.

Cardoso, Y.P., and J.I. Montoya-Burgos. 2009. Unexpected diversity in the catfish *Pseudancistrus brevispinis* reveals dispersal routes in a Neotropical center of endemism: The Guyanas Region. Molecular Ecology, 18: 947–964.

Carvalho, L.N., J. Zuanon and I. Sazima. 2007. Natural History of Amazon Fishes, *In:* Del-Claro, K. (org.). Encyclopedia of Life Support Systems, UNESCO, Oxford.

Collin, S.P., and J. Shand. 2003. Retinal sampling and the visual field in fishes, p. 139–169 *In:* Collin, S.P., and N.J. Marshall (eds.). Sensory Processing in Aquatic Environments. Springer, New York.

Curran, D.J. 1989. Phylogenetic relationships among the catfish genera of the family Auchenipteridae (Teleostei: Siluroidea). Copeia, 1989: 408–419.

Dagosta, F.C.P., and M. de Pinna. 2017. Biogeography of Amazonian fishes: deconstructing river basins as biogeographic units. Neotropical Ichthyology, 15(3): e170034, 2017.

Dahdul, W.M., J.G. Lundberg, P.E. Midford, J.P. Balhoff, H. Lapp, T.J. Vision, M.A. Haendel, M. Westerfield and P.M. Mabee 2010. The Teleost Anatomy Ontology: Anatomical Representation for the Genomics Age. Systematic Biology, 59: 369–383.

Datovo, A., and R.P. Vari. 2013. The jaw adductor muscle complex in teleostean fishes: evolution, homologies and revised nomenclature (Osteichthyes: Actinopterygii). PLoS ONE, 8: e60846.

Datovo, A., and R.P. Vari. 2014. The adductor mandibulae muscle complex in lower teleostean fishes (Osteichthyes: Actinopterygii): Comparative anatomy, synonymy, and phylogenetic implications. Zoological Journal of the Linnean Society, 2014: 1–69.

Diogo, R. 2004. Morphological evolution, adaptations, homoplasies, constraints and evolutionary trends: Catfishes as a case study on general phylogeny and macroevolution. Science Publisher, Inc., Enfield, 600 p.

Ferraris, C.J., Jr. 1988. The Auchenipteridae: Putative monophyly and systematics, with a classification of the neotropical doradoid catfishes (Ostariophysi: Siluriformes). Unpublished Ph. D. Dissertation, The City University of New York, New York, 229 p.

Ferraris, C.J., Jr. 2007. Checklist of catfishes, recent and fossil (Osteichthyes: Siluriformes), and catalogue of siluriform primary types. Zootaxa, 1418: 1–628.

Ferraris, C.J., Jr., and R.P. Vari. 1999. The South American catfish genus *Auchenipterus* Valenciennes, 1840 (Ostariophysi: Siluriformes: Auchenipteridae): monophyly and relationships, with a revisionary study. Zoological Journal of the Linnean Society, 126: 387–450.

Ferraris, C.J., Jr., and R.P. Vari. 2000. The deep-water South American catfish genus *Pseudepapterus* (Ostariophysi: Auchenipteridae). Ichthyological Explorations of Freshwaters, 11: 97–112.

Franke, H.J. 1990. The first breeding of the starry woodcat, *Tatia galaxias*. Tropical Fish Hobbyist, 39: 20–34.

Friel, J.P. 1994. A phylogenetic study of the Neotropical banjo catfishes (Teleostei: Siluriformes: Aspredinidae). Unpublished Ph. D. Dissertation, Duke University, Durham, 256 p.

Ghiot, F., P. Vandewalle and M. Chardon. 1984. Anatomical and functional comparison of barbel muscles and ligaments in 2 families of bagroid fishes. Annales de la Societe Royale Zoologique de Belgique, 114: 261–272.

Goloboff, P.A., and S.A. Catalano. 2016. TNT version 1.5, including a full implementation of phylogenetic morphometrics. Cladistics, 32: 221–238.

Gosline, W.A. 1973. Considerations regarding the phylogeny of cypriniform fishes, with special reference to structures associated with feeding. Copeia, 1973: 761–776.

Grant, S. 2015. Four new subgenera of *Centromochlus* Kner, 1858 with comments on the boundaries of some related genera (Siluriformes: Auchenipteridae: Centromochlinae). Ichthyofile, 3: 1–16.

Hara, T.J. 1994. Olfaction and gustation in fish: an overview. Acta Physiologica Scandinavica, 152: 207–217.

Hennig, W. 1950. Grundzüge einer Theorie der phylogenetischen Systematik. Deutsche Zentralverlag, Berlin. 370 p.

Hennig, W. 1966. Phylogenetic Systematics. University of Illinois Press, Urbana. 263 p.

Higuchi, H. 1992. A phylogeny of the South American thorny catfishes (Osteichthyes; Siluriformes; Doradidae). Unpublished Ph. D. Dissertation, Harvard University, Boston, 372 p.

Hoedeman, J.J. 1961. Notes on the ichthyology of Surinam and other Guianas. 8. Additional records of siluriform fishes. Bulletin of Aquatic Biology, 2: 129–139.

LeClair, E.E., and J. Topczewski. 2010. Development and Regeneration of the Zebrafish Maxillary Barbel: A Novel Study System for Vertebrate Tissue Growth and Repair. PLoS ONE, 5(1): e8737.

Loir, M., C. Cauty, P. Planquette and P.-Y. le Bail. 1989. Comparative study of the male reproductive tracts in seven families of South American catfishes. Aquatic Living Resource, 2: 45–56.

Lujan, N.K., and J.W. Armsbruster. 2011. The Guiana Shield, p. 211–224 *In:* Albert, J. S., and R.E. Reis (eds.). Historical Biogeography of Neotropical Freshwater Fishes. University of California Pres, Berkeley.

Lundberg, J.G. 1970. The evolutionary history of North American catfishes, family Ictaluridae. Unpublished Ph.D. Thesis, University of Michigan.

Lundberg, J.G. 1982. The comparative anatomy of the toothless blincat, *Trogloglanis pattersoni* Eigenmann, with a phylogenetic analysis of the ictalurid catfishes. Miscellaneous Publications of the Museum of Zoology, University of Michigan, 163: 1–85.

Lundberg, J.G., L.G. Marshall, J. Guerrero, B. Horton, M.C.S.L. Malabarba and F. Wesselingh. 1998. The stage for Neotropical fish diversification: A history of tropical South American rivers p. 13–48 *In:* Malabarba, L.R., R.E. Reis, R.P. Vari, Z.M.S. Lucena and C.A.S. Lucena (eds.). Phylogeny and classification of Neotropical fishes, Edipucrs, Porto Alegre.

Lundberg, J.G., T.M. Berra and J.P. Friel. 2004. First description of small juveniles of the primitive catfish *Diplomystes* (Siluriformes: Diplomystidae). Ichthyological Explorations of Freshwaters, 15: 71–82.

Mazzoldi, C., V. Lorenzi and M.B. Rasotto. 2007. Variation of male reproductive apparatus in relation to fertilization modalities in the catfish families Auchenipteridae and Callichthyidae (Teleostei: Siluriformes). Journal of Fish Biology, 70: 243–256.

Mees, G.F. 1974. The Auchenipteridae and Pimelodidae of Suriname (Pisces, Nematognathi). Zoologische Verhandelingen, 132: 1–256.

Meeuse, A.D.J. 1965. The cleaning of skeletons by means of larvae of dermestid beetles. Bijdragen tot de Dierkunde, 35: 135–139.

Meisner, A.D., J.R. Burns, S.H. Weitzmann and L.R. Malabarba. 2000. Morphology and histology of the male reproductive system in two species of internally inseminating South American catfishes, *Trachelyopterus lucenai* and *T. galeatus* (Teleostei: Auchenipteridae). Journal of Morphology, 246: 131–141.

Melo, R.M.C., F.P. Arantes, Y. Sato, J.E. Santos, E. Rizzo and N. Bazzoli. 2011. Comparative Morphology of the Gonadal Structure Related to Reproductive Strategies in Six Species of Neotropical Catfishes (Teleostei: Siluriformes). Journal of Morphology, 272:525–535.

Miranda Ribeiro, P. 1968. Apontamentos ictiológicos III. Boletim do Museu Nacional do Rio de Janeiro, Nova Série, Zoologia, 263: 1–14.

Nakatani, K., A.A. Agostinho, G. Baumgartner, A. Bialetzki, P.V. Sanches, M.C. Makrakis and C.S. Pavanelli. 2001. Ovos e larvas de peixes de água doce, desenvolvimento e manual de identificação. Universidade Estadual de Maringá, Maringá, Brazil, 378p.

Nixon, K.C. 2002. WinClada ver. 1.00. 08. Published by the author, Ithaca, NY.

Nixon, K.C., and J.M. Carpenter 1993. On outgroups. Cladistics, 9(4): 413-426.

Pereira, L.H., A. Bialetski and A.C. Bonecker. 2017. Larval and juvenie development of *Tatia intermedia* (Siluriformes : Auchenipteridae). Journal of Fish Biology, 90: 1098–1103.

de Pinna, M.C.C. 1996. A phylogenetic analysis of the Asian catfish families Sisoridae, Akysidae, and Amblycipitidae, with a hypothesis on the relationships of Neotropical Aspredinidae (Teleostei, Ostariophysi). Fieldiana, 1478: 1–83.

de Pinna, M.C.C. 1998. Phylogenetic relationships of Neotropical Siluriformes (Teleostei: Ostariophysi): historical overview and synthesis of hypotheses, p. 279–330 *In:* Malabarba, L.R., R.E. Reis, R.P. Vari, Z.M.S. Lucena and C.A.S. Lucena (eds.). Phylogeny and Classification of Neotropical Fishes. Edipucrs, Porto Alegre.

Poll, M. 1971. Révision des *Synodontis* Africains (Famille Mochocidae). Annales du Musée Royal de l'Afrique Centrale, series in 8º, Sciences Zoologiques, 191: 1–497.

Regan, C.T. 1911. The classification of the teleostean fishes of the order Ostariophysi. 2. Siluroidea. Annals and Magazine of Natural History, 8: 553–577.

Reis, R.E., and T.A.K. Borges. 2006. The South Americn Catfish Genus *Entomocorus* (Ostariophysi: Siluriformes: Auchenipteridae), with the Description of a New Species from the Paraguay River Basin. Copeia, 2006: 412–422.

Rengifo, B., N.K. Lujan, D. Taphorn and P. Petry. 2008. A new species of *Gelanoglanis* (Siluriformes: Auchenipteridae) from the Marañon River (Amazon Basin), northeastern Peru. Proceedings of the Academy of Natural Sciences of Philadelphia, 157: 181–188.

Ribeiro, A.C. 2006. Tectonic History and the Biogeography of the Freshwater Fishes from the Coastal Drainages of Eastern Brazil: An Example of Faunal Evolution Associated with a Divergent Continental Margin. Neotropical Ichthyology, 4: 225–246.

Rojo, A.L. 1991. Dictionary of evolutionary fish osteology. Taylor & Francis Group, Boca Raton, 230 p.

Royero, R. 1987. Morfologia de la aleta dorsal en los bagres (Teleostei: Siluriformes), con especial referencia a las familias americanas. Unpublished graduated monography, Universidad Central de Venezuela, Caracas, 285 p.

Royero, R. 1999. Studies on the systematics and phylogeny of the catfish family Auchenipteridae (Teleostei: Siluriformes). Unpublished Ph.D. Dissertation, University of Bristol, London, 534 p.

Sabaj, M.H. 2020. Codes for Natural History Collections in Ichthyology and Herpetology. Ichthyology and Herpetology [ex Copeia], 108: 1–76.

Santos, J.A.D., R.M. Passos, A.A. Agostinho and A. Bialetzki. Early ontogeny of *Tatia neivai* (Ihering, 1930) (Osteichthyes, Auchenipteridae), a small catfish from Neotropical region. Zootaxa, 4353: 540–550.

Sarmento-Soares, L.M., and M. Porto. 2006. Comparative anatomy of the cheek muscles within the Centromochlinae subfamily (Ostariophysi, Siluriformes, Auchenipteridae). Journal of Morphology, 267: 187–197.

Sarmento-Soares, L.M., and R.F. Martins-Pinheiro. 2008. A systematic revision of *Tatia* (Siluriformes: Auchenipteridae: Centromochlinae). Neotropical Ichthyology, 6: 495–542.

Sarmento-Soares, L.M., and R.F. Martins-Pinheiro. 2013. *Glanidium botocudo*, a new species from the rio Doce and rio Mucuri, Minas Gerais, Brazil (Siluriformes: Auchenipteridae) with comments on taxonomic position of *Glanidium bockmanni* Sarmento-Soares and Buckup. Neotropical Ichthyology, 11: 265–274.

Sarmento-Soares, L.M., H. Lazzarotto, L.H.R. Py-Daniel and R.P. Leitão. 2016. A new *Centromochlus* (Siluriformes: Auchenipteridae: Centromochlinae) from the transition between Amazon floodplain and Guiana shield, Brazil. Neotropical Ichthyology, 14: 1–12.

Sazima, I., J. Zuanon and V. Haddad. 2005. Puncture wounds by driftwood catfish during bucket baths: local habits of riverside people and fish natural history in the Amazon. Wilderness and Environmental Medicine, 16: 204–208.

Sereno, P.C. 2007. Logical basis for morphological characters in phylogenetics. Cladistics, 23: 565–587.

Soares-Porto, L.M. 1998. Monophyly and interrelationships of the Centromochlinae (Siluriformes, Auchenipteridae), p. 331–350 *In:* Malabarba, L.R., R.E. Reis, R.P. Vari, Z.M.S. Lucena and C.A.S. Lucena (eds.). Phylogeny and Classification of Neotropical fishes. Edipucrs, Porto Alegre.

Soares-Porto, L.M., S.J. Walsh, L.G. Nico and J. Maia. 1999. A new *Gelanoglanis* from the Orinoco and Amazon River basins, with comments on miniaturization within the genus (Siluriformes: Auchenipteridae: Centromochlinae). Ichthyological Explorations of Freshwaters, 10: 63–72.

Sousa, L.M. 2010. Revisão Taxonômica e Filogenia de Astrodoradinae (Siluriformes, Doradidae). Unpublished Ph.D. Dissertation, Universidade de São Paulo, São Paulo, 276p.

Spadella, M.A., C. Oliveira, H. Ortega, I. Quagio-Grassiotto and J.R. Burns. 2012. Male and female reproductive morphology in the inseminating genus *Astroblepus* (Ostariophysi: Siluriformes: Astroblepidae). Zoologischer Anzeiger, 251: 38–48.

Stewart, T.A. 2014. The origins of adipose fins: an analysis of homoplasy and the serial homology of vertebrate appendages. Proceedings of the Royal Society, 281: 1–8.

Swofford, D.L., and W.P. Maddison, 1987. Reconstructing ancestral character states under Wagner parsimony. Mathematical Biosciences, 87(2): 199-229.

Swofford, D.L., and W.P. Maddison, 1992. Parsimony, Character-State Reconstructions, and Evolutionary Inferences, p. 186–223 *In:* R.C. Mayden (ed.). Systematics, historical ecology, and North American freshwater. Stanford University Press, Palo Alto.

Taylor, W.R., and G. Van Dyke, 1985. Revised procedures for staining and clearing small fishes and other vertebrates for bone and cartilage study. Cybium, 9: 107–119.

Vanscoy, T., J.G. Lundberg and K.R. Luckenbill. 2015. Bony ornamentation of the catfish pectoral-fin spine: comparative and developmental anatomy, with an example of fin-spine diversity using the Tribe Brachyplatystomini (Siluriformes, Pimelodidae). Proceedings of the Academy of Natural Sciences of Philadelphia, 164: 177–212.

Vari, R.P., and C.J. Ferraris, Jr. 2006. The catfish genus *Tetranematichthys* (Auchenipteridae). Copeia, 2006: 168–180.

Vari, R.P., and C.J. Ferraris, Jr. 2013. Two new species of the catfish genus *Tatia* (Siluriformes: Auchenipteridae) from the Guiana Shield and a reevaluation of the limits of the genus. Copeia, 2013: 396–402.

Vigliotta, T.R. 2008. A phylogenetic study of the African catfish family Mochokidae (Osteichthyes, Ostariophysi, Siluriformes), with a key to genera. Proceedings of the Academy of Natural Sciences of Philadelphia, 157: 73–136.

Walsh, S.J. 1990. A systematic revision of the Neotropical catfish family Ageneiosidae (Teleostei: Ostariophysi: Siluriformes). Unpublished Ph.D. Dissertation, University of Florida, Florida, 363 p.

Wiley, E.O., D. Siegel-Causey, D.R. Brooks and V.A. Funk. 1991. The Compleat Cladist. A Primer of Phylogenetic Procedures. Museum of Natural History, The University of Kansas, Lawrence, 172 p.

Winterbottom, R. 1974. A descriptive synonym of the striated muscles of the Teleostei. Proceedings of the Academy of Natural Sciences of Philadelphia, 125: 225–317.

APPENDIX A

Material examined

Auchenipteridae: Centromochlinae

Centromochlus carolae.—Brazil: Roraima State: MZUSP 9347, 1, 29.4 mm SL; Uraricoera River, Maracá island, near Fazenda Canadá. Guyana: USNM 401514, holotype, Rx, 37.2 mm SL; Cuyuni River, sand island in middle of river just downstream from Kurutuku, Essequibo River basin, Cuyuni-Mazaruni. USNM 401511, 1, paratype, Rx, 31.9 mm SL; Cuyuni River, Cuyuni-Mazaruni. ANSP 175836, 9, 22.3–30.5 mm SL and MNRJ 30491, 1, cs, 23.7 mm SL; Essequibo River.

Centromochlus existimatus.—Brazil: Acre State: MZUSP 48880, 1, 90.2 mm SL; and MZUSP 57643, 1, 80.1 mm SL; Porto de Rio Branco, Branco River. Pará State: INPA 40662, 6, 46.5–59.0 mm SL; right margin of Xingu River, Porto de Moz.

Centromochlus heckelii.—Brazil: Acre State: MZUSP 48910, 2, 80.0–83.2 mm SL; Acre River between seringal Paraíso and lagoa Amapá. Amapá State: MNRJ 12130, 8, 33.4–61.8 mm SL; Fazendinha, Amazonas River, near Macapá. MNRJ 12135, 10, 40.5–55 mm SL, 1 mi; Amazonas River, Macapá. Amazonas State: INPA 8203, 2, 73.3–81.8 mm SL; Manacapuru. INPA 10967, 2, 106.2–108.7 mm SL; Jamari River. INPA 8369, 5, 62.3–74.0 mm SL, 1 mi; Amazonas River, downstream from Paraná da Eva, Itacoatiara. INPA 12643, 6, 86.7–90.5 mm SL; Jaú River, Novo Airão. MZUSP 83268, 80.2 mm SL; Amazonas River. MZUSP 44128, 3, 1 CS, 69.8–77.0 mm SL; Pauini. Pará State: MZUSP 8336, 2 cs, 53.4–62.0 mm SL; Tapajós River, Santarém. MPEG 4977, 14, 68.5–83.5 mm SL; Pará. Venezuela: MCNG 23921, 2, 83.7–83.8 mm SL; Orenoco River, Porto Venado.

Centromochlus macracanthus.—BRAZIL: AMAZONAS STATE: INPA 6565, 1, paratype, 129.7 mm SL; Negro River. INPA 43009, 6, 55.4–71.9 mm SL; Negro River, Cachoeira Curucui, São Gabriel da Cachoeira. MZUSP 30605, 2, paratypes, 65.7–71.8 mm SL; MZUSP 30619, 1, 42.0 mm SL; and MZUSP 52924, 6, 1 cs, paratypes, 41.0–68.2 mm SL; Negro River, São Gabriel da Cachoeira.

Centromochlus melanoleucus.—BRAZIL: AMAZONAS STATE: INPA 36773, 6, 27.3–32.3 mm SL; central amazonian, Catalão, Manaus. PARÁ STATE: INPA 43676, 4, 43.2 mm SL; Xingu River, on flooded vegetation along left bank, Altamira. MNRJ 35521, 1, 48.5 mm SL; Tapajós River, Mirituba along boat cross at Transamazônica, Itaituba. MZUSP 8535, 6, 1 CS, 46.9–76.5mm SL; Tapajós River, Santarém. MZUSP 21837, 1, 38.5 mm SL; Tapajós River, São Luiz. MZUSP 30585, 6, 1 CS, 35.0–48.4 mm SL; Tapajós River, Alter do Chão.

Centromochlus musaicus.—VENEZUELA: AMAZONAS. AMNH 58795, 3, 25.1–29.0 mm SL; paratypes, MBUCV-V 15663, 47.1 mm SL; holotype, MBUCV-V 17727, 1, paratype, 26.8 mm SL; Atabapo River, approximately 3 km from its mouth, San Fernando de Atabapo. ANSP 160656, 1, 57.0 mm SL; Sipapo River, above Pendare. MCNG 21796, 1, 50.8 mm SL; stream La Chimita 3–15 km above confluence with Atacavi River.

Centromochlus orca.—BRAZIL: PARÁ STATE: INPA 35086, 14, 1 CS, 40.5–56.8 mm SL; INPA 35087, 4, 21.0–47.7 mm SL; paratypes, MBML 11220, 1, 51.0 mm SL; paratypes, MBML 11221, 1 CS, 50.6 mm SL; paratypes, MNRJ 45072, 5, 1 CS, 38.2–52.3 mm SL; paratypes, mouth of Igarapé Jamari with lago de Terra Santa, Nhamundá River basin, Terra Santa. INPA 43875, 4, 43.2–54.1 mm SL; INPA 43883, 3, 37.2–49.4 mm SL; Nhamundá River.

Centromochlus cf. *orca*.—BRAZIL: PARÁ STATE: ANSP 196655, 1, 56.0 mm SL; Xingu River, 4.5 km northeast of Vitória do Xingu, Senador José Porfírio. ANSP 196666, 1, 44.2 mm SL; Xingu River, upstream of mouth of Veiros River, Porto de Moz. ANSP 198628, 1, 42.2 mm SL; Xingu River at right bank about 20 Km southeast of Vitória do Xingu. ANSP 197862, 2, 41.2–45.5 mm SL; INPA 47841, 2, 49.7–51.3 mm SL; Acarai River, about 1 km above confluence with Xingu River, Porto de Moz.

Centromochlus schultzi.—BRAZIL: GOIÁS STATE: MNRJ 12139, 38, 1 CS, 85.0–108.9 mm SL; Serra da Mesa dam, upper Tocantins River. MATO GROSSO STATE: MNRJ 9417, 2, 32.7–60.8 mm SL; upper Xingu River. TOCANTINS STATE: UNT 850, 1, 94.0 mm SL; Paranã River at Fazenda Traçadal, Paranã. UNT 851, 1, 89.2 mm SL; Tocantins River at Brejinho de Nazaré. UNT 16340, 7, 80.1-102.5 mm SL; Tocantins River at Porto Nacional.

Gelanoglanis nanonocticolus.—BRAZIL: AMAZONAS STATE: MZUSP 28308, 2, 16–16.8 mm SL; Rx, paratypes, Paraná do Jacaré, Negro River, Amazon River basin. MZUSP 81212, 2, 20.5–23.3 mm SL; Tiquié River, community of Caruru, beach downstream waterfall. MZUSP 81524, 1, 25.3 mm SL; Tiquié River, community of Boca do Sal. VENEZUELA: MCNG 22690, 1, Rx, 22.2 mm SL; holotype, Asisa River, upstream from confluence with Paru River, Ventuari River drainage, Orinoco River basin.

Gelanoglanis pan.—BRAZIL: MATO GROSSO STATE: MZUSP 96032, 5, 1 CS, 11.8–26.4 mm SL; paratypes, Teles Pires River, Itaúba, tributary to upper Tapajós River basin. BRAZIL: PARÁ STATE: INPA 53085, 1, 20.1 mm SL; Xingu River. INPA 12419, 1, 20.1 mm SL; Xingu River, near Vitória do Xingu.

Gelanoglanis stroudi.—COLOMBIA: META DEPARTMENT: ANSP 142937, 22.6 mm SL; holotype, ANSP 142938, 5, 2 Rx, paratypes, 25.9–36.6 mm SL; and ANSP 142940, 1, Rx, paratype, 24.8 mm SL; Metica River approximately 22 km southwest from Puerto Lopez and 3 Km southeast from Hacienda Mozambique. FMNH 83912, 1, 24.6 mm SL; CS, paratype, Manacacias River 4 km east from Puerto Gaitan. VENEZUELA: MBUCV-V 27965, 1, 29.7 mm SL; Río Apure, Apure, Amazonas.

Gelanoglanis travieso.—PERU: ANSP 182807, 1, Rx, 29.7 mm SL; paratype, and ANSP 182808, 1, CS, 29.2 mm SL; paratype, Nieva River, Maranon River drainage, Amazonas.

Gelanoglanis varii.—BRAZIL: TOCANTINS STATE: MCP 49095, 2, 10.6- 11.9 mm SL; CS, paratypes, Tocantins River at Tupiratins, Amazon basin.

Gephyromochlus leopardus.—GUYANA: MNHN 1989-43, 1, 106.0 mm SL. FRENCH GUIANA. ZMA.PIS 102.233, 1, 100 mm SL; Rx, holotype, Litany River, Aloiké village, Maroni River basin. RMNH.PIS 28575, 1, 48.0 mm SL; Acarouany, Mana River basin. RMNH.PIS 28573, 2, 56.0–71.0 mm SL; RMNH.PIS 28574, 2, 85.0–94.0 mm SL; and RMNH.PIS 28576, 4, 1 CS, 38.5–82.6 mm SL; Balaté creek, Mana River basin. ZMA.PIS 107.825, 2, 87.2–90.1 mm SL; stream Yawapa, Yawapa village, upper Oyapock River, Oyapock River basin. SURINAME: ZMA.PIS 105.854, 12, 59.0–99.7 mm SL; Maka creek, right margin of Lawa River, 10 km south from Stoelmans island. Marowijne/Maroni River basin.

Glanidium albescens.—Brazil: Minas Gerais State: UZMK 335, 1, syntype, 101 mm SL; Rx, UZMK 336, 1, syntype (Rx), 94 mm SL; UZMK 337, 1, 93 mm SL, Rx, syntype, Velhas River, São Francisco River basin. DZUFMG unnumbered, 2, 40–47 mm SL; Rx, São Francisco River at Manga. MNRJ 16262, 4, 107.5–121.5 mm SL; Paraopeba River, São Francisco River basin. MCNIP 1084, 4, 91.5–101.9 mm SL; MBML 11230, 23.1 mm SL; and MCNIP 1085, 1, 71.7 mm SL; São Francisco River, Rio Acima village, São Francisco River basin.

Glanidium botocudo.—Brazil: Minas Gerais State: MNRJ 32538, 93.2 mm SL; holotype, and DZUFMG 047, 1, 95.2 mm SL; Rx, paratype, Mucuri River, downstream from Santa Clara dam, Nanuque, on boundary with Minas Gerais and Bahia states. DZUFMG 048, 1, paratype, 83.0 mm SL and MNRJ 32539, 1, paratype, CS, 82.0 mm SL; Ponte Nova, Piranga River, Doce River basin. MBML 2047, 2, Rx, 86.8–95.5 mm SL; Santa Cruz do Escalvado, Doce River basin. MNRJ 31460, 2, 83.0–91.0 mm SL; córrego Joanésia, tributary of Santo Antônio River, Joanésia, Doce River basin.

Glanidium catharinensis.—Brazil: Santa Catarina State: MNRJ 5169, 1, Rx, holotype, 89.0 mm SL; Braço do Norte River, São Ludgero, Tubarão. MCP 25588, 3, 116.5–138.3 mm SL; Capivari River, tributary of Tubarão River, São Martinho. MCP 29701, 3, 115.0–123.2 mm SL; Braço do Norte River, tributary of Tubarão River. MNRJ 1109, 6, 83.9–134.2 mm SL; Novo River, tributary Itapocu River, Humboldt-Corupá. São Paulo State: MZUSP 9308, 1, CS, 103.2 mm SL; MZUSP 45189, 2, 118.8–139.6 mm SL; and MZUSP 55490, 6, 93.9- 169.0 mm SL; Ribeira do Iguape River. MZUSP 55494, 8, 110.3–118.5 mm SL; Barra do Turvo, Ribeira do Iguape River. MZUSP 44260, 1, 71.3 mm SL; São Lourenço River, Oliveira Barros, Miracatu, Ribeira do Iguape River basin.

Glanidium cesarpintoi.—Brazil: Goiás State: MNRJ 41724, 3, 1 CS, 65.2–83.2 mm SL; and NUP 5699, 7, 77.7–87.9 mm SL; Corumbá River, tributary of Paranaíba River, Pires do Rio near Ipameri, Paranaíba River basin. NUP 11519, 7, 1 CS, 60.2–72.2 mm SL; Rx, Jacotuba River in Mineiros, Paranaíba River basin. São Paulo State: DZSJRP 4570, 1, 89.7 mm SL; Rx, Tietê River, downstream from Salto Grande reservatory, Tietê River basin. DZSJRP 6343, 1, 13.6 mm SL; Borá River, between Nova Aliança and Potirendaba, Tietê River basin. MZUEL 108, 3, 87.5–94.7 mm SL; Tibagi River, Paranapanema River basin. MZUEL 9539, 1, 74.7 mm SL; Lajinha River tributary of Paranapanema River. Mato Grosso do Sul State: NUP 5455, 2, 75.5–80.2 mm SL; Piquiri River, Nova Laranjeiras, Upper Paraná River basin. Paraná State: MZUSP 51046, 1, 14.3 mm SL; lake near Abrigo stream, Jupiá river dam, Upper Paraná basin.

Glanidium melanopterum.—Brazil: São Paulo State: MZUSP 52573, 1, 130.3 mm SL; Paraíba do Sul River. Espírito Santo State: LIRP 6416, 1, 111.2 mm SL; and LIRP 7036, 4, 95.9–99.3 mm SL; Itabapoana River, on area of UHE Rosal, Guaçuí. MBML 2118, 2 Rx, 125.2–144.6 mm SL; Santa Maria da Vitória River in Mangaraí, Santa Leopoldina, Santa Maria da Vitória River basin. MBML 2566, 2 Rx, 136.8–154.0 mm SL; and MBML 2571, 1 Rx, 153.8 mm SL; Benevente River downstream from Alfredo Chaves, Benevente River basin. MBML 3913, 1, 131.9 mm SL; Itapemirim River downstream from Itaóca stream, Itapemirim River basin. Rio de Janeiro State: MNRJ 12137, 2, 107–134.5 mm SL; Juturnaíba Lagoon, between Araruama and Silva Jardim, São João River basin. MNRJ 12359, 1, CS, 105.0 mm SL; Paraíba do Sul River, Três Rios. MNRJ 17485, 2, 129.0–190.0 mm SL; ribeirão das Lajes. CAS 52128, 1, 84.5 mm SL, Paraíba do Sul River. MNRJ 16061, 1, 51.3 mm SL; Itaocara, Coronel Teixeira, Paraíba do Sul River basin. USNM 41506, 1, 98.6 mm SL; Paraíba do Sul River basin. MZUSP 42572, 3, 61.3–90.4 mm SL; Paraíba do Sul River, São Fidélis. MZUSP 44130, 1, 70 mm SL; rio Muriaé, Itaperuna.

Glanidium ribeiroi.—Brazil: Paraná State: AMNH 37924, 1, 126.0 mm SL; Iguaçu River, upstream from cataracts. FMNH 54243, 1, 134.4 mm SL; holotype, Porto União da Vitória. MNRJ 27963, 3, 1 CS, 92.9–192.5 mm SL; MZUSP 45044, 4, 82.2–90.5 mm SL; Iguaçu River upstream from Salto Santiago, Laranjeiras do Sul. NUP 5463, 15, 5 Rx, 87.1–105.4 mm SL; NUP 5471, 19, 77.3–137.9 mm SL, and NUP 5698, 4, 172.1–193.4 mm SL; Iguaçu River, downstream from Caxias reservatory, Capitão Leônidas Marques. NUP 5474, 7 Rx, 72.6–91.5 mm SL; Jordão reservatory, lower Iguaçu River, Foz do Jordão. NUP 11868, 3 Rx, 52.7–75.1 mm SL; tributary of Iguatemi River, lower Iguaçu River, Tapejara do Oeste.

Tatia altae.—Colombia: USNM 121965, 1, 35.5 mm SL; Dedo River, tributary of Orteguazo River.

Tatia aulopygia.—Bolivia. AMNH 39818, 2, 25.8–27.8 mm SL; Itenez River, Beni. INHS 37034, 1, 75.2 mm SL; Matos River, Apure River drainage, Amazon basin; MNHN 1988–994, 1, Rx, 56.3 mm SL; Mamoré River drainage; UMMZ 204834, 1 24.6 mm SL; Baures River, about 500 m upstream from mouth of Itenez River. Brazil: Amazonas State: ZMA.PIS 114.280, 2, Rx, 39.6–46.8 mm SL; Humaitá, Madeira River drainage. Rondônia State: FMNH 58015, 3, 21.8–43.8 mm SL, Guaporé River in Maciel. INPA 11078, 1, 76.2 mm SL, INPA 11079, 1, 159.0 mm SL and INPA 11080, 3, 1 CS, 80.0–104.6 mm SL; Guaporé River.

Tatia bockmanni.—BRAZIL: BAHIA STATE: MZUSP 82351, 8, 1 CS, paratypes, 29.4–35.8 mm SL, Preto River at Formosa do Rio Preto.

Tatia boemia.—BRAZIL: RIO GRANDE DO SUL STATE: MCP 12949, 6, 1 CS, paratype, 33.1–61.1 mm SL; and MZUSP 47921, 2, Rx, paratypes, 52.4–64.5 mm SL; Pelotas River on road Anita Garibaldi to Pinhal da Serra, Esmeralda.

Tatia britskii.—BRAZIL: SÃO PAULO STATE: MZUSP 115271, holotype, 39.2 mm SL, MZUSP 43251, 2, 1 CS, 33.5–36.3 mm SL, paratypes, and MNRJ 41787, 2, 36.0–38.6 mm SL, paratypes, Paraná River, upper Paraná River basin.

Tatia brunnea.—BRAZIL: AMAZONAS STATE: CAS 76790, 2, 70.3–80.2 mm SL, Cuieras River. INPA 14228, 2, 96.9–97.4 mm SL, Urubu River, igarapé of Gavião, Farm Esteio, Negro River basin. INPA 15989, 1, 66.6 mm SL, Presidente Figueiredo, Urubu River, Negro River basin. INPA 29988, 4, 17.9–42.4 mm SL, Preto da Eva River, Cabo Frio, Manaus. MZUSP 31075, 1, 34.0 mm SL, Negro River, island lake, Barcelos. FRENCH GUIANA. RMNH.PIS 28571, 4, 1 CS, 25–37 mm SL, Balaté stream. SURINAME: RMNH.PIS 26196, holotype, Rx, 56.5 mm SL; Compagnie creek. AMNH 58390, 1, Rx, paratype, 54.6 mm SL; Kamaloe stream, right margin of Marowijne River. RMNH.PIS 26197, 3, paratypes, 47.6–60.0 mm SL, Compagnie creek. RMNH.PIS 26198, 3, 1 CS, paratypes, 35.1–40.3 mm SL, Kwambaolo stream, near dam. ZMA.PIS 105.849, 7, 2 Rx, 27.0–52.2 mm SL, Maka stream, tributary of Lawa River, Marowijne district.

Tatia caxiuanensis.—BRAZIL: PARÁ STATE: MPEG 6201, 7, 1 CS, paratypes, 29.3–40.7 mm SL, and MNRJ 28821, 2, paratypes, 31.3–35.3 mm SL, Estação Científica Ferreira Pena, Curuá River, Caxiuanã, Melgaço.

Tatia caudosignata.—COLOMBIA: AMAZONAS DEPARTMENT: IAvH-P 8932, 2, 1 CS, 91.4 - 101.3 mm SL, quebrada Sufragio, in front of the Reserva Biológica El Zafire, Leticia. IAvH-P 9394, 3, 67.3- 123.7 mm SL; 1 CS, tributary stream to the río Pureté, 3 hours from Salado Varios, Parque Nacional Natural Amacayacu, Leticia.

Tatia concolor.—SURINAME: ZMA.PIS 106210, holotype, 33.4 mm SL, Rx and ZMA.PIS 106209, 2,Rx, paratypes, 29.0–30.6 mm SL, Coppename River.

Tatia dunni.—BRAZIL: AMAZONAS STATE: CAS 52124, 3, 28.4–40.8 mm SL, Castelo Branco, lago Grande, Amazonas River. INPA 3017, 1, 69.0 mm SL, Igarapé Madalena, Catalão, Solimões River. INPA 18477, 3, 72.0–87.8 mm SL, Tupinambaranas Island. COLOMBIA: ANSP 71705, holotype, Rx, 83.3 mm SL, upper Amazonas River, Caquetá River drainage, Morelia. ANSP 71706, 1, paratype, 50.1 mm SL, upper Amazonas River, Caquetá River drainage, Morelia. ECUADOR: FMNH 88187, 3, 66.1–84.2 mm SL, Conambo River, mouth of Shiona River, eastern Ecuador. FMNH 92007, 2, 1 CS, 90.0–96.9 mm SL, Conambo River, mouth of Shiona River, eastern Ecuador.

Tatia ferrarisi.—BRAZIL: TOCANTINS STATE: MNRJ 41924, 1, paratype, 57.6 mm SL and MZUSP 115352, 2, 1 CS, paratypes, 50.4–68.1 mm SL; Conceição River, headwater of Balsas River, Estação Ecológica Serra Geral do Tocantins.

Tatia galaxias.— COLOMBIA: ANSP 138105, 2, 54.2–64.6 mm SL, El Viento rivulet, Finca El Viento south of Matazul. VENEZUELA: CAS 6568, 4, paratypes, 49.0–56.6 mm SL, and RMNH.PIS 26493, 2, Rx, paratypes, 48.5–55.6 mm SL, Quiribana stream, near Caicara, Orinoco basin. AMNH 91381, 1, 125.6 mm SL, Mavaca River. ANSP 160648, 1, 44.0 mm SL, Sipapo River above Pendare. MCNG 15001, 3, 1CS, 25.3–29.4 mm SL, San Bartolo River, Parque Aguaro. MCNG 25983, 1, 85.6 mm SL, Siapa River. MCNG 27966, 1, 39.3 mm SL, Orinoco River in El Tigre island. COLOMBIA: ANSP 138105, 2, 54.2–64.6 mm SL, El Viento rivulet, Finca El Viento south of Matazul.

Tatia gyrina.—BRAZIL: AMAZONAS STATE: MCZ 8182, 1, 32.7 mm SL, Solimões River in Codajás. INPA 18478, 1, 38.2 mm SL, Tefé. INPA 20970, 2, 29.0–36.2 mm SL, igarapé Branco, Reserva de Desenvolvimento Sustentável Amanã, Tefé. INPA 20971, 4, 1 CS, 26.0–28.3 mm SL, Igarapé of Veado, Reserva de Desenvolvimento Sustentável Amanã, Tefé. SURINAME: RMNH.PIS 19440, holotype of *Centromochlus creutzbergi*, Rx, 25.2 mm SL, creek Djai. RMNH.PIS 28617, 10, 1 CS, 25.0–34.1 mm SL, Sipaliwini: tributary on right margin of Nickerie River, above Stondansie Camp; RMNH.PIS 28618, 8, 31.2–35.0 mm SL, tributary on right margin of Fallowatra River, Nickerie River basin. RMNH.PIS 28619, 7, 26.3–34.0 mm SL, Forest stream, above Stondansie, Nickerie River basin.

Tatia intermedia.—BRAZIL: AMAPÁ STATE: MNRJ 12132, 1, 66.0 mm SL, Maruanum River, tributary of Matapi River, Macapá. MNRJ 12133, 1, 31.9 mm SL, and MNRJ 12134, 9, 40.2–65.1 mm SL, Aporema River in Fazenda Modelo do Aporema, tributary of Araguari River. AMAZONAS STATE: INPA 35380, 4, Tapauá River, Indigenous land Paumari of lake Manissuã, Tapauá. INPA 47933, 124.0 mm SL, Castanho River. PARÁ STATE: INPA 11076, 1, 84.7 mm SL, Tocantins River. MZUSP 43139, 5, 35.2–42.0 mm SL, MZUSP 47504, 1, CS, 40.0 mm SL, and RMNH.PIS

26492, 1, 40.0 mm SL, Igarapé Paracuri, near Icoaraci, Belém. Suriname: RMNH.PIS 26199, 12 (38.5–50.0 mm SL), Sipaliwini. ZMA.PIS 105.791, 3, Rx, 51.2–74.2 mm SL, stream on left margin of Suriname River, 2,5 km north from Botopasi Village, Brokopondo district.

Tatia jaracatia.—Brazil: Paraná State: MNRJ 31909, 1, paratype, 42.9 mm SL, lower Iguaçu River, Capitão Leônidas Marques. MNRJ 31910, 1, paratype, 57.0 mm SL, Jaracatiá River, Salto do Lontra.

Tatia marthae.—Venezuela: ANSP 146201, holotype, Rx, 23.1 mm SL, and ANSP 199070, 1, Rx, 19.0 mm SL, Cuchima rivulet, tributary of Cusimi River, upstream from confluence of Caura River and Erebato River at Entre Ríos, Bolivar.

Tatia meesi.—Guyana: INHS 99772, holotype, 44.3 mm SL, INHS 49549, 9, 1 CS, 30.3–46.6 mm SL, and MBML 2046, 3, 32.2–42.6 mm SL, Waratuk cataract, Essequibo River Drainage, lower Potaro River, Potaro-Siparuni.

Tatia meridionalis.—Brazil: Mato Grosso State: INPA 37893, 10, paratypes, 40.4–47.9 mm SL; INPA 37897, 2 CS, paratypes, 29.7–39.2 mm SL; MBML 5616, 1 CS, paratype, 39.1 mm SL; MBML 5617, 3, 32.2–46.2 mm SL; paratypes, and MNRJ 40702, 3, 32.6–38.3 mm SL; paratypes, Loanda stream, a small tributary of Roquete River, Cláudia.

Tatia neivai.—Mato Grosso do Sul State: MZUSP 35882, 1, 26.6 mm SL, Piquiri River, Santo Antônio do Paraíso farm, Itiquira. MZUSP 36364, 2, 27.7–46.8 mm SL, Corixão, Capão Grande, Nhecolândia, Corumbá. MZUSP 42145, 2, 23.6–33.9 mm SL, lake about 25 Km from Poconé, on road to Porto Cercado. Paraguay. MHNG 2355.92, 12, 50.7–63.7 mm SL, Yuguyry stream, about 17 km south of Yhu, Caaguazu. MHNG 2430.19, 1, Rx, 76.1 mm SL, lake on Iguazu River, upper Paraná. MHNG 2537.73, 8, 1 CS, 37.2–46.6 mm SL, Tagatija-mi River, about 30 Km east from Puerto Max.

Tatia nigra.—Brazil: Amazonas State: INPA 11081, 6, paratypes, 86.6–107.8 mm SL, and MNRJ 32024, 2, 1 CS, paratypes, 97.0–98.2 mm SL, Uatumã River, Samaúma lake, Presidente Figueiredo. INPA 43876, 2, 100.5 –106.6 mm SL, Nhamundá River below Sete Ilhas Lake.

Tatia perugiae.—Brazil: Acre State: MZUSP 31880, 1, 28.2 mm SL; Rx, Tarauacá River, Tarauacá. Ecuador: ANSP 130611, 14, 30.1–45 mm SL; Aguarico River in Santa Cecilia, Napo. FMNH 92005, 1 CS, Rutun Celutu River. MNRJ 30489, 1, 38.5 mm SL; Aguarico River, Napo. Peru: MNRJ 30490, 1, 38.4 mm SL; Huanuco, Amazonas. MZUSP 26029, 2, 22.3–29.8 mm SL; Chiriaco River, provincia Bagua. MZUSP 26684, 4, 26.2–35.9 mm SL; stream Ivita–Pucallpa, Caserio Neshuya, Coronel Portillo Province. Venezuela: MCNG 21691, 5, 1 CS, 24.6–29.4 mm SL; Sipapo River, about 50 m from Salto Remo, Ucayali, Amazonas.

Tatia punctata.—Brazil: Pará State: RMNH. PIS 26494, 2, Rx, paratypes, 33.3–43.2mm SL, Igarapé Kumadueni, tributary of Paru River. Suriname: RMNH. PIS 26495, holotype, 45.0 mm SL, and RMNH.PIS 26496, 3, 36.2–39.3 mm SL, Rx, paratypes, rivers between Kabel and Lombé.

Tatia reticulata.—Brazil: Amazonas. INPA 35394, 6, 18.3–28.8 mm SL; Tapauá River, indigenous land Paumari do Cuniuá, Purus River. Guyana: RMNH.PIS 26744, 2, Rx, 18.3–39.8 mm SL; paratypes, Karanambo, Rupununi. Colombia: MNRJ 30492, 1, CS, 30.8 mm SL and ANSP 128797, 4, 30.7–34.2 mm SL; Emma stream, Finca El Viento, ca 33.5 km NE Puerto Lopez, Meta.

Tatia romani.—Venezuela: AMNH 91382, 2, 32.5–32.7 mm SL; Siapa River, Amazonas. INHS 27999, 1, 31.0 mm SL; Michay River, Apure drainage, Barinas. MCNG 14896, 18, 1 Mi, 29.0–31.3 mm SL; San Jose River, Guanare. RMNH.PIS 30491, 3, 27.1–31.3 mm SL; Rx, paratypes, Monagas, Maturin.

Tatia simplex.—Brazil: Mato Grosso State: MZUSP 47506, 1 CS, Igarapé do Aeroporto, Humboldt, Aripuanã. Pará State: INPA 18475, 1, 19.9 mm SL, Tocantins River, corredeiras Jatobal. MZUSP 36862, 2, 28.4–29.6 mm SL, Xingu River. MZUSP 44071, 2, 26.0–48.3 mm SL, lake in front of Jatobal, Tocantins River drainage. MZUSP 44074, 1, 26.5 mm SL, lake near Capitariquara channel, close to Jatobal, Tocantins River drainage.

Tatia cf. *simplex*.—Brazil: Tocantins State: MZUSP 82359, 14, 28.7–36.2 mm SL, Palma River, near village of Taipas, on road Dianópolis-Conceição do Tocantins. UFOPA-I 670, and UFOPA-I 671, 38.4 mm CP, Brazil, Tocantins, Perdida River, Tocantins River drainage.

Tatia strigata.—Brazil: Amazonas. MCZ 78092, 1, paratype, 55.0 mm SL, lake Cristalino, off Negro River near Manaus. MZUSP 7357, 35, paratypes, 20.5–38.6 mm SL, Maués, Igarapé Limãozinho. MZUSP 7298, 23, paratypes, 16.3–31.2 mm SL, and MZUSP 44066, 2 CS, paratypes, 37.0–38.9 mm SL, Igarapé of Marau River, Maués. Roraima State: INPA52138, 4, 14.8–25.9 mm SL, Jufari River, Igarapé Caicubi, near margin, on nocturnal sampling, Caicubi.

Auchenipteridae: Auchenipterinae

Asterophysus batrachus.—BRAZIL: AMAZONAS STATE: MNRJ 915, 1, upper Negro River, frontier Brazil with Venezuela. MNRJ 985, 1 CS, Manaus. MZUSP 12420, 1, Negro River, Paricatuba.

Entomocorus benjamini.—BRAZIL: MATO GROSSO DO SUL STATE: MZUSP 40085, 1, Onça bay, Fazenda Alegrete, rio Aquidauana, Aquidauana.

Entomocorus gameiroi.—VENEZUELA: MZUSP 9357, 1 CS, laguna El Pavoncito, close to San Fernando de Apure, Apure.

Epapterus dispilurus.—BRAZIL: AMAZONAS STATE: MZUSP 28750, 1 CS, Javari.

Liosomadoras oncinus.—MNRJ 15906, 1 cs, 92.0 mm SL; and MNRJ 17640, 1 cs, 125 mm SL, aquarium store. BRAZIL: AMAZONAS STATE: MNRJ 12351, 9, 80–135.0 mm SL, Inambu, right margin of upper rio Negro. LIA unnumbered, 1, 95.0 mm SL, Amazonas. VENEZUELA: MZUSP 105828, 3, 1 Sk, 99–101 mm SL, río Ventuari, Rio Orenoco basin.

Pseudauchenipterus nodosus.—BRAZIL: MARANHÃO STATE: INPA 729, 1, Rio Pericumã, Pinheiro.

Parauchenipterus striatulus.—BRAZIL, RIO DE JANEIRO STATE: MNRJ 12133, 3, 1 CS, rio Paraiba do Sul.

Pseudotatia parva.—BAHIA STATE: FMNH 70580, holotype, and FMNH 57807, 4, 2 cs, paratypes, 34.0–35.0 mm SL, Juazeiro, rio São Francisco.

Tocantinsia piresi.—BRAZIL: GOIÁS STATE: CAS 6573, holotype of *Tocantinsia depressa*, 71.0 mm SL, Rio Tocantins near Porto Nacional. MNRJ 13502, 1, 130 mm SL, Rio Tocantins, on locality of future hydroelectric dam Cana Brava, between Ilha do Orgulho and Porto do Garimpo, on boundary between municipalities of Minaçu and Cavalcante. PARÁ STATE: MZUSP 98301, 1, Sk, 250.0 mm SL, Jacareacanga, rio Teles Pires.

Doradidae

Kalyptodoras bahiensis.—BRAZIL: BAHIA STATE: MZFS 12878, 7, Paraguaçu River on Fazenda Deus Andou, Iaçu. MBML 5500, 5, Paraguaçu River, Marcionílio Souza.

Wertheimeria maculata.—BRAZIL: MINAS GERAIS STATE: MZUSP 40229, 15, rio Jequitinhonha confluence with Araçuaí, Araçuaí.

APPENDIX B

Data matrix of 133 characters (numbered 0 to 132) examined for 47 potential ingroup species of Centromochlinae and one species of Auchenipterinae (outgroup: OG). Missing data indicated by (?); inapplicable characters indicated by (-).

OG *Tocantinsia piresi*
0000000000000?00000000000?0000000000000000000000000000000000000000000000000000000000
0000000000000000000000000000000000

Centromochlus carolae
001000100000100100000000000010000001010100101111101??0110000100010100011000001?00100000011010111
010001000000000000001000110100 2011010

Centromochlus existimatus
0010001001001001011010000?00000000111101001011000110001101001000101010001000000?0110001001101111 10
10012001000000000000110111010020 11010

Centromochlus heckelii
001000100100101101101000000000000001111010010110001100011010010001010100010 0000?011000100110101 11
010012001000000000001101110100 2011010

Centromochlus macracanthus
0010001000001001001000000000010000001110100101100000000110100100000100011000000?0110001001101 0111
0100110000000000000010011101002011010

Centromochlus melanoleucus
001000100000100100000000000010000001010100101110000000110000100000100011000000?00100000011010111
0100010000000000000010001101002001000

Centromochlus musaicus
0010001000001001000000000000100000010101001011111010?0110000100010100011000001?00100000011010111
0100010000000000000010001101002011010

Centromochlus orca
0010001000001001000000000000100000010100001011100100001100001000101010110000 01?00100000011010111
0100010000000000000010001101002011010

Centromochlus schultzi
00100010000010010000000000001000000101010010110000000011010010000010001100000 1?00100010011010111
0100010000000000000010011101002011010

Gelanoglanis stroudi
1102?0?00?10100100000101?00101?1??1101111111211000 1001?100001?1002100011000001?001?2001111100 11121
0001000000000000000100?????????????

Gelanoglanis nanonocticolus
1102?1?01?11100100000101?00101?1??11011101112110001001?100001?10021000 11011??0?0?1?1101????1111211
0020000100000000 0100?????????????

Gelanoglanis pan
1102?1?01?1110010000010010 0101?1??110111011121100 01001?100001?100210001100000000 1?1001111100 11121
1001000000000000000100?????????????

Gelanoglanis travieso
1102?0?00?10100100000101?00101?1??1101111111211000100 1?100001?1002100011001??110?1?200111110011121
0001000000000000000100?????????????

Gelanoglanis varii
1102?1?01?1110010000100?00101?1??1101110111211000100 1?100001?1002100011011?????01?1101111100111 21?
0010000000000000100?????????????

Gephyromochlus leopardus
0000000000001??1000000000?2000000000110100000000000000011000011?000100000000001100100000 1111?01110
1100000000020000000100011000 00?0?

Glanidium albescens
0000000000001101000100000110000000000000000000000000000000100101000000000000000100001000000000000110
0101000000002000000010000000000100101

Glanidium botocudo
0000000000001101000100000110000000000000000000000000000000100101000000000000000100001000000000000110
0101000000002000000010000000000100101

Glanidium catharinensis
0000000000001001000000000010000000000000000000000000100001001010100000000000010000100000000000110
0101000000012000000010000010100100100

Glanidium cesarpintoi
0000000000001001000100000110000000000000000000000000?0000100101000000000000010000100000000000110
0101000000002000000010000000000100101

Glanidium melanopterum
0000000000001001000000000010000000000000000000000000100001001010100000000000010000100000000000110
0101000000012000000010000010100100100

Glanidium ribeiroi
0000000000001001000000000010000000000000000000000000100001001010100000000000010000100000000000110
0101000000012000000010000010000100100

Pseudotatia parva
000000000000?0000???000000000000010000000000000000000000???000000000000000000000000000000000000
000000000000200000000000?????????????

Tatia intermedia
0000000100001011000010000000000011000000000000111000101100100000000000000000000011000000000111
1100010101100101001110101100011000100

Tatia aulopygia
0000000100001011000010001000000011000000000000111000101100100000000000000000000011000000000111
1120010101100101001110101100011000100

Tatia boemia
0000000100001011000010000000000011000000000000111000101100100000000000?000000000110000000000111
1100010101100001001010101100000000000

Tatia brunnea
00000001000010110100100000000000110000000000001110001011001000000000000000000000111000000000111
11000101011001O?01111010110000000100

Tatia caudosignata
00000001000010110000100000000000110000000000001110001011001000000000000000000000111000000000111
11000101011001010111101?????????????

Tatia caxiuanensis
00000000000010111000100000000000010000000000001110001011001000000100000000000000110000000000111
1100010?01100001001010001100001000000

Tatia dunni
00000001000010110100100000000000110000000000001110001011001000000000000?000000000111000000000111
11000101011001O?01111010110000000100

Tatia galaxias
00000001000010110000100000000000110000000000001110001011001000000000000000000000110000000000111
11000101011001010011101011000010001000

Tatia gyrina
00000000000010111000101000000010010000000010001110001011001000000100000000000000110000000000111
11000100001000?0100101000110000010000000

Tatia jaracatia
00000001000010110000100000000000110000000000001110001011001000000001010000000000110000000000111
11000101011000010010101?1100000000000

Tatia meesi
00000000000010111000100000?0000100100000000000011100010110010000001000000000000001100000000001111
11000100001000010010100011000010000000

Tatia neivai
00000001000010110000100000000000110000000000001110001011001000000001010?000000000110000000000111
11000101011001?0100101010110000000000

Tatia nigra
00000001000010110000100000000000110000000000001110001011001000000000000000000000111000000000111
11000101011001010111101011000000000100

Tatia strigata
00000001000010110000100000000000110000000000001110001011001000000000000000000000110000000000111
11200101011001010011101011000110001000

Tatia meridionalis
00010000000010110000100000000000000000000000001000000110010000000002011000l?110011000000000111
01000110001010011010100011000000000000

Tatia perugiae
00000000000010110000101010000020000000001000000100001?011001000000000200?000000100110000000000111
01000110101010011010100011000000000000

Tatia altae
00000000000001011000010101000002000000000100000010000?01100100000000200?000000100110000000000111
01000110101010011010100?????????????

Tatia ferrarisi
00010000000011111000010000000000000000000000000100000011001000000000201100000110011000000000111
01000110001010011010100?????????????

Tatia reticulata
00000000000001111000010000000000000?000000000001?000?01100100000000020 1?000000100110000000000111
01000100001010010010100011000000000000

Tatia romani
00000000000001111000010100000002000000000000000001?000?01100100000000020110001?01001100000000000111
01000110101010011010100011000000000000

Tatia bockmanni
00000000000001111000000000000000000000000000000000000001100100000000000110000010101100000000000111
01000100001000100010100011000000000000

Tatia britskii
00001?2000001111000000000000000000000000000000000000001100100000000000110000010101100000000000111
01000100001000100010100?1100000000000

Tatia concolor
0000000000001??100???000000000000000000000000000000001100100000000000110000000001100000000000111
01000100001000100010100?????????????

Tatia marthae
0000000000001??10????000000000000000000000000?0?????0?1?0???00000??00110000000001100000000000?????
??01????????1???1?100?????????????

Tatia punctata
0000000000001??100???000000000000000000000000000000001100100000000000110000000001100000000000111
01000100001000100010100?????????????

Tatia simplex
0000?02000001111000000000000000000000000000000000000001100100000000000110000010101100000000000111
01000100001000100010100011000000000000